Materials Today Bio 29 (2024) 101348

Contents lists available at ScienceDirect

Materials Today Bio

journal homepage: www.journals.elsevier.com/materials-today-bio

Recent advancements and clinical aspects of engineered iron oxide nanoplatforms for magnetic hyperthermia-induced cancer therapy

Arunima Rajan [a], Suvra S. Laha [b,c], Niroj Kumar Sahu [d], Nanasaheb D. Thorat [e,*], Balakrishnan Shankar [a,f,**]

[a] Centre for Flexible Electronics and Advanced Materials, Amrita Vishwa Vidyapeetham, Amritapuri, 690525, India
[b] Centre for Nano Science and Engineering (CeNSE), Indian Institute of Science, Bangalore, 560012, India
[c] Department of Materials Science and Engineering, Clemson University, Clemson, SC, 29634, USA
[d] Centre for Nanotechnology Research, Vellore Institute of Technology, Vellore, 632014, India
[e] Department of Physics, Bernal Institute and Limerick Digital Cancer Research Centre, University of Limerick, Castletroy, Limerick, V94T9PX, Ireland
[f] Department of Mechanical Engineering, Amrita Vishwa Vidyapeetham, Amritapuri, 690525, India

ARTICLE INFO

Keywords:
Iron oxide
Reactive oxygen species
Lysosomal membrane permeabilization
Magnetic hyperthermia
Cancer therapy

ABSTRACT

The pervasiveness of cancer is a global health concern posing a major threat in terms of mortality and incidence rates. Magnetic hyperthermia (MHT) employing biocompatible magnetic nanoparticles (MNPs) ensuring selective attachment to target sites, better colloidal stability and conserving nearby healthy tissues has garnered widespread acceptance as a promising clinical treatment for cancer cell death. In this direction, multifunctional iron oxide nanoparticles (IONPs) are of significant interest for improved cancer care due to finite size effect associated with inherent magnetic properties. This review offers a comprehensive perception of IONPs-mediated MHT from fundamentals to clinical translation, by elucidating the underlying mechanism of heat generation and the related influential factors. Biological mechanisms underlying MHT-mediated cancer cell death such as reactive oxygen species generation and lysosomal membrane permeabilization have been discussed in this review. Recent advances in biological interactions (in vitro and in vivo) of IONPs and their translation to clinical MHT applications are briefed. New frontiers and prospects of promising combination cancer therapies such as MHT with photothermal therapy, cancer starvation therapy and sonodynamic therapy are presented in detail. Finally, this review concludes by addressing current crucial challenges and proposing possible solutions to achieve clinical success.

1. Introduction

Cancer, in terms of morbidity and mortality rates, is the second leading cause of death globally according to the World Health Organization (WHO) report 2020 [1]. At present, millions of people in the world are carrying this potentially fatal disease. Intensive research in the field of cancer treatment spanning over the past few decades offers only limited outcomes considering the fatality and adverse side-effects [2]. Cancer (generally termed as tumor) is a stage of unregulated cell growth in the body, which happens when the cells instruction carried by DNA gets damaged from its proper functioning causing cell mutation. This loss of growth control occurs as a result of accumulated abnormalities in multiple cell regulatory systems therefore reflected in numerous aspects of cell activity which distinguish tumor cells from normal healthy cells. The root cause of cancer can be traced back to an alteration of basic biological cell cycle process which is the cell cycle regulation. Cancer cells differ from normal cells depending on the nature of cell division in the cell cycle [3]. The growth and progression of cancer are generally linked to a series of changes in the activity of cell cycle. The process of cell division in normal cells are intricately controlled by hundreds of genes. Normal cells become cancerous after mutations accumulate in various genes which control cell proliferation. A cell cycle composes of

* Corresponding author. Department of Physics, Bernal Institute and Limerick Digital Cancer Research Centre, University of Limerick, Castletroy, Limerick, V94T9PX, Ireland.
** Corresponding author. Centre for Flexible Electronics and Advanced Materials, Amrita Vishwa Vidyapeetham, Amritapuri, 690525, India.
E-mail addresses: arunimarajan11@gmail.com (A. Rajan), ss.laha@gmail.com (S.S. Laha), nirojs@vit.ac.in (N.K. Sahu), thoratnd@gmail.com (N.D. Thorat), bala@am.amrita.edu (B. Shankar).

https://doi.org/10.1016/j.mtbio.2024.101348
Received 31 August 2024; Received in revised form 31 October 2024; Accepted 15 November 2024
Available online 21 November 2024

DNA replication and division of cells.

Tumors can be categorized as benign or malignant. Benign tumors grow without spreading to other parts of the body and are not usually life threatening whereas malignant tumors are invasive cancer cells, proliferating through blood or lymph system and eventually creating a secondary growth (metastases) [4]. In order to reach blood or lymph vessels, invasive cancer cells in solid epithelial tumors must cross the basement membrane first and then migrate through the stroma, where they can be carried to other organs. Removal of malignant tumor through surgery is not treated as an effective approach due to its invasive nature. Therefore, many new strategies are being developed for diagnosis and fight against cancer. Tumors often exhibit a more complex tissue structure which can be rendered to their unregulated growth and their deposit causes low pH and low oxygen pressure to the surrounding tissues as a result of defective blood perfusion (chaotic vascularization) [5,6]. These conditions impart a challenge to the prevailing standard therapeutic procedures as outlined below.

Besides surgical treatment, radiation therapy and chemotherapy are well authenticated oncological therapies for cancer [7,8]. In radiation therapy, high energy radiation of X-rays, gamma rays or charged particles are exploited to damage the DNA thereby shrinking the tumor or killing the cancer cells. Chemotherapy is the administration of drugs to specifically targeted cancer sites leading to slowing down its growth eventually destroying it. These therapies are often combined with each other to obtain a synergistic effect for better outcomes. However, it is found from the literature that many cancer cells are chemo resistant [9–12]. Immunotherapy is another potential technique to potentially fight against cancer by providing the body's own immune system [13]. Provenge is the first autologous vaccine applied successfully for prostate cancer which works by forcefully stimulating the immune system to target cancer cells, however it limits in producing large quantities [14]. The limited efficiency due to an immunosuppressive tumor microenvironment and systemic toxicity limits the extensive cancer immunotherapy applications [15]. Even though cancer cells are more sensitive to these therapies, there are still issues relating to the unavoidable effects on normal healthy cells which make these treatments not a better option. Therefore, there is extensive research to search for alternative effective techniques of cancer theranostics (diagnosis and therapy).

Apart from these therapies, hyperthermia (HPT) has been confirmed as a minimally invasive thermal therapy that alleviates severe adverse effects to the tumor cells thereby enhancing the treatment to bring a new hope to cancer patients [16,17]. In medical oncology, the term HPT is used for exposing the tumor loaded tissues to an elevated temperature for a given period of time to achieve a specific therapeutic effect, to induce cell death. Cancer cells are more vulnerable to temperatures greater than 41 °C than compared to their normal cell counterparts, due to the higher rates of metabolism as well as the hypoxic nature of cancer tissues [18]. This observation affirmed the immense potentiality of HPT as an effective therapeutic procedure assuring the conservation of normal tissue structure. HPT complements conventional oncological modalities such as chemotherapy, radiation therapy, hormone therapy, surgery, and immunotherapy as an attractive substitute owing to the fact that it lacks notable side effects [19]. In Germany, HPT in conjunction with chemotherapy (thermal chemosensitization) and radiation (thermal radiosensitization) has been clinically used and detected profound metabolic changes in tumor cells, compared to other therapies [17]. Thus, HPT is often used as an adjuvant cancer therapy causing a synergistic effect *i.e.* it often aims for the enhancement of the results caused by other treatment modalities through these synergistic effects. In spite of the fact that combinatorial approaches result in elevated metabolic rates and oxygenation, inhomogeneous tumor-heating has shown limited clinical results [20–22].

In the history of HPT, magnetic hyperthermia (MHT) or magnetic fluid hyperthermia (MFH) where colloidal dispersion of magnetic nanoparticles (MNPs) is exploited, has attained a promising success owing to its propensity in the field of material science and medicine [23–25]. In vivo MHT studies result in promising outcomes when tested in animal tumor models, paving way for future clinical studies [23, 26–30]. MNPs, as tumor specified heat sources, have the ability to be guided by external AC magnetic field (ACMF) and targeted directly to the localized tumor sites for controlled homogeneous heating, rendering MHT distinctive from other traditional modalities. To achieve highly efficient carcinogenic cell destruction and for the optimization of heat dissipation, understanding and tuning the physico-chemical properties of MNPs and applied magnetic field parameters are crucial. The effective application of MHT is dependent on forming biocompatible surface functionalized MNPs exhibiting enhanced magneto-thermal properties thereby ensuring effective heating under an ACMF. MNPs can be injected intra-tumorally or by intravenously to the target sites [31]. Intra-tumoral injection where MNPs bypass the arterial pathway, is very beneficial due to the specific heat dissipation at tumor area, however heterogenous distribution limits this method. Intravenous injection of MNPs involves localized delivery of MNPs to the specific cancer sites based on enhanced permeability and retention (EPR) phenomenon. Among the MNPs, nano-sized iron oxide, a versatile biocompatible metal oxide with unique magnetic properties, biochemical functionality, safety, cost-effective fabrication processes, large surface area, high chemical stability and high versatility in terms of shape and size has shown great potential as an advanced platform for MHT [32,33] Among IONPs, magnetite (Fe_3O_4) and maghemite (γ-Fe_2O_3) forms have been extensively researched and preferred for cancer theranostics [28,29,34]. Moreover, pharmacokinetics of IONPs can be enhanced through surface modification strategies to yield better colloidal stability and improved blood circulation with minimal toxicity [35–39].

The present review seeks to focus on comprehensive and multidisciplinary perception of MHT from fundamentals to clinical translation (Fig. 1). There are several pertinent recently published reviews [40–44] in this research field in terms of synthesis strategies, surface functionalization, heating mechanisms and related factors influencing the heat dissipation for MHT and conventional combined MHT-chemotherapy. This proposed review article aims to explore various aspects of HPT, extensive clinical aspects of IONPs as thermal nanomedicine in MHT, biological mechanism such as reactive oxygen species (ROS) and lysosomal membrane permeabilization (LMP), novel combinational therapies such as photothermal therapy (PTT), cancer starvation therapy (CST) and sonodynamic therapy (SDT) in conjunction with MHT and addressing the future perspectives. This article begins with a general discussion of HPT and its traditionally established heating modalities used for cancer therapy followed by a comprehensive explanation of heating mechanism of MNP-mediated cancer HPT. Recent advances in biological interactions (in vitro and in vivo) of IONPs and their translation to clinical applications will be briefed. Clinical studies conducted, currently being investigated in the clinic, along with the preclinical works which can be translated to the clinical stage will be discussed. Understanding the principles underlying the combination therapies such as MHT with photothermal therapy (PTT), cancer starvation therapy (CST) and sonodynamic therapy (SDT) and its recent applications will be detailed. This review will rationalize and focus research efforts at various stages of MHT to address the challenges and existing open problems from basic to applications in day-to-day life. Overall, this review will aid in providing insights to be considered for progress in magnetic nanomaterials for cancer therapy which is still one of the most pervasive diseases globally.

2. Hyperthermia (HPT)

The term 'hyperthermia' is a combination of two Greek words-hyper (rise) and therme (heat) *i.e.* to raise the body temperature higher than normal. The practice of using heat for cancer therapy has a long history that dates back to ancient ages [45]. Ancient Greeks, Romans, and Egyptians used heat to treat breast tumors which is still a preferable self-care therapy for engorged breasts [46]. Cancer cells typically have a

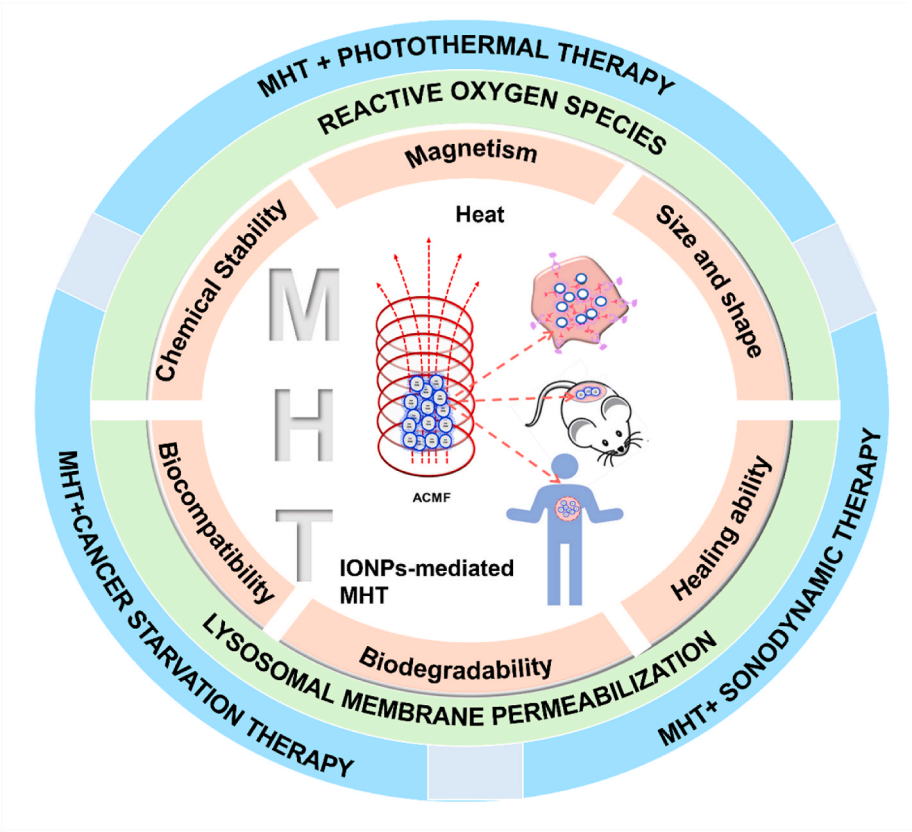

Fig. 1. Schematic illustration of the focus of this review. IONP-mediated MHT under an ACMF for cancer cell destruction and synergistic approaches employing PTT, CST and SDT emphasizing the ROS and LMP mechanism.

lower thermal tolerance compared to healthy cells. Cancer cells often exhibit increased sensitivity to heat due to their rapid proliferation and altered metabolic states, making them more susceptible to thermal stress. Heat generation induces a heat shock response in the body affecting the protein structure and function thereby disrupting the cellular pathways resulting cell death [47]. The amount of thermal dosage required for cell death is approximately about 140 kcal/mol in vitro as well as in experimental tumors which is close to the energy required for cellular protein denaturation [48]. Heat response during exposure varies among cells according to the four phases in cell cycle such as G1 (gap 1), S (synthesis), G2 (gap 2), and M (mitotic) phase. G1, S, and G2 together are known as interphase or resting phase of the cell cycle in which the cell prepares for division by undergoing both cell growth and DNA replication. Cell growth occurs in G1 phase, DNA replication in its nucleus occurs in S phase and more cell growth for making proteins and organelles occurs in G2 phase where this phase ends when mitosis begins. M phase composed of mitosis process in which the nucleus of the cell divides (mitotic nuclear division) followed by the process of cytokinesis in which the cytoplasm divides to form two daughter cells. Each phase of cell cycle progression is reliant on the proper completion of the previous cell cycle phase. Cancer is characterized by continuous cycles of cell division, which is steered by mutations that hinder cell death, compromising cell cycle exit, ensuing uncontrolled cell cycle progression [3,49,50]. During HPT treatment, G1 phase in the interphase stage does not show any microscopic damage, however follows a rapid cell death whereas S phase cells undergo chromosomal damage after heat exposure. M phase cells in the mitotic stage damage their mitotic apparatus leading to an incomplete mitosis. Cells that enter mitosis under hyperthermic conditions may undergo apoptosis if they cannot properly divide. Acute exposure to moderate heat shock can induce transient arrest of cells at two check points such as G1/S and G2/M [51]. Heat sensitivity is observed highest during the mitotic phase. HPT along with other forms of cancer therapies such as radiation therapy and chemotherapy may make some tumor cells more prone to radiation or may harm more cancer cells which are not affected while using only radiation. In a conjoint treatment trial of HPT and radiation therapy, an enhanced response in the survival rates were observed [21]. HPT can also enhance the effects of certain anticancer agents [8]. Since chemotherapy fails at certain drug resistance tumor cells, a combination of drug and heat can effectively exhibit a tumoricidal effect. For combined therapies, not all types of cancer have shown a significant reduction in tumor size. Common HPT treatments have focused on different cancer types including sarcoma, melanoma and cancers in brain, liver, lung, esophagus, breast, bladder, rectum, appendix, cervix and peritoneal lining [17,52].

HPT treatment can be grouped under three classes depending on the generated temperatures - thermoablation (46 °C < T < 56 °C), moderate HPT (41 °C < T < 46 °C) and diathermia (T < 41 °C). Traditionally treated HPT therapy is moderate HPT (41 °C < T < 46 °C) which has various effects both at the cellular and tissue levels. In moderate HPT, the cells undergo heat stress resulting in (i) activation and/or initiation of many intra and extracellular degradation mechanisms (ii) induction and regulation of cell death, signal transduction, multidrug resistance and heat shock protein (HSP) expression and (iii) pH changes, increasing blood perfusion and oxygenation of tumor environment by modifying tissue structure. The efficacy can be attributed to various factors viz. the attained temperature during the medication, the time of exposure and cell-tissue characteristics. The temperature applied to the tumor cells as well as the surrounding tissues are continuously monitored during treatment so as to ensure that the temperature will not exceed its critical limit to elicit any adverse effects to healthy cells.

2.1. Treatment modes of HPT

Depending on the extent of area, location and depth, clinical treatment modes of HPT are categorized as local, regional and whole-body. Treatment can either be internal or external subjected on whether heat is applied through inserting suitable foreign substances into the human body (internal treatment) or externally using instruments that can generate electromagnetic fields (microwaves or radio waves) or ultrasound. Many clinical HPT strategies have emerged for inducing homogeneous heat distribution in targeted cancer tissues. Most of the therapies employed external applicators for transferring energy to tissues directly. Local, regional and whole-body HPT deliver heat to localized, deep seated and disseminated malignancies, respectively. Local HPT is considered as the commonly used therapy as it induces minimal side effects compared to the other two.

Local HPT involves effective heat application to a small area of tumor inside a tissue locally with the aid of various energy sources (microwave, radio wave, and ultrasound). This method of treatment can further be classified on the basis of tumor location viz. external, interstitial and endocavitary approaches. External HPT approach makes use of external applicators, such as antennas for emitting radio or micro waves, which can be focused nearby or around the affected tissues to heat localized tumor areas in or just below the skin. Interstitial approaches can be utilized to treat tumors such as brain tumor by employing probes or needles which can generate high temperatures deep within the body as compared to external approach. Endocavitary method treats tumor within or near body cavities such as natural openings of hollow organs like esophagus or rectum using probes or antennas inserted into these cavities.

Regional HPT is related to the heating of large tissue areas such as an organ, limb or a body cavity i.e., treating deep seated tumors commonly such as those associated with pelvis or abdomen. This therapeutic procedure is more complicated than local HPT since it requires more treatment monitoring and planning regarding heating adjacent deep-seated tumors without potentially affecting the nearby tissues. This therapy often uses in conjunction with radiation therapy or chemotherapy. Deep regional HPT, continuous hyperthermic peritoneal perfusion (CHPP) and regional perfusion HPT are some of the typical approaches under this category. The metastatic or disseminated tumor that has spread throughout the body is usually treated by whole body HPT. Heating blankets, thermal chambers, warm water immersion are frequently used for elevating body temperature for whole body treatment. There are three main approaches in this sort for achieving a controlled and reproducible outcome such as thermal conduction (surface heating), extracorporeal induction and radiant or EM induction. Among the three treatment modes, local HPT has gained much more acceptance as it involves intracellular heating of localized tumor regions [53].

2.2. Different techniques of heat generation

Most of the HPT treatments are carried out with the aid of external devices transferring energy to tissues by electromagnetic technologies. Various heating sources such as laser irradiation, radio-frequency (RF) waves, microwaves and ultra sonic waves are available for solid tumor destruction. The choice of energy source depends on the nature of diseased tissues, geometry of applicator used and perfusion. Laser HPT involving laser tissue interaction has significant application in cancer therapy. It is often combined with surgery, chemotherapy or radiation therapy to achieve the best outcome. Optimum laser heating for apoptosis is governed by certain factors such as type of laser used and depth of penetration. Lasers used for HPT therapy are often operated in the near-infrared (NIR) range (700–1100 nm), which is ideal for penetrating tissues without causing damage. It is well known that biological tissues absorb light radiation in the NIR wavelength range of 650–950 nm [54]. Different wavelengths vary in absorption rates in tumor tissues, influencing the heat generation [55,56]. Therapy often aims to achieve power densities around 1–2 W/cm^2 which helps to achieve the desired thermal effect sparing surrounding healthy tissues [57]. Diode lasers, Nd:YAG lasers and CO2 lasers are commonly used lasers for effective heating of deep-seated tissues [58]. Thermal effects of laser HPT at 40–50 °C (HPT domain) will lead to the reduction of enzyme activity and cell immobility. Multiple interaction effects such as necrosis, coagulation, vaporization, carbonization or melting can be seen in biological tissues due to laser interactions depending on the temperature achieved. One of the main disadvantages of this therapy is the repeated exposure of laser irradiation for a patient to get a full recovery. Apart from laser, mostly used local heating sources for clinical HPT includes radiowaves, microwaves and ultrasonic waves. RF HPT employs frequencies in the range of 0.5–30 MHz have the ability to heat human tissues. This non-invasive RF ablation method at 13.56 and 27.1 MHz has provided a means for effective clinical HPT applications [59]. Still this therapy exhibits inconsistent responses towards irregular, large tumors and occurrence of heat-sink effect due to blood vessels surrounding the tumor. This therapy application is also limited to certain organ sites such as liver, kidney, breast, lung, bone. Microwave HPT employs 433, 915 and 2450 MHz frequencies for the therapy [60]. Since tumors have a structure of high-water content, high energy microwaves can easily penetrate and heat such physiology rapidly. Exposure of these microwaves causes the water molecules inside the tumor to vibrate developing frictional forces and consequently heat dissipation. However, relatively longer wavelengths of operation limit the microwaves to directly focus on tumor sites. This type of HPT is often used in conjunction with radiation therapy. In addition to these thermal therapy techniques, external energy can also be supplied in the form of ultra sonic waves. Ultrasound therapies of 0.5–2 MHz frequencies of acoustic energy have a good penetration in soft tissues [61,62] which can be focused for selective heating of tumor loaded tissues. Unlike the other electromagnetic radiations, ultrasound does not propagate effectively in air medium. These acoustic waves get totally deflected at the tissue interface and become ineffective near hollow regions such as near oral-nasal cavity, respiratory and gastrointestinal tracts owing to the high acoustic impedance mismatch between air and soft tissues.

Owing to low absorption efficiency of natural tissue absorbents, photothermal agents are administered externally into the tumor sites for a successful photothermal therapy (PTT). HPT-mediated by PTT is a newly developed therapeutic strategy which employs near-infrared (NIR) laser photothermal agents that dissipate heat resulting in thermal damage of cancer cells [63]. Photothermal agents (eg. Au/IONPs) converts light energy into heat energy to induce tumor cell death. This process involves absorption of light and conversion to heat via electron–electron and electron-phonon relaxation mechanisms leading to thermal apoptosis or necrosis due to increased temperature. PTT operates through a variety of cell death pathways, depending on temperature profile and duration, and the use of external photoabsorbers such as nanoparticles (NPs) [29]. Stable NPs within a particular size range (20–300 nm) exhibiting EPR effect and possessing an optical absorbance in NIR region are currently being investigated as photoabsorbing agents. Gold-based NPs with varying morphologies such as gold nano-shells, nanorods, nanocages etc., carbon nanotubes (CNTs), graphene and graphene oxide and semiconductor quantum dots (QDs) are extensively used candidates [64]. PTT utilizing IONPs are also predominant for potential heat dissipation [63,65–67]. This therapy is often combined with the existing therapies for effective treatment of cancer metastasis. Direct exposure to cancer cells by NIR laser can effectively induce tumor ablation. Due to the difficulties in penetrating deep seated tissues and the heterogeneous distribution of laser irradiation might lead to incomplete cancer cell death. All these non-invasive methods have its own limitations, such as non-uniformity of temperature and failure to heat tissues in depth, depending on the nature of tissue response to these radiation interactions. In addition, tumor reoccurrence, skin burns, lesions, and skin puckering also limits these methods from extensive

clinical applications.

3. Heat generation by magnetic field – magnetic hyperthermia

MHT offers an effective approach for attaining therapeutic temperature with the aid of MNPs in presence of external magnetic field. MNPs, also termed as nanoheaters, under an external ACMF convert electromagnetic energy thereby heating tumor area specifically sparing normal cells [Fig. 2 (a)]. MHT is a truly localized therapy employing biocompatible MNPs. Compared to other conventional cancer therapies, MHT effectively generates localized heat which induces cancer cell death. Applied field frequencies utilized during MHT to attain the therapeutic limit are in low radiofrequency range, i.e., at 100–300 kHz [68]. Hauff et al. experimented clinical trials of MHT in brain tumor patients under the applied field frequency of 100 kHz and therapeutic temperature in the range of 42–49 °C [69]. It was found that patients were able to tolerate MNP based MHT in this temperature limit and the applied field parameters with minimal side effects. The utilization of MNPs was initially put forward by Gilchrist (1957) [70]. Maghemite ferromagnetic NPs with particle sizes in the range of 20–100 nm were employed for MHT applications under an ACMF of 1.2 MHz. It has been inferred that MNPs have the excellent ability for heat generation than their bulk counterparts. An in vivo MHT study by Tong et al. [71] proved 40 nm sized IONPs could effectively reach the hyperthermic temperature and selectively heat the tumor tissues with a minimal concentration of MNPs sparing the normal healthy cells. MNPs have unique advantages of magnetic controllability, reduced (nanometer) size and high colloidal stability which make them preferred choice for therapeutic applications. These particles in varying magnetic fields dissipate heat by magnetic losses. Conventionally, two techniques are used to deliver MNPs inside the body. Either delivering MNPs to the tumor vasculature through its supplying artery or by injecting directly into the extra cellular space in the tumor. First method is ineffective in the case of poorly perfused or irregular structured tumors. In such cases, inadequate distribution of MNPs may cause under dosage heating of tumors or overdosage of surrounding tissues. The second method offers the multi-site injection of MNPs to cover the whole tumor region even though it possesses an irregular shape. Owing to the advantageous magnetic and fluidic properties of MNPs, magnetic nanofluids (magnetic colloids) have been attracted for maintaining a stable state in biological media. Application of ferrofluids for HPT treatment was initially conducted by Jordan et al. and Chan et al. during 1993 [72,73]. Uniformly dispersed colloids exhibit an enhanced heating efficiency than poly dispersed ones. Agglomeration as a result of magnetic interactions is negligible in such fluids ensuring the stabilization of colloids since these MNPs are often coated with surfactants or polymers. These magnetic fluids when injected will uniformly get diffused and distributed inside the tumor tissue assuring a successful MFH procedure. The injection volume and the infusion flow rate of these fluids are the two important factors responsible for dispersion and concentration of MNPs within the tissues. The success of MHT strongly lies on certain factors such as (a) minimal concentration of MNPs to be injected for maximal thermal response (b) maximum specific heating power of the MNPs in ACMF at the therapeutic temperature (c) desired magnetic material should be biocompatible. Owing to the immense potentiality featuring attractive magnetic features such as low remanence, low coercivity, high saturation magnetization, fast response to external fields, researchers globally are designing and fabricating multifunctional MNPs which can effectively interact with a variety of bio molecules [74]. MNPs are also utilized as drug carriers when combined with HPT to achieve an enhanced drug release and thermotherapy in a single platform [Fig. 2 (b)]. The therapeutic efficacy of drugs for instance, doxorubicin (DOX) is enhanced when combined with HPT [75]. In addition, MNPs modified with biomimetic cancer cell membrane aids for specific tumor targeting and high internalization ability, makes them suitable for efficient MHT procedure and tumor growth inhibition. A schematic illustration of tumor targeting cell membrane-coated iron based nanorings via homotypic targeting [76] for MHT-mediated tumor ablation is displayed in Fig. 2 (c).

The concept behind the utilization of MNPs for major biomedical applications is the easy penetration and attachment of nano-sized

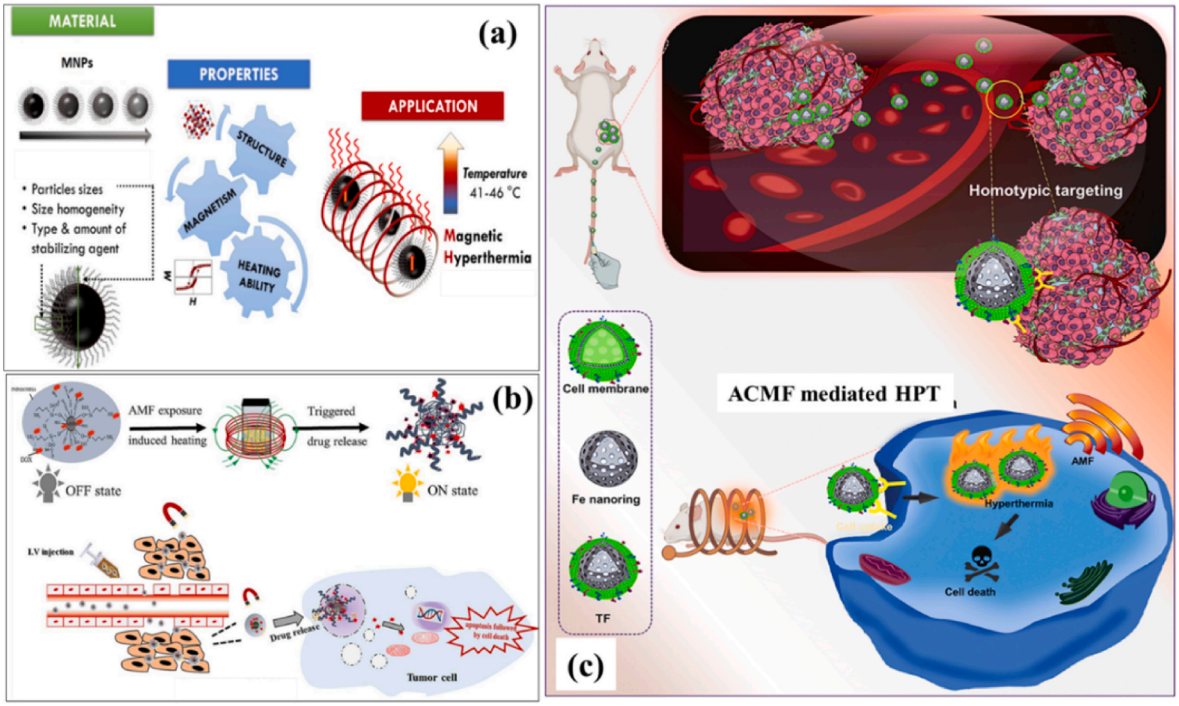

Fig. 2. Schematic representation of (a) MNP-mediated MHT where the targeted MNPs with desired structural and magneto-thermal properties dissipate heat when exposed to an ACMF for selective tumor cell destruction, (b) drug conjugation using MNPs for controlled drug release and thermotherapy [77] and (c) tumor-targeting cell membrane-coated iron nanorings for ACMF-mediated HPT (reprinted with permission from Ref. [76]).

particles throughout the body and exploiting the immense magnetic potentialities such as selective attachment of drugs or to heat a particular tissue which can be easily guided by an external magnetic field. Fabricating such magnetic nano-sized uniform functionalized particles producing a consistent response are necessary for MHT applications. Magnetic properties both intrinsic and extrinsic properties, differ in each magnetic material. Intrinsic properties such as saturation magnetization (M_s), Curie temperature (T_c) and magnetocrystalline anisotropy (K_u) are influenced by the chemical composition and crystalline structure and are considered as the equilibrium properties. Extrinsic properties such as coercivity (H_c), remanence (M_r) are non-equilibrium properties depending on the size, shape and microstructural factors which are related with the magnetic hysteresis. Enhanced magnetization and susceptibilities of MNPs are the vital requirements for potential applications of MHT. MNPs with a higher M_s yields a higher thermal energy loss. For HPT applications, such MNPs are considered more effective as the movement of such particles in blood stream by external field can be easily controlled [78]. The magnetic properties of ferromagnets are greatly influenced by 'temperature'. Entropy effects dominate while increasing the temperature, and thus a reduction in magnetization can be observed. At the curie temperature (T_c), saturation magnetization becomes zero and above this temperature, the material becomes paramagnetic. This ferro to paramagnetic transition has been applied for the HPT applications and such materials are designed in such a way that the required temperature for HPT should match with T_c. However, T_c of most magnetic materials is much greater than the desired HPT temperature (for example, T_c of bulk Fe_3O_4 is 576 °C). The unique feature of ferro-to-paramagnetic transition at T_c is an important intrinsic property of MNPs similar to bulk magnetic materials [79,80]. MNPs offer self-control-temperature favorable for MHT applications. When the temperature of MNPs (generally ferromagnetic NPs) exceeds T_c during MHT treatment, MNPs transform to behave as paramagnetic which cannot be further over-heated even under the continuous application of ACMF. Here T_c acts as the threshold temperature for MHT and T_c acts as a switch to automatically control the temperature of MHT. T_c can be optimized to control the maximum power dissipated by a ferro/ferrimagnetic material at a given temperature when exposed to ACMF in case of MHT application [79]. Tuning physical parameters such as chemical composition, crystal structure, geometric shape, and size of MNPs can reduce high value of T_c favorable for MHT conditions. Biocompatible MNPs with T_c between 42 and 60 °C are the best candidates for effective MHT treatment, as MNPs act as in vivo temperature control switches thereby hindering over-heating [81]. One of the special distinctive features of MNPs from their bulk counterparts are the size dependence magnetic properties. Ferromagnetic materials have different magnetic domains with groups with natural alignment of atomic magnetic moments in a same specific direction pertains. It is interesting to note that the size of NPs is comparable to that of the size of a magnetic domain.

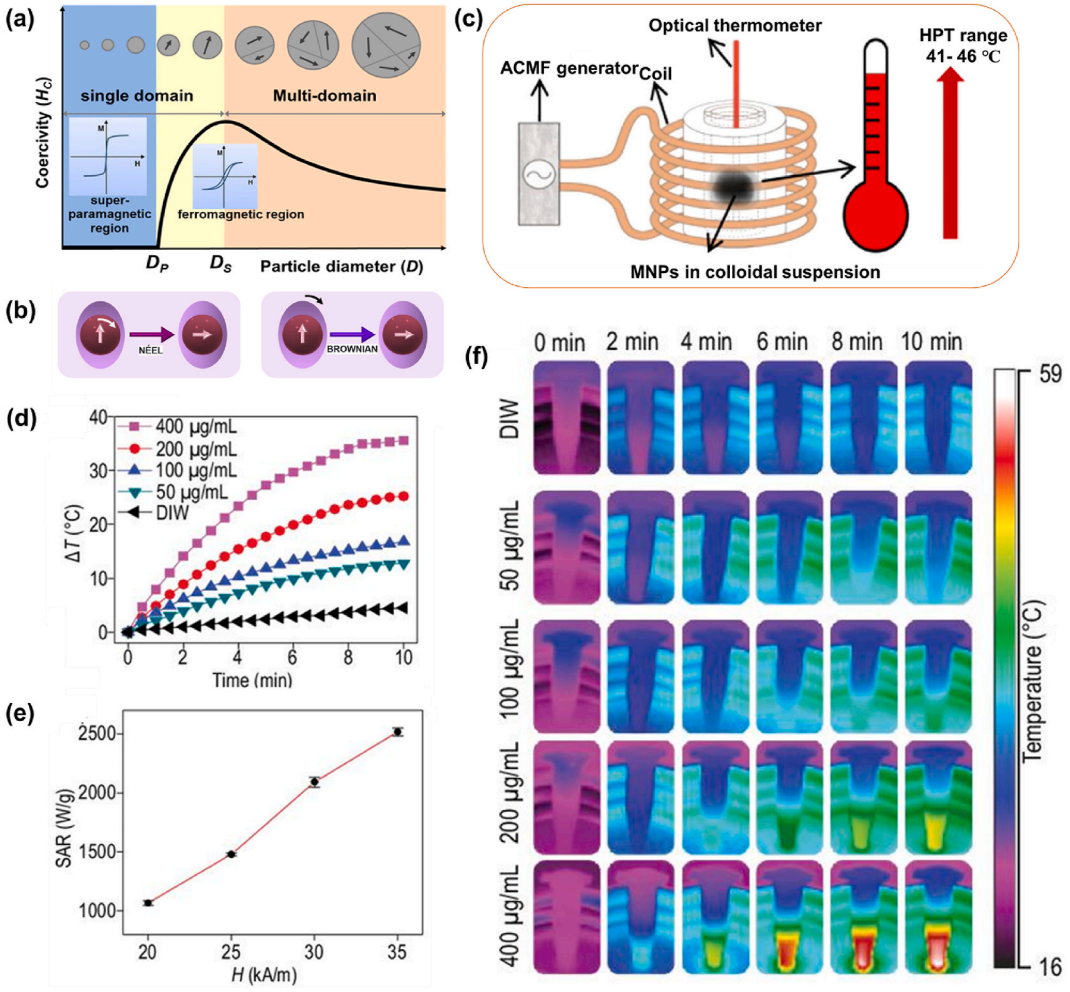

Fig. 3. (a) Multi-domain versus single-domain magnetic materials (reprinted with permission from Ref. [98]), (b) Neel and Brownian relaxation heat generation mechanism under the application of ACMF, (c) experimental apparatus for MHT application (reprinted with permission from Ref. [99], (d) temperature-time profile of IONPs with varying particle concentrations with an ACMF of 312 kHz and 35 kA/m, (e) SAR values of IONPs for varying amplitudes for a particle concentration rate of 200 µg/mL and (f) thermal images of (d) (reprinted with permission from Ref. [97]).

This leads to the occurrence of two pertinent classes such as single-domain superparamagnetic NPs and single-domain ferro/ferrimagnetic NPs [Fig. 3 (a)]. Moreover, MNPs with diameters in the range of 3–25 nm are considered to be superparamagnetic [82–84] and sizes greater than 25–80 nm generally falls under single-domain ferro-/-ferrimagnetic particles [85].

In MHT, thermal energy dissipation by magnetic losses is mainly attributed to two independent mechanisms such as (1) hysteresis heat loss and (2) susceptibility or relaxation heat loss which includes Neel and Brownian relaxation loss. Irreversible magnetization of a magnetic material leads to hysteresis heat loss, a major contribution of heat dissipation during MHT and the optimal heat loss is evaluated from the area of loop. Hysteresis mechanism varies with single and multidomain (bulk) magnets. For a single domain magnet, combined coherent rotation of atomic magnetic moments comprising the material results in hysteresis *i.e.,* only coherent magnetization rotation occurs to overcome the effective anisotropy of the particle whereas for a multi domain magnet, it is due to shifting of domain wall motion resulting a net magnetization. Since domain wall shifting requires a high magnetic field in multi domain magnet, single domain nanomagnets are considered for MHT. In addition, it is proven that single domain NPs are more susceptible to varying magnetic fields as compared to multi domain particles [86]. According to Stoner-Wohlfarth (SW), the total energy (E) of a single domain magnetic particle result from the sum of anisotropy energy (E_A)and Zeeman energy (E_z) given by Ref. [87],

$$E = E_A + E_Z = K_u V \sin^2\theta - HVM_s \cos(\theta - \phi) \tag{1}$$

where K_u is the anisotropy energy, V is the volume of MNP, θ is the angle between the easy axis and magnetization, H is the applied magnetic field, M_s is the saturation magnetization and ϕ is the angle easy axis makes with the applied magnetic field. The factor K_uV referred to the anisotropy energy barrier separating the two energetically equivalent easy directions of magnetization. Anisotropy factor *(K)* varies with anisotropy field H_K, the field required to change the anisotropy, as given by:

$$\mu_0 H_K = \frac{2K}{M_S} \tag{2}$$

where μ_0 is the permeability of free space. If the applied field exceeds the anisotropy field, $H > H_K$, then the magnetization reverses leading to heat generation resulting in an open hysteresis loop. There are certain limits for this applied frequency above which inadequate time results in insufficient attempts to overcome the energy barrier for magnetization reversal. Consequently, no hysteresis loop and no heat will be dissipated.

Since MNPs get filtered via reticular endothelial system (RES) and other biological routes, particles need to be confined to a critical size limit. 10–100 nm sized MNPs are beneficial for easy penetration, and assistance for prolonged retention in physiological environment [38, 88–92]. This confined size regime coincides with single domain superparamagnetic nanostructures. Superparamagnetism is a distinctive characteristic of single-domain magnets dependent on finite size and surface properties that govern magnetic behavior of individual NPs. Magnetization of superparamagnetic materials are much higher (nearly to ferromagnetic materials) than normal paramagnetic materials. A finite particle size of 3–25 nm within the superparamagnetic limit which absorbs much power at biologically tolerated magnetic field strength and frequency, is favorable for attaining higher saturation magnetization, a desired property, for MHT applications [93]. Linear Response Theory (LRT) first proposed by Rosenweig effectively explains the heating mechanism of a system of single domain MNPs in the superparamagnetic regime from a theoretical perspective [94]. According to this theory, thermal energy produced is solely based on the rotational relaxation of non-interacting single domain particles and the resulting magnetization varies linearly with the applied magnetic field. For single domain superparamagnetic nanoparticle suspension, each particle will maintain a constant magnetic moment. At zero magnetic field, the orientation of this moment will be determined by the anisotropy energy barrier, K_uV, of the particle. Under an optimal field, the applied magnetic energy is enough to overcome this energy barrier thereby switching the magnetic moment from the preferred orientation to the direction of applied field and relaxation back to equilibrium releases thermal energy resulting in local heating. This heat dissipation also referred to as susceptibility loss is attributed to the magnetization delay of magnetic NPs during relaxation process. Relaxation can occur in two ways - Neel relaxation (internal spin relaxation) and Brownian relaxation (external particle rotation) [Fig. 3 (b)]. Neel relaxation occurs when the magnetic dipole moment oscillates rapidly within a particle when thermal energy (K_BT) exceeds magnetic anisotropy energy (K_uV). Brownian relaxation is effectuated due to the physical rotation of particle in a dispersed medium. Brownian motion depends predominantly on the medium viscosity. These particle rotations (internal and external) induce a phase lag between magnetic moment direction and ACMF leading to heat loss. Neel motion dominates in the case of smaller sized particles while Brownian motion governs larger particle sizes in viscous fluids. Thus, the thermal energy by Neel motion is due to the rearrangement of dipole moments within the crystal and by Brownian motion is due to shear stress in the fluid medium. Heat loss processes depend on the anisotropy energy of the material and the carrier fluid viscosity of the dispersed medium. In MHT, magnetic fluids (colloidal suspension of MNPs) under external magnetic field produce heat losses only by (i) Neel's spin relaxation (ii) Brownian rotational loss. Thus, the effective relaxation time, τ, can be calculated considering the relative contributions of both Neel and Brownian relaxation denoted by τ_N and τ_B respectively [95] as

$$\frac{1}{\tau} = \frac{1}{\tau_N} + \frac{1}{\tau_B} \tag{3}$$

where

$$\tau_N = \tau_o \, e^{\frac{K_u V}{K_B T}} \tag{4}$$

$$\tau_B = \frac{3\eta V_H}{K_B T} \tag{5}$$

Equation (4) represents the Neel relaxation time where K_u is the anisotropy constant, V is the volume of MNP, K_B is the Boltzmann's constant, T is the temperature, τ_0 is in the range of 10^{-13}–10^{-9} s [96]. Equation (5) represents the Brownian relaxation time where $V_H = \frac{\pi (2+\delta)^3}{6}$, is the hydrodynamic volume (including the ligand layer thickness, δ) and η is the viscosity of the medium.

One of the main aspects of superparamagnetic single domain NPs is the characteristic time scale for thermally activated switching of magnetic moments. When the magnetic field reversal time is less than the magnetic relaxation times of particles on exposure to an AC magnetic field, heat will be dissipated due to the delay in the relaxation of the magnetic moment through either Brownian or Neel relaxation. The relaxation time depends on the particle diameter. Therefore, from the LRT model, an expression for the total power (heat) dissipated in relation with a strong dependence of the applied frequency and amplitude can be expressed as:

$$P = \mu_0 \pi \chi'' f H^2 \tag{6}$$

where f,H are the frequency and amplitude of the applied field and χ'' is the out-of-phase component or the imaginary part of susceptibility (loss component of susceptibility). [Since susceptibility ($\chi = M/H$) is expressed as a complex number; $\chi = \chi' - i\chi''$]. The mentioned loss component of susceptibility χ'' represents a phase lag of magnetization, M, with time varying field, H due to the thermal motion of the particle's magnetic moment. It can be also interpreted as the portion of magnetization which is in quadrature with the applied magnetic field. This lag

contributes the conversion of magnetic work ($dW = H.dM$) into internal energy. The effective time relaxation in relation with susceptibility can be now expressed as:

$$\chi'' = \left[\frac{\omega\tau}{1+(\omega\tau)^2}\right]\chi_0 \tag{7}$$

where angular frequency, $\omega = 2\pi f$, χ_0 is the initial static susceptibility and τ is the effective relaxation time. Heat relaxation dominates or the loss component of susceptibility χ'' is maximum when the relaxation time of the particle is equal to the field frequency as $\omega\tau = 1$.

Modified power dissipation equation can now be expressed as:

$$P = \mu_0\pi\chi_0 f H_{max}^2 \frac{2\pi f\tau}{1+(2\pi f\tau)^2} \tag{8}$$

where the initial susceptibility,

$$\chi_0 = \frac{\mu_0 M_s^2 V}{K_B T}, \tag{9}$$

Hence, equation (9) becomes,

$$P = \frac{\pi\mu_0^2 f H_{max}^2 M_s^2 V}{K_B T}\frac{2\pi f\tau}{1+(2\pi f\tau)^2} \tag{10}$$

Heating efficiency or power dissipation responsible for MHT is calculated in terms of specific absorption rate/specific loss power (SAR/SLP). SAR/SLP is defined as the absorbed power or the power loss normalised by the mass of MNPs under an ACMF at certain frequency and intensity. SAR values can be conveniently evaluated from predetermined Brownian and Neel relaxation times using LRT model. Higher the SAR value, higher is the heat generated. SAR maximizes when $\omega\tau = 1$ as the applied frequency must be in correlation with the relaxation time. This may not be true in certain cases until the relaxation time matches with the magnetic frequency. A stable colloid in equilibrium results in enhanced hysteresis losses due to the spontaneous effects of particle rotation (Neel and Brownian) leading to higher SAR.

$$\text{SAR} \Big/ \text{SLP} = \frac{P(f,H)}{\rho_{MNP}} = \frac{\pi\mu_0\chi'' H^2 f}{\rho_{MNP}} \tag{11}$$

where P is the heat power dissipated and ρ is the mass density of the magnetic NPs [11]. From the above equation, it is evident that SAR vary linearly with the applied magnetic field frequency and are proportional to the square of magnetic field intensity as $P \propto H^2 f$.

SAR values can be experimentally determined by two methods viz. magnetometric and calorimetric method [95]. SAR values can be interpreted from the area enclosed by the hysteresis loop through the magnetometric method. Calorimetric method is the most commonly used method in which SAR is measured in terms of the temperature increase of the colloidal suspension exposed to AC magnetic field.

$$\text{SAR} = C_s * \frac{dT}{dt} * \frac{M_{sol}}{M_{mnp}} \tag{12}$$

where, C_s is the specific heat capacity of the colloidal solution, M_{sol} is the mass of solvent used, M_{mnp} is the mass of the MNPs, and $\frac{dT}{dt}$ is the initial slope of the temperature variant versus time interval. Besides SAR, intrinsic loss power (ILP), is an effective parameter for evaluating the heating ability with respect to ACMF parameters (frequency and amplitude) which is calculated as follows:

$$\text{ILP} = \frac{SAR}{H^2 f} \tag{13}$$

Fig. 3c shows a representative image of MHT experimental apparatus where MNPs in colloidal form are placed within the designed coil. Fig. 3 (d, e and f) exhibits representative images of (d) temperature rise versus time curves (experimentally obtained) of IONPs with varying particle concentrations with an ACMF of 312 kHz and 35 kA/m, (e) calculated SAR values [using equation (12)] of IONPs for varying amplitudes for a particle concentration rate of 200 μg/mL (highest SAR of 2518 W/g at 35 kA/m was achieved) and (f) infrared thermal images corresponding to Fig. 3d of the IONPs dispersion with varying concentrations, confirming the magneto-thermal heating performance [97].

4. Use of iron oxide nanoparticles as thermal nanomedicine in MHT

Spinel metal–oxide NPs of MFe_2O_4 (where M = Mn, Co, Fe, Ni or Zn) and metallic alloys of $A_{1-x}B_x$ (A, B = Fe, Pt, Pd, Co, Ni and x = mole percentage) have attracted plenty of attention in various biomedical fields due to their remarkable size and shape dependent magnetic properties [100–102]. The properties of MNPs are strictly related to size, shape, composition and structure, which are governed by polymer-based modification during fabrication. Some of the common synthesis methods for the formation of MNPs with controlled parameters are co-precipitation, solvothermal, microemulsion, thermal decomposition and sol–gel method [103]. Among MNPs, iron oxide maintains a stable magnetic response and exhibits less oxidation effects compared to other pure metals such as Fe, Co, and Ni [104]. Moreover, these materials possess better chemical stability, lower toxicity and biodegradability. Surface modification is necessary using suitable biocompatible polymers for improved colloidal stability, extended blood circulation and minimal toxicity. IONPs inside the body can be metabolized with heme oxygenase-1 to produce hemoglobin and have the ability to expel from the body [105]. Among IONPs, magnetite (Fe_3O_4) has been empowered as a bioactive therapeutic agent for MHT [106–109] owing to its superior biocompatibility, tunable magnetic properties and excellent chemical stability. Magnetite displays the strongest magnetism of all the natural minerals existing on the Earth. Iron atom has four unpaired electrons in 3d orbital, therefore possess a strong magnetic moment. Magnetite is a black ferrimagnetic mineral with iron contents in two oxidation states, i.e., Fe^{2+} and Fe^{3+} denoted by Fe_3O_4. Magnetite differs from other phases of iron oxide as it constitutes both di and tri-valent iron cations. Iron oxides by its chemical structure are in closed pack hexagonal or cubic lattices, in which partial filling of interstitial sites by Fe^{2+} or Fe^{3+}, commonly in octahedral positions and some cases with a tetrahedral geometry. Crystal geometry of magnetite (Fe_3O_4) is different from other forms of iron oxides due to the presence of both divalent as well as trivalent iron ions. These ferrimagnetic structures constitute metallic cations in two sublattices which are antiferromagnetically coupled. Because of different site occupancies in the sublattices, ferrites display a net magnetic moment. The iron and oxygen ions form a face-centered cubic (fcc) crystal system and the oxygen ions are in the cubic close-packed arrangement i.e., it form a close-packed cubic lattice with the iron ions located at interstices between the oxygen ions. Magnetite has an inverse spinel structure with a unit cell consisting of 32 oxygen ions in a fcc structure [110]. Unit cell of 32 oxygen (O^{2-}) ions is arranged along (111) plane with a cell parameter of 0.839 nm. In the inverse spinel structure, half of the Fe^{3+} cations (8 ions) occupy all the tetrahedral sites (A-type) and the remaining half of Fe^{3+} (8 ions) and Fe^{2+} (8 ions) cations occupy the octahedral sites (B-type) with a stoichiometry Fe^{3+}/Fe^{2+} of 2 [Fig. 4 (a)]. This is represented as $(Fe^{3+})_{tet}[Fe^{2+}Fe^{3+}]_{oct}O_4$. The ferrimagnetic order results from antiferromagnetic coupling between A and B type cations. The Fe^{2+}cations in Fe_3O_4 can be substituted with other metal cations, which produce different types of metal ferrites. Changes in ferrite compositions affect the heating mechanism accordingly. Spinel metal oxide ferrite NPs such as $CoFe_2O_4$, $NiFe_2O_4$, $ZnFe_2O_4$, $CuFe_2O_4$, $MnFe_2O_4$, zinc manganese–doped iron oxides and gadolinium–doped iron oxides have also been considered for achieving higher heating efficiency for HPT [111–118]. Incorporating rare-earth (RE) ions such as gadolinium, cerium, erbium or yttrium into IONPs have exhibited much-improved MHT performance in comparison to bare IONPs [119–122]. However,

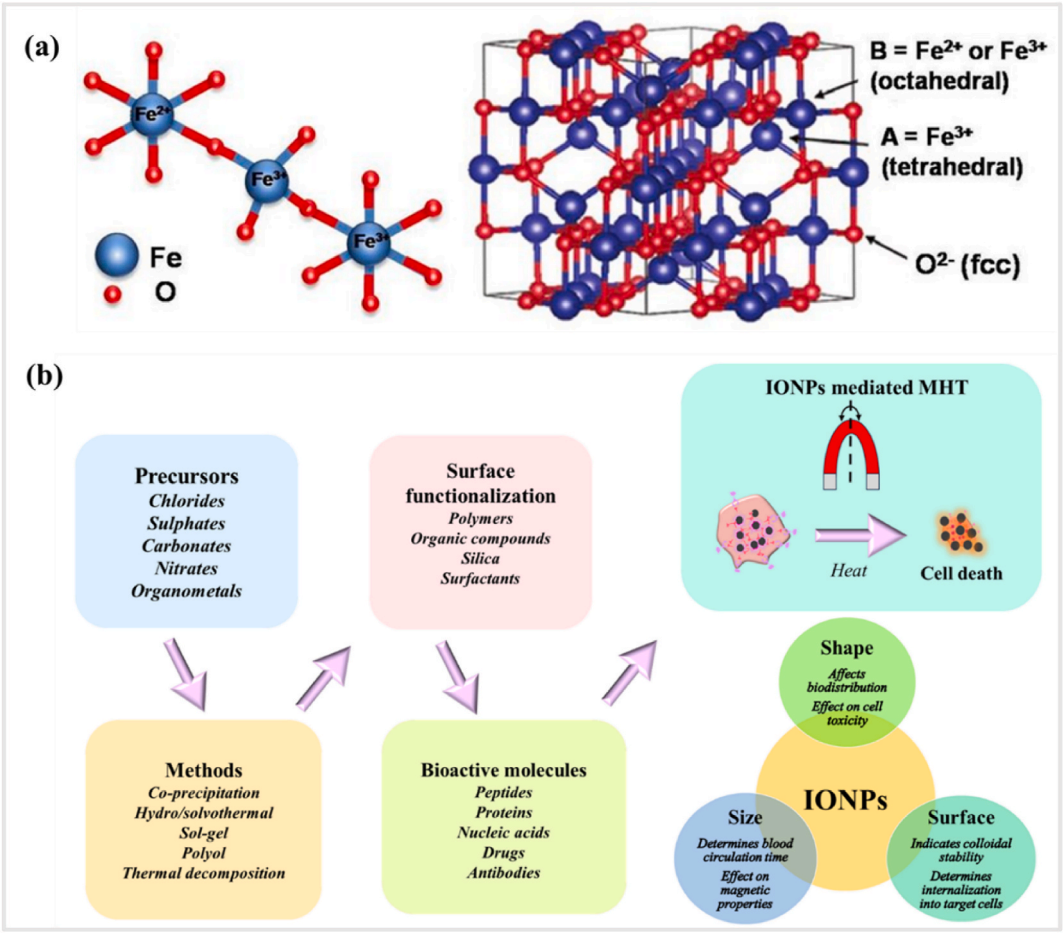

Fig. 4. (a) Inverse spinel fcc crystal structure of magnetite (reprinted with permission from Ref. [110]) and (b) schematic showing the various process of synthesis and surface modification of IONPs for MHT.

toxicity investigation in vivo models with different ferrite compositions are still limited, in comparison with cost-effective and simple in vitro analysis [123].

Expanded investigations in MHT focusses on superparamagnetic iron oxide nanoparticles (SPIONs) due to its biocompatibility, self-heating ability, high magnetic response to release heat and high versatility. SPIONs have the advantageous property of colloidal stability as it prevents agglomeration leading to the formation of embolus in the capillary vessels which makes them appropriate for HPT applications. SPIONs could be easily functionalized and guided within biological entities by an external magnetic field. At thermal equilibrium, SPIONs obey the Langevin's theorem of paramagnetism by exhibiting elevated saturation magnetization and susceptibility upon ACMF application and complete de-magnetization with the field removal. This results in zero remanence and zero coercivity as magnetic moments reverse back to their original easy axis thereby leading to random orientation of grains. This innate property of SPIONs can be effectively utilized for HPT applications. Accordingly, SPIONs when introduced to tumor tissues exhibit feeble magnetic dipolar interactions between particles, eventually preventing aggregation and avoiding detrimental conditions resulting thrombus formation in cardiovascular system. SPIONs approved by EMA have paved way for the first human MHT trial [124]. Intravenously administered SPIONs have the ability to get expelled from the reticulo endothelial system (RES) of the liver, spleen, lymph and bone marrow without creating any adverse toxic effects. Clinical studies have revealed that SPIONs can be precisely targeted to achieve an appropriate intratumoral deposition inducing controlled heating to therapeutic temperatures with minimal side effects. SPIONs when conjugated with organic dyes or with some semiconductor quantum dots enhance the theranostic efficacy. This multifunctional theranostic nanohybrid would find promising application in MRI as well as in MHT [125,126].

Heating performance of MNPs is inherently entwined with intrinsic factors such as size, shape, composition and magnetic anisotropy and extrinsic factors such as dosage of MNPs, medium viscosity and ACMF parameters (amplitude and frequency). Heating efficacy strongly correlates with the magnetic properties of MNPs such as magnetization and coercivity, which in turn depend on size. It is crucial to gain insights into these factors for an improved SAR for therapeutic applications.

Tuning size, shape, composition and surface modification are the major parameters to be focused while designing MNPs suitable for MHT. Localised heating of targeted cells and cellular uptake during MHT therapy relate to the finite size-dependent properties of MNPs. MNPs in the size limit of 10–100 nm are considered to be favorable for easy penetration and prolonged blood circulation time [91]. MNPs $<$10 nm size will be quickly eliminated via renal clearance; on the contrary NPs $>$200 nm size will lead to phagocytic uptake, both being unfavorable for therapeutical efficacy [92,127–131]. However, MNPs within superparamagnetic (SPM) size regime of 3–25 nm [82–84] are regarded as suitable candidates for MHT and exhibit superior magnetic properties leading to an improved SAR. Heat dissipation mechanisms such as Néel and Brownian relaxation losses are predominant in SPM size regime particles. Beneath the size range ($<$3 nm), spin canting phenomenon predominates resulting in a reduced magnetization and hence a minimized SAR. Shape of the NPs holds a profound impact to fine-tune the magnetic anisotropy which is an appropriate choice for an improved magnetic response and an enhanced SAR. On exposure to ACMF, SPM

NPs get magnetized equally along one of its easy axes. A high anisotropy energy arising from interaction of magnetic moments, is required to reroute the magnetic moment from easy to hard direction in a single crystal. Magnetic anisotropy cannot be altered easily since it is an intrinsic factor. In the context of MHT applications, the efficacy of MNPs can be enhanced by fine-tuning the anisotropy. Optimizing the anisotropy of MNPs is an appropriate choice for an improved magnetic response and an enhanced SAR. Magnetic anisotropy arises from the collective contributions of (a) magnetocrystalline anisotropy (MCA), (b) shape-surface anisotropy and (c) exchange anisotropy. In case of MNPs, MCA contribution is weak when compared to other anisotropies. Shape and surface anisotropy play a key role for the effective magnetic anisotropy of MNPs particularly in soft ferrites [132,133]. Exchange anisotropy occurs in exchange coupled nanostructures (core-shell) arising from the magnetic interaction across an interface between two magnetic materials with different magnetic ordering. IONPs with different morphologies can be fine-tuned for an enhanced heating performance pertinent for MHT applications. For instance, cube shaped IONPs self-accumulate to develop closely packed chain-like formation, which are capable of changing effective anisotropy leading to a higher SAR when compared to spherical counterparts [134]. Similarly, a highest SAR of 200 W/g for cube shaped FeO/Fe_3O_4 NPs in comparison with spherical shaped ones of same composition is reported [132]. In this work, surface anisotropy along with shape anisotropy contributed to the total effective magnetic anisotropy, which resulted in an enhanced SAR. Boubeta et al. [133] investigated chain-like arrangement of biomimicking magnetotactic bacteria which was proved for enhanced heating performance when aligned with respect to ACMF. This multiplicative heating effect is due to the reorientation of chains under applied ACMF. Serantes et al. [135] proved that the assembling of IONPs into chains with a uniaxial anisotropy is the way to reach the maximum possible SAR. Later, rod shaped NPs has been reported to achieve improved SAR of 862 W/g in comparison with cubes (314 W/g) and spheres (140 W/g) according to Das et al. [136] and proved and proved unidirectional shape anisotropy in rod shaped NPs lead to SAR enhancement. These experimental results unfold the relevance of shape anisotropy in maximizing the MHT performance of MNPs [137–141]. Apart from magnetic anisotropy, magnetic interactions between particles are also crucial in the magnetic behavior of NPs. Such interactions produce aggregation/agglomeration eventually leading to enhanced SAR [142], which need to be hindered prior to MHT applications. In such cases, MNPs do not rotate (magnetic spins in freezed state) under the magnetic field to dissipate heat via magnetic losses as they are considered as large entities. Hence, MNPs should be surface modified with biocompatible surfactants in order to minimize magnetic exchange-coupling effect and magnetic dipolar interactions for a better half-life of MNPs and lower toxicity inside the human body.

Relevant surface functionalization on IONPs using hydrophilic biocompatible coating materials is requisite for improving the biological interactions. Bare IONPs on exposure to physiological environment pose a tendency to aggregate and oxidize owing to its high reactivity. Surface functionalization avoids colloidal agglomeration, destabilisation, opsonisation and non-specific cellular uptake which can influence their orientation under an ACMF. Such surfaces improve colloidal stability which assist in directing IONPs towards target cancer sites with minimum direct exposure to the biological media. Surfaces of IONPs are modified commonly using biocompatible surfactants such as polymers/non-polymers/biomolecules [143–147] which act as a protective coating enabling a suitable attachment with tumor surface receptors. These coatings not only avoid aggregation but also alters the surface chemistry of IONPs propitious for meliorating the biological interactions (with proteins, cells or tissues) in the physiological environment. Apart from these, surface functionalization improves steric as well as electrostatic repulsion within NPs to prevent self-aggregation and surface oxidation. This modification can further improve cellular uptake, target specificity, cellular proliferation and viability and opsonization prevention before biological interactions. In case of core-shell structured IONPs, modified surfaces can diminish exchange coupling effect and short-range magnetic dipolar interactions within the NPs. Commonly used biocompatible coatings for IONPs useful for biomedical applications are PEG and its derivatives [148]. In addition, utilization of biocompatible surfactants is pertinent to synthesize monodisperse NPs to attain colloidally stable ferrofluids beneficial for MHT.

Moreover, cellular uptake properties have a profound impact on the MHT heating efficiency when MNPs are localized inside cells or tissues [149]. MNP interaction with cells depends on certain factors encompassing size, surface coatings, surface charge, and binding with biological molecules which critically influence the in vivo pharmacokinetics and biodistribution [150–152]. IONPs with a size of 10–100 nm and with a neutral surface charge facilitate for longer circulation time and reduced uptake by the phagocyte system due to decreased opsonization, compared to positive or negative surface charge [91]. One of the primary challenges for a specific distribution and localization to enhance the therapeutic efficiency is to prolong the MNPs blood circulation duration to facilitate target-tissue accumulation. Generally, IONPs are administrated to the tumor sites via passive targeting. The main clearance pathways are via liver as well as spleen in the RES system and it is crucial to avoid the sudden uptake by this system to improve the retention time of IONPs [153]. Opsonization, a major factor which hinders the therapeutic efficacy, is a phenomenon by which blood plasma opsonin proteins adsorb to the surface of IONPs when exposed to blood media. Cabrera et al. [154] reported the reduction of heating efficiency due to the presence of intracellular IONP clustering compared to intracellular IONPs immobilization. Opsonization leads to receptor mediated phagocytosis by macrophages and other phagocytic cells resulting in an enlarged hydrodynamic size of NPs which favors rapid hepatic clearance [152]. These adverse outcomes can be prevented via surface modification strategies using biocompatible hydrophilic polymers to form a protective barrier against protein corona formation and augments the cellular uptake of IONPs [155]. Therefore, a thorough understanding of cell uptake properties is vital to utilize MNPs as efficient heat mediators. A schematic illustration of distinctive precursor salts as well as coatings or bio molecules for fabrication and surface modification of IONPs for MHT is displayed in Fig. 4 (b). Table 1 exhibits summary of studies conducted using surface modified ferrites for MHT in terms of SAR upon varying magnetic field parameters (magnetic field frequency and amplitude).

5. Biological mechanism underlying MHT induced cancer cell death: ROS and LMP

MNPs get internalized into the cells via endocytosis process which involves a number of processes such as clathrin-mediated endocytosis, caveolin-mediated endocytosis, macropinocytosis, phagocytosis and membrane fusion are the basic mechanisms involved during the endocytosis process [184–187]. Following the endocytosis pathway, MNPs are confined inside endocytic vesicles which mature into early endosomes, late endosomes and lysosomes. Endocytosed MNPs are finally destroyed in lysosomes or get recycled towards the cell membrane. However, this entrapment limits the therapeutic efficiency of MNPs [188]. These MNPs therefore must be released from endocytic vesicles to escape from degradation or recycling. Endosomal escape of MNPs is a vital mechanism required for the selective transport of MNPs focusing on intracellular target [189,190]. Nontoxic, biodegradable and biocompatible endosomal escape agents such as peptides, proteins, toxins, polymers or small chemical molecules such as chloroquine are being employed during the synthesis process of MNPs, for the endosomal escape of MNPs for biomedical applications [191]. Fusion of endosomal escape agent with lysosomes (acidic and presence of hydrolytic enzymes) breaks the endosomal membrane, which further contributes towards cytotoxicity.

MHT exploiting MNPs effectively generates localized heat which

Table 1
Recent works of surface modified ferrites used for MHT in terms of SAR upon varying magnetic field parameters (magnetic field frequency and amplitude).

Types of Ferrites	Stabilizers	Synthesis method	Particle factors		ACMF product limit (f x H) (10^9 A/ms)	SAR (W/g)	ILP (nHm^2/kg)	Ref.
			Size (nm)	Shape				
Fe_3O_4	Dextran	Solvothermal	17.609 ± 2.44	Sphere	5.01	233.28	3.12	[156]
Fe_3O_4	PEG	Thermal decomposition	19	Cube	15	2452	5.6	[141]
Fe_3O_4	Citric acid	Co-precipitation	10.9 ± 2.6	quasi-spherical	4.8	170	0.73	[157]
Fe_3O_4	Ammonium bicarbonate	Polyol	8.69 ± 1.44	nearly-spherical	6.6	69.6 ± 5.2	0.613 ± 0.051	[158]
Fe_3O_4	Graphene oxide	Thermal decomposition method	45	Cluster form	13	5020	12.21	[159]
Fe_3O_4	Oleic acid	Solvothermal	31.09	Rod	2.4	228.51	4.3	[160]
Fe_3O_4	Polycaprolactone	Co-precipitation	15.67	sphere	4.17	85.4 ± 3.9	0.62	[161]
Fe_3O_4	Polyethylene glycol	Co-precipitation	12.2	–	21	145.84	0.24	[162]
Fe_3O_4	Oligonucleotides	Seeded-growth thermal decomposition	23 ± 3	Flower	4.8	1540	13.4	[140]
$CoFe_2O_4$	Chitosan	Solvothermal	14.2	sphere	5.028	179.5	2.3	[163]
$CoFe_2O_4$	Citric acid	Co-precipitation	15 ± 1	Core-shell	7.15	135.2	1.19	[164]
$CoFe_2O_4$	Citric acid	Hydrothermal	9 ± 4.3	sphere	14.2	297	0.46	[165]
$CuFe_2O_4$	Dextran	Solvothermal	19.3 ± 1.0	Chain-like	5.02	591.3	1	[166]
$CuFe_2O_4$	–	Co-precipitation	45.02	Nearly-spheroid	5.04	162	2.1	[167]
$NiFe_2O_4$	Graphene oxide	Solvothermal	12.87	Cubic-octahedron	7.25	15	0.08	[168]
$NiFe_2O_4$	Polyvinylpyrrolidone	Co-precipitation	17.26	quasi-spherical	4.49	54.71	0.9	[169]
$MnFe_2O_4$		Polyol method	10.7 ± 2.0	sphere	5.5	32.8 ± 3.5	0.3 ± 0.04	[114]
$MnFe_2O_4$	Chitosan	Co-precipitation	10.4	Irregular	1.4	129.1	4.6	[170]
$MnFe_2O_4$	Sodium oleate	Co-precipitation	9.6	Irregular	4.04	510	14.4	[171]
$MnFe_2O_4$	Polyethylene glycol	Solvothermal	25.81 ± 1.78	quasi-cubic	11.3	296	0.73	[172]
$ZnFe_2O_4$	–	Hydrothermal	42.4	Irregular	3.2	70.2	0.68	[173]
Cu-$CoFe_2O_4$	Chitosan	Solvothermal	10.7 ± 0.91	sphere	5.02	446	5.9	[174]
Zn-$MgFe_2O_4$	Oleic acid	Sol-gel	45.16 ± 2.5	Core-shell	9.2	112	1.17	[175]
Mn-$ZnFe_2O_4$	Oleic acid	Solvothermal reflux	12	–	11.1	107.79	0.27	[176]
Mn-$ZnFe_2O_4$	Lauric acid	Co-precipitation	11.7 ± 0.5	sphere	4.1	105.55	2.03	[177]
Zn-Mg-$CuFe_2O_4$	Oleic acid	Solvothermal reflux	13	sphere	11.1	127.88	0.32	[178]
Ni-$MgFe_2O_4$	Oleic acid	Solvothermal reflux	10	sphere	11	328.64	0.83	[179]
Co-$NiFe_2O_4$	–	Sol-gel	20.8	cube	4.9	22.90	0.4	[180]
Zn-doped $CoFe_2O_4$	Polyvinyl alcohol	Hydrothermal-assisted co-precipitation	15.2	–	2.9	25.25	0.35	[181]
Zn-$NiFe_2O_4$	Oleic acid	Solvothermal reflux	10	sphere	11	410	1.04	[182]
Ni-$ZnFe_2O_4$	Citric acid	Sol-gel	8.2	sphere	11	131.5	0.69	[183]

induces cancer cell apoptosis (programmed cell death) via various mechanisms such as thermal stress, protein denaturation, oxidative damage, and mitochondrial dysfunction [192]. Localized increase in temperature creates thermal stress within cancer cells, disrupting the normal cellular functions and signalling pathways, leading to cell death. In addition, this elevated temperature causes proteins to unfold or misfold, impairing their function. HSPs may be activated, but excessive heat can overcome these protective mechanisms, leading to cell damage. Although the exact pathways leading to cell killing during MHT are still not fully understood, it appears that protein denaturation is crucial in such process. Heat can stimulate the production of ROS, which damage cellular components, including lipids, proteins, and DNA [193]. High ROS levels can trigger apoptotic pathways. The heat-induced stress can disrupt mitochondrial function, leading to the release of pro-apoptotic factors (e.g., cytochrome *c*) into the cytosol, activating caspases that initiate the apoptotic process [194] termed as mitogen-activated protein kinase (MAPK) pathway, which is one of the signaling pathways that ROS can activate. Increased temperature can affect the integrity of cellular membranes, leading to increased permeability and the release of apoptotic signals.

The two major mechanisms responsible for MHT induced cancer cell death are ROS generation and LMP. IONPs with enhanced magneto-thermal properties and ROS generation ability serve as potential nanomedicine for non-invasive localized ferroptosis induced cancer treatment [Fig. 5 (a)]. Iron ions play a crucial role in ferroptosis as well as in MHT where the combination of two therapies is anticipated to significantly amplify the therapeutic effects of tumors [195]. Ferroptosis is a form of regulated cell death, depending on Fe ions and intracellular ROS generation. In the presence of H_2O_2, ferrous (Fe^{2+}) ion catalyzes the Fenton reaction, producing hydroxyl radicals (•OH), a highly reactive form of ROS. These hydroxyl radicals are capable of attacking poly-unsaturated fatty acids present in cellular membranes, leading to lipid peroxidation process. This process generates lipid peroxides, which further contributes to cell damage and can propagate oxidative stress. Lipid peroxides can decompose to generate additional ROS, creating a vicious cycle that intensifies oxidative damage. This amplification is crucial in promoting ferroptosis, as elevated levels of lipid peroxides are characteristic of this form of regulated cell death. In certain cases, excessive ROS leads to mitochondrial dysfunction, further amplifying oxidative stress and contributing to the ferroptotic process. Hence, ferroptosis not only leads to cell membrane damage via lipid peroxidation but also amplifies oxidative stress, driving the ferroptotic cell death pathway [196]. The detailed reaction mechanism of ROS generation in ferroptosis is as follows:

Fenton reaction starts with the oxidation of ferrous to ferric ions in the presence of hydrogen peroxide (acts as an oxidizing agent), to form

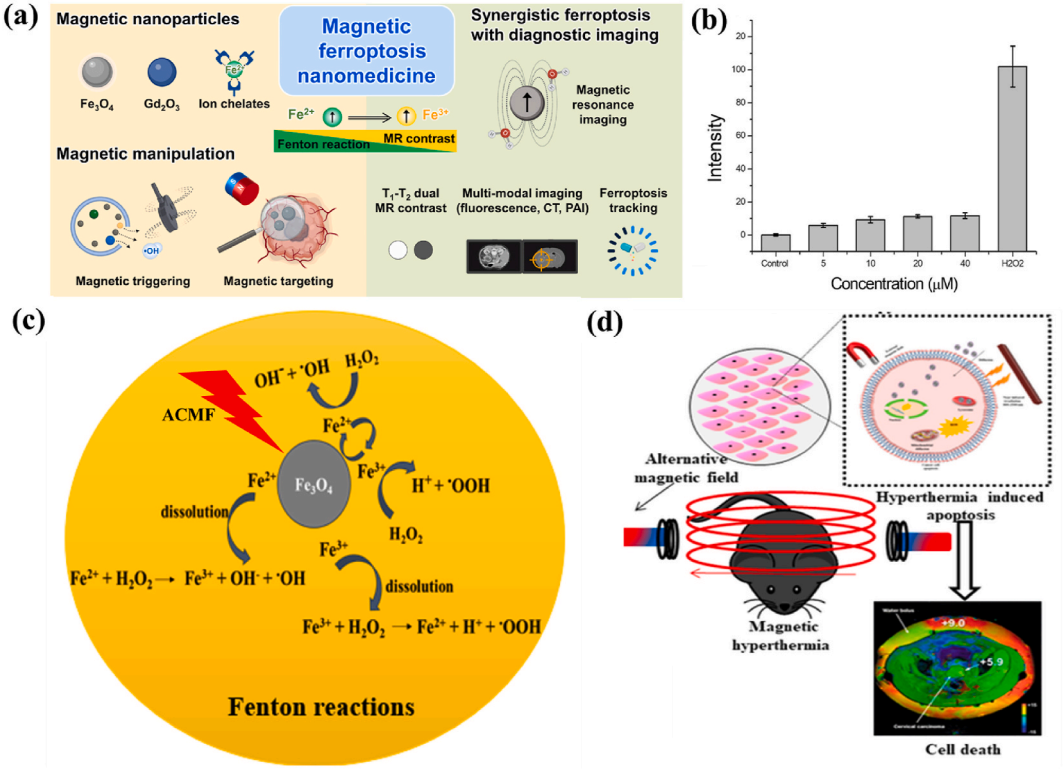

Fig. 5. (a) Multifunctional theranostic MNP-mediated ferroptosis cancer nanomedicines (reprinted with permission from Ref. [205]), (b) quantification of ROS generated from IONPs evaluated by DCFDA assay (H_2O_2 as positive control) (reprinted with permission from Ref. [198]), (c) role of IONPs towards ROS generation in the presence of an ACMF via Fenton reaction and (d) MHT induced apoptosis due to ROS generation for targeting cancer (reprinted with permission from Ref. [203]).

byproducts such as a hydroxide (OH^-) ion and a highly toxic hydroxyl ($^{\bullet}OH$) free radical (equation (14)). Fe^{3+} ion reduces back into Fe^{2+}ion in the presence of another H_2O_2 molecule, which results in hydroperoxyl (•OOH) free radical, Fe^{2+}ion and a proton (H^+) (equation (15)). The presence of ferric ions with H_2O_2 facilitates the disproportionation of H_2O_2 molecules thereby resulting for the formation of highly toxic free radical species. •OH and •OOH radicals are formed due to the splitting of O–O bond in H_2O_2 either by absorbing an electron or by ejecting an electron. Oxidation–reduction pair Fe^{2+}–Fe^{3+} serves as the electron donor and acceptor in these reactions. •OOH radical is very weak, hence give rise to superoxide radical (O_2^-) when it loses a proton (equation (16)). This superoxide radical reduces H_2O_2 to form •OH radicals, leads to Haber-Weiss reaction (Equation (17)) [197].

$$Fe^{2+} + H_2O_2 \rightarrow Fe^{3+} + OH^- + \bullet OH \quad (14)$$

$$Fe^{3+} + H_2O_2 \rightarrow Fe^{2+} + H^+ + \bullet OOH \quad (15)$$

$$\bullet OOH \rightarrow H^+ + \bullet O_2^- \quad (16)$$

$$\bullet O_2^- + H_2O_2 \rightarrow O_2 + OH^- + \bullet OH \quad (17)$$

Nazeer et al. quantified intracellular ROS generation due to IONPs on HepG2 cancer cells [198] using 2′7′-dichlorodihydrofluorescein diacetate (serve as a cell permeable probe) as shown in Fig. 5 (b). A basal level of fluorescence signals generated from ROS production due to IONPs concentrations up to 40 μM was observed, which proves the ability of IONPs for killing cancer cells.

ROS generation can be enhanced under the application of external magnetic field providing a synergistic effect of thermal stress and ROS generation for cancer cell death i.e., the heat generated from MHT could potentially induce ferroptosis in cancer cells by promoting lipid peroxidation and affecting iron metabolism [199,200]. This enhanced effect leads to an efficient internalization and significant apoptosis. In addition, abundant generation of ROS are able to mitigate the thermal resistance in HPT [193]. At the HPT range of temperature, ROS levels are amplified resulting in long-term cellular death. This observation can be attributed to increased kinetic activity of the Fenton-like reaction with temperature or the decreased ability of cancer cells to scavenge ROS at the elevated temperature. Sola-Leyva et al. [201] reported ROS production in HepG2 human hepatoma cells induced by the incorporation of biomimetic MNPs with MHT application. Intracellular ROS production was found to be higher in cells when incubated with MNPs + ACMF stimulation whereas negligible ROS was found in cells exposed with NPs alone. Hauser et al. [202], studied the effect of dextran-coated IONPs with TAT peptide functionalization on A549 and H358 cells. The results show significant increase in percentage cell death by ROS generation in the presence of ACMF compared to the control. Fig. 5 (c) depicts a schematic illustration representing the role of magnetite (Fe_3O_4) NPs towards ROS generation in the presence of an ACMF via Fenton reaction and Fig. 5 (d) represents MHT induced apoptosis due to IONPs [203].

LMP, a potential anticancer practice in apoptosis-resistant cancer tissues, is one of the other mechanisms for inducing lysosomal-dependent cell death. Lysosomes are membrane-bound organelles comprising enzymes involved in cellular digestion and waste degradation. LMP occurs when the lysosomal membrane is damaged, leading to the release of these enzymes into the cytoplasm. This event can trigger various cellular responses such as cell apoptosis or necrosis. LMP indeed plays certain role in MHT cell death. Upon an external ACMF, MNPs when immobilized in cells specifically heats the area leading to lysosomal damage and hence LMP to occur. High concentrated MNPs within lysosomes produces hot spots which damages or permeabilize the lysosomal membrane [Fig. 6 (a)]. The release of lysosomal enzymes into the cytoplasm triggers the apoptotic pathways or cause direct damage to cellular structures, ultimately leading to cell death. A schematic illustration of LMP by targeted and non-targeted MNPs in an ACMF is shown

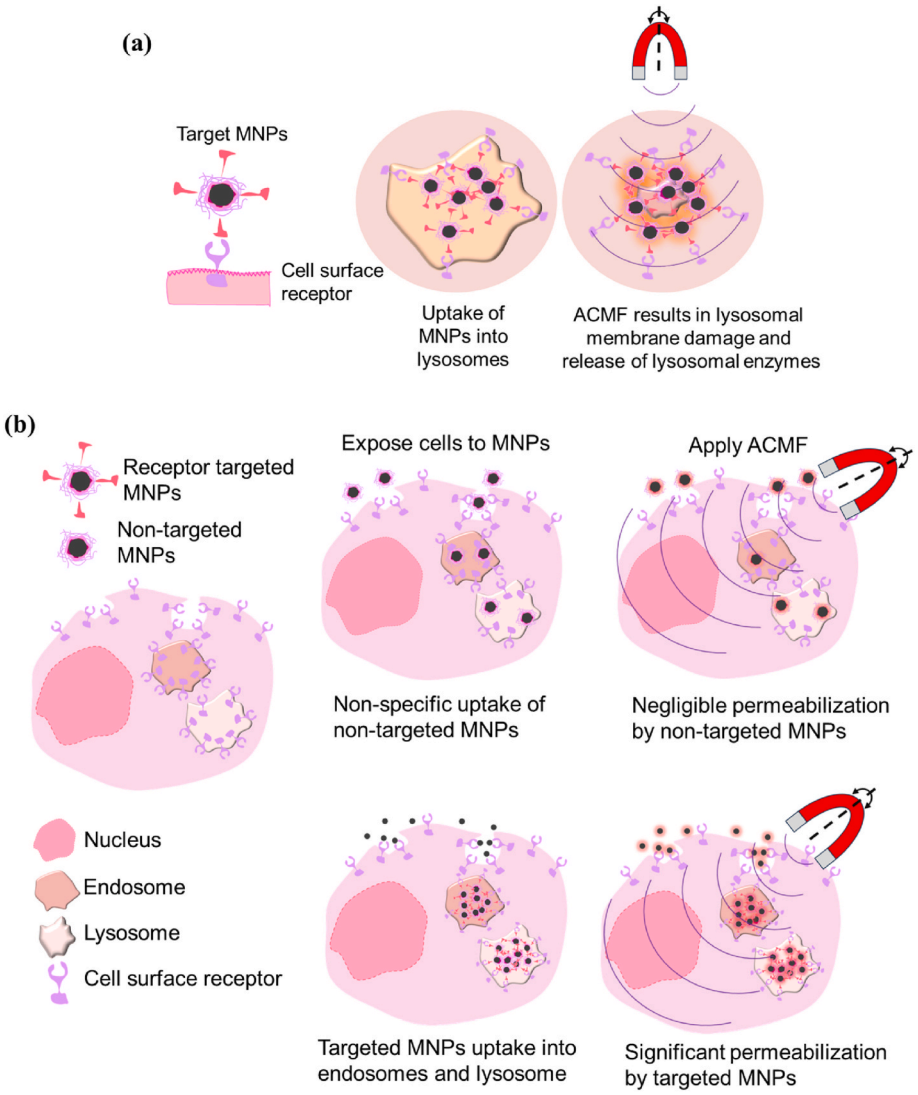

Fig. 6. Schematic representation of (a) uptake of targeted MNPs facilitating lysosomal membrane damage and release of enzymes and (b) difference in uptake of non-targeted and targeted MNPs under an ACMF (adapted from Ref. [204]).

in Fig. 6 (b). Targeted MNPs are taken up into endosomes and lysosomes due to receptor mediated endocytosis of the targeted receptor whereas non-targeted MNPs are taken up by non-specific mechanisms. Both types of MNPs dissipate heat under the guidance of an external magnetic field. However, targeted MNPs deliver heat specifically to endosomes and lysosomes thereby causing permeabilization and the release of their contents into the cytoplasm leading to selective killing of targeted cancer cells. Domenech et al. [204] demonstrated IONPs targeted to the epidermal growth factor receptor (EGFR) selectively promote LMP in cancer tissues overexpressing the EGFR with the aid of ACMF. Heat treatment along with improved cathepsin B cytosolic activity as well as enhanced ROS generation were observed to be responsible for lysosomal-dependent cell death. Hence, LMP occur better with targeted MNPs compared to non-targeted MNPs.

Pucci et al. [206] studied the anticancer efficacy of drug loaded IONPs induced by MHT. The NPs taken up by the lysosomes were permeabilized during ACMF stimulation with consequent release of lysosomal cysteine protease enzyme named cathepsin B suggesting LMP. It was inferred that the intracellular temperature was not enough to induce cell toxicity however, localized heating results in LMP induction. Conversely, Fenton reactions facilitated by the ACMF stimulus might produce enough ROS to trigger LMP. LMP can be hence triggered with high concentration of ROS production near the lysosomal membrane. ROS generation can cause a negative effect on lysosome stability rendering LMP easier in tumor cells.

Understanding these two mechanisms (ROS and LMP) is crucial for optimizing the efficacy and safety of MHT in cancer therapy. Few articles have discussed the underlying mechanism of cytotoxicity induced IONPs guided MHT [207–210]. Further research in this area may uncover new insights into the interplay between MNPs, cellular organelles and cell death pathways leading to the development of more targeted and efficient therapies.

6. Bench to bedside clinical translation using IONPs in MHT

With increasing developments in MHT, the biological effects of NPs in human body need to be emphasized. The toxicity of various nanosized particles is being investigated both in vitro and in vivo. Several studies have indicated that the exposure of human cells to MNPs can induce adverse biological effects such as toxicity, oxidative stress, pulmonary inflammation and genotoxicity [211,212]. Kim et al. [213] studied the whole body MHT efficacy for treating malignant cancer using leukemia cell-specific iron based NPs. MHT was performed by targeting MNPs to the blood circulating system. The removal of cancer cells via MHT (310 kHz, 316 A) was experimented in vitro and in vivo. In this study, an epithelial cellular adhesion molecule (EpCAM) antibody was conjugated

on the surface of MNPs (EpCAM-MNPs) to target human monocytic leukemia cells (THP1). Fig. 7 depicts the bio-TEM images of THP1 cells before and after MHT in vitro and in vivo. In vitro studies where THP1 cells treated with bare MNPs (In-MNPs) [Fig. 7 (a)] and human epithelial cellular adhesion molecule antibody on MNPs (hEpCAM-MNPs) [Fig. 7 (b)] without MHT, displayed a globular and intact cell shape. Cells treated with In-hMNPs along with MHT [Fig. 7 (c)] had a similar morphology compared to those without MHT. However, other cells were seen to be destroyed and small-size debris was seen (Fig. 7 (c), two right panels). Conversely, hEpCAM-MNPs within cells had destroyed the cell morphology and MNPs were adhered to their surface as seen in Fig. 7 (d). Cell viability was reduced to 40.8 % compared to control, when cells treated with hEpCAM-MNP-mediated MHT. In vivo MHT inducing on AKR mice with T-cell lymphoblastic leukemia proved that MHT could induce selective removal of leukemia cells from the blood circulatory system due to the specific adhesion of mouse EpCAM-modified MNPs (mEpCAM-MNPs) to the leukemia cells [Fig. 7 (e) and 7 (f)]. It was observed that some cells were adhered to mEpCAM-MNPs however not to In-mMNPs. This study proved that MHT employing EpCAM-modified MNPs selectively removes the leukemia cells hence considered whole body MHT as a promising approach for depleting cancer cells from the blood circulatory system.

6.1. *In vitro studies*

IONPs will be internalized by the cells when incubated for in vitro studies. The concentration-dependent toxicity, time-dependent internalization, and efficiency of IONPs as MHT agents have been recently investigated in multiple cancer cell lines such as pancreatic carcinoma, uveal melanoma, breast adenocarcinoma, triple-negative breast cancer, lung cancer and colon cancer cell lines [140]. NPs were found to be internalized inside the cytoplasm in all cell lines. Reduction in cell viability (after 72 h) due to MHT (23.8 kA/m and 202 kHz) was observed and found to have a strong dependence on the cell line. The influence of dimercaptosuccinic acid modified IONPs on cellular oxidative stress in five different cell lines such as macrophage, endothelial, pancreatic cancer, breast cancer and glioma cell lines were evaluated by Daviu et al. [214]. The effect was found to be strongest in macrophage cell lines and MDA-MB-231 breast cancer cells whereas glioma and pancreatic cells which were less affected. However, no changes were observed in endothelial cells. Grudzinski et al. studied the cytotoxic effect of hydrophilic IONPs with sizes from 15 to 100 nm on lung cancer cells such as A549, H1703, DMS 114 along with normal bronchial cells BEAS-2B with and without exposure to ACMF. Aqueous suspension of IONPs with 0.1–100 μg/mL under applied magnetic field parameters of 18.3 kA/m and 110.11 kHz were examined and found negligible cytotoxicity when NPs and ACMF were tested individually [215]. Under ACMF, a significant decrease in cell viability and proliferative capacity due to the enhanced effects of IONPs and ACMF were observed. Specifically engineered NP surfaces have exhibited distinct cell responses and polymer encapsulation reduces the cytotoxicity of IONPs [216]. Surface coated NPs exhibited enhanced cell proliferation and viability compared to uncoated particles [217,218]. Pradhan et al. [219] investigated cytocompatibility studies of lauric acid and dextran-coated SPIONs in two different cell lines (mouse fibroblast and human cervical carcinoma). A higher uptake and lesser cytocompatibility performance were observed in SPIONs coated with lauric acid than with dextran which could be due to the loss of dextran shell during enzymatic degradation. Thus, dextran has been limited in most HPT applications. The cytotoxicity effects of uncoated and polyvinyl alcohol (PVP) coated SPIONs were compared by employing MTT assay using L929 cells [122]. The coated NPs exhibited enhanced cell viability compared to uncoated ones. In addition, protein affinity to the NPs surface was found to be a significant factor in determining the interaction of NPs with living matter and thus protein interaction with different surfaces can induce varying effects. NPs with positive surface charges are more prone to easy attachment towards negatively charged cytoplasmic membranes. The effect of internalization of positively charged 3-aminopropyltriethoxysilane (APS)-coated SPIONs and low charged amino-dextran (AD)-coated SPIONs on HeLa cancer cell lines were studied [220]. The uptake of APS coated IONPs was observed to be significant than that of AD coated IONPs. Chen et al. [221] evaluated the biocompatibility of Fe_3O_4 NPs and investigate their therapeutic effects when combined with MHT on cultured MCF-7 cancer cells. The NPs exhibited better heating ability during in vitro MHT and observed reduced blood, cellular and genetic toxicities. Our group has performed in vitro MHT using Fe_3O_4 @TMAAD NPs on MCF-7 cell lines

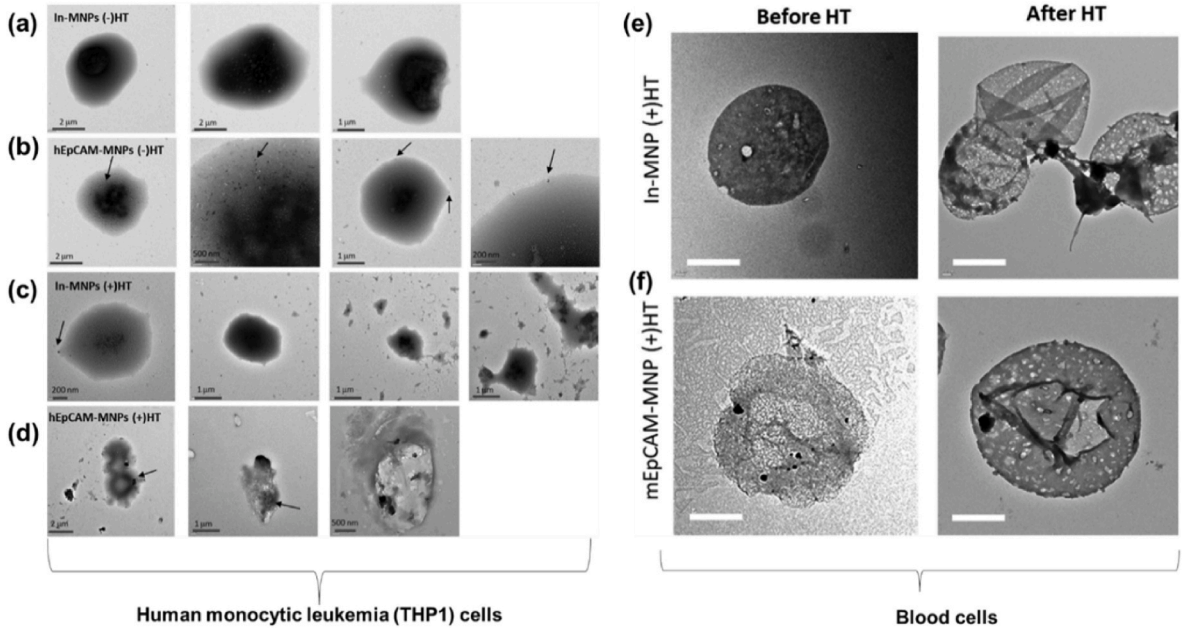

Fig. 7. Bio-TEM images of (a–d) human monocytic leukemia (THP1) cells with MHT [(+HT)] or without MHT [(−)HT] following the treatment of inactivated form of hEpCAM-MNPs (In-MNPs) and hEpCAM-MNPs [arrows indicate the localization of MNPs] and (e,f) blood cells from In-mMNPs (+)HT and mouse EpCAM-modified MNPs (mEpCAM-MNP) (+)HT groups (reprinted with permission from Ref. [213]).

to evaluate the cytotoxicity and hemolytic response [137]. NPs have shown concentration-dependent anticancer activity toward MCF-7 cancer cells and nonhemolytic response, suitable for cancer HPT. All these studies affirm the biocompatibility of IONPs and ensure their suitability for use in cancer HPT applications. Fig. 8 exhibits the MHT potential of alginate coated IONPs on hepatocellular carcinoma cells (HepG2) [198]. Cells injected with IONPs were incubated for 4 h followed by the exposure of ACMF at 33.8 mT and 275 kHz for 15 min. Control cells and cells incubated with IONPs without ACMF exhibited predominantly green signal, showing the characteristic of live cells in live/dead assay. However, most of MNPs incubated cells exposed to ACMF were shown positively stained for apoptotic cell death. Membrane blebbing, loss of structural integrity, cell shrinkage and rupture of cell membrane were seen indicating the complete cell destruction after MHT. These studies reveal the potential use of IONPs as targeted nano heating agents for in vitro MHT applications.

6.2. *In vivo studies*

A systematic in vivo analysis of the MHT effects of IONPs in orthotopic Dunning R3327 tumor model of prostate cancer in rat was demonstrated in an earlier study [222]. MHT led to a tumor inhibition rate of 44–51 % and 82.5 % iron content was found to be in the prostate of the rat. In later years, the biodistribution, iron clearance and biocompatibility of surface modified IONPs were tested in vivo in rats to ensure their safe clinical use and the results exhibited neither long term effects nor oxidative stress [223]. Moreover, the results demonstrated that the biodistribution of MNPs depends on the size, shape and surface characteristics. Oxidative stress was found to be reduced and iron levels in various organs were within safer margins. Lee et al. extensively investigated the biocompatibility of core–shell Fe_3O_4 at Au nanocomposite injected in mice and beagle dogs [224]. No significant problems related to cytotoxicity, acute toxicity and histopathological studies were reported. Kim et al. investigated in vivo MHT efficacy (Fig. 9) on SCC7 tumor-bearing mice using polyethylene glycol coated Fe_3O_4 multigranular nanoclusters (PEG-MGNCs) and PEG coated single iron oxide nanoparticles (PEG-NPs) [225]. Mice were injected via tail vein with saline (control), PEG-NPs and PEG-MGNCs. Tumors were then subjected to ACMF with parameters 389 kHz and 19.5 kA/m for 30 min after 24 and 48 h postinjection of MNPs. Temperature rise from 37 to 45 °C was observed for mice treated with PEG-MGNCs, whereas a slight temperature increment of 34.8 °C and 35.2 °C were observed respectively for saline and PEG-NPs, which was measured using an IR camera [Fig. 9 (a)]. Significant tumor growth inhibition and negligible antitumor effect was observed respectively in mice treated with PEG-MGNCs and PEG-NPs under MHT application. Antitumor effect for control group was found to be similar in case of mice treated with PEG-NPs [Fig. 9 (b)]. The tumor weight of the mice [Fig. 9 (c)] with PEG-MGNCs along with MHT application was found to be reduced compared to control and PEG-NPs, which indicates an enhanced therapeutic efficacy. The pictures of mouse and tumor tissues attained after the end of the studies established a correlation with the obtained experimental results [Fig. 9 (d)]. These results evidenced that PEG-MGNCs can be used as an excellent therapeutic agent to induce heat in tumors in vivo. Ding et al. [226] synthesized magnetite nanorings with an average outer diameter of 70 nm and investigated the cellular HPT efficiency on mice bearing MCF-7 breast cancer. The heating efficacy was compared with commercially available IONPs named Resovist under same experimental conditions (400 kHz, 40 kA/m, 150 μg/mL) and the tumor volume was monitored up to 40 days (Fig. 10). A remarkable reduction in tumor volume from day 1 and a complete disappearance of tumor after day 6 was observed when mice treated with magnetite nanorings with MHT application. However, mice treated with Resovist MHT treatment exhibited tumor growth similar to those of control. It has been inferred that these unique shape-induced magnetite nanorings holds potential for enhanced heating output compared to commercially available ones, hence desirable for MHT-mediated cancer therapy. Localized MHT effect in combination with amino-silane coated IONPs applied multiple times in brain tumor of Wistar rats under ACMF parameters of 300 G and 309 kHz was evaluated [227]. Intratumoral HPT exhibited anti-tumoral effects and intravenous administration demonstrated almost total reduction tumor size. A magnetic IONPs-PEG–TRA core-shell structure was designed and examined for efficient in vivo MHT effect in HER2+ breast cancer bearing female balb/c mice [228]. When the NPs were accumulated in the tumor sites, the temperature was enhanced and maintained to about 45 °C for 20 min. The temperature of the tumor was

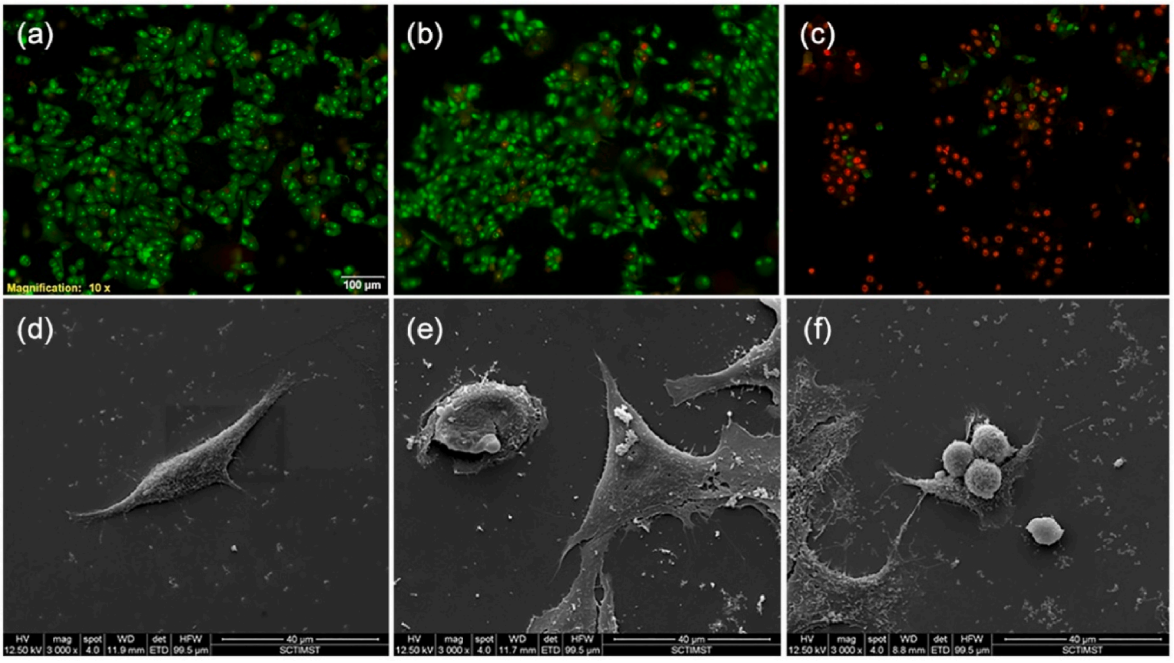

Fig. 8. In vitro MHT using IONPs (a–c) live-dead cell assay and (d–f) ESEM (Environmental Scanning Electron Microscopy) images of HepG2 cells. (a & d) controls, (b & e) with IONPs treatment without exposure to ACMF and (c & f) with IONPs treatment and exposure to ACMF (reprinted with permission from Ref. [198]).

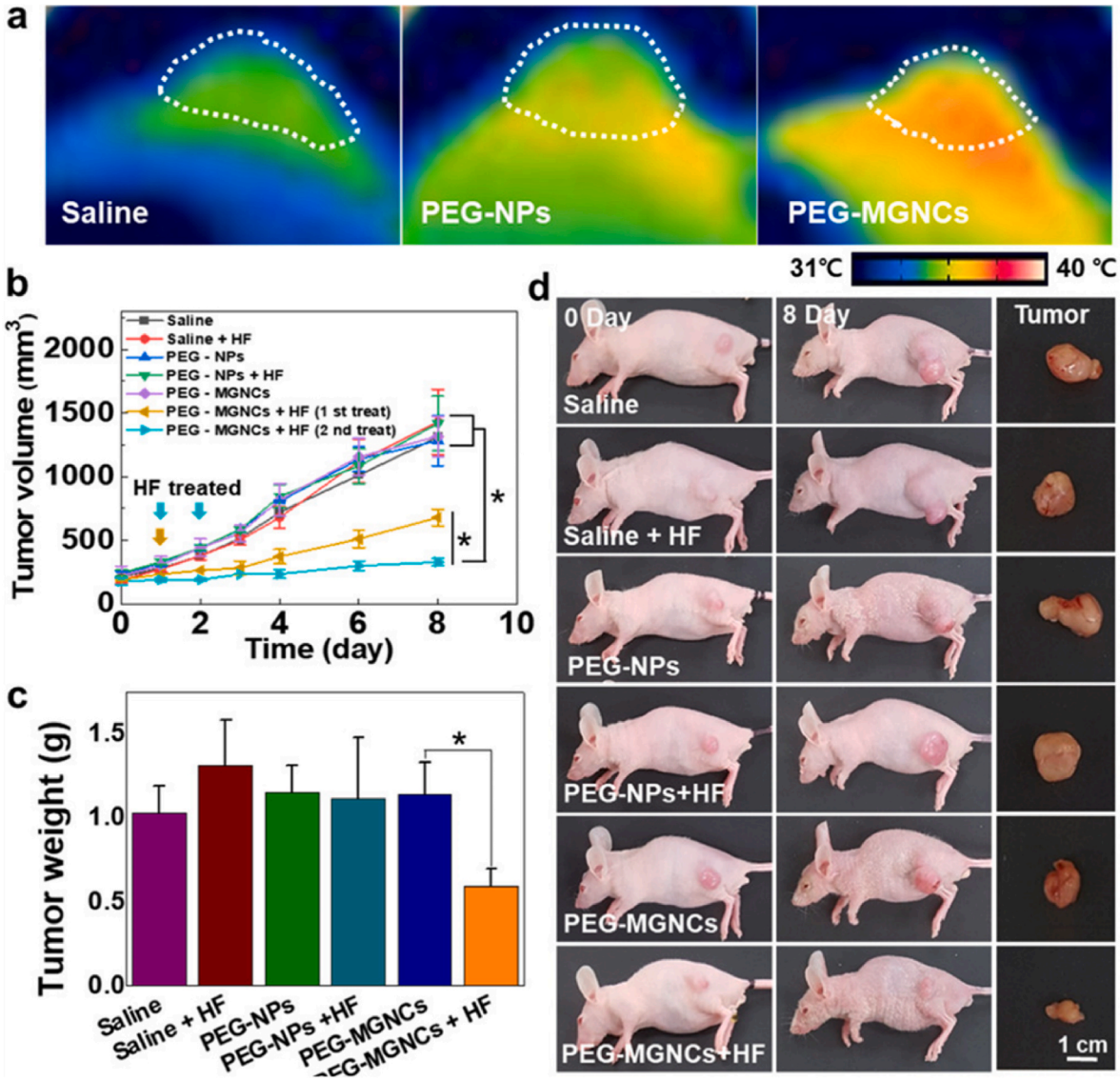

Fig. 9. (a) Thermal image of tumor tissues 24 h after intravenous injection of PEG-NPs and PEG-MGNCs (8 mg/kg) upon ACMF of 19.5 kA/m and 389 kHz, (b) inhibition of tumor growth where samples treated with hyperthermia field (HF) are highlighted with arrows, (c) tumor weight after MHT treatment and (d) photographs of mice and tumor from day 0 to day 8 after MHT (reprinted with permission from Ref. [225]).

found to be specifically increased sparing the surrounding normal tissues inducing MHT with minimal toxicity. MHT therapeutic efficacy of IONPs against pancreatic tumors such as BxPC3 and MIA PaCa-2 in mice was demonstrated [26]. A steady increment in tumor temperature with minimal increment in rectal temperature of the mice was observed. Higher heating was observed in BxPC3 compared to MIA PaCa-2 and inferred that higher heating response was achieved due to the physico-chemical properties of IONPs, concentration of NPs, applied field parameters and tumor nature. Recently, Yan et [229] designed a bio applicable magnetic iron oxide-based hydrogel for elucidating thermal responsiveness for the treatment of hepatocellular carcinoma in mice. In vivo studies evaluated the anti-recurrence efficacy and specified that the hydrogel can decrease postoperative recurrence rate. When the mice were exposed to ACMF, the temperature of tumor sites reached up to 46 °C within 15 min and a significant tumor growth was observed. This significant reduction is due to the effective inhibitory properties of hydrogel in combination with applied ACMF. Routes of administration of MNP in vivo and the real time monitoring via MRI are schematically represented in Fig. 11 (a). SPIONs are administered caudally (I) or by carotid (II) artery and being transported by the blood flow (III). An ACMF is applied to target the tumor loaded SPIONs (IV), which are concentrated in the tumor tissue (V). MRI showing SPIONs accumulation (arrow) in tumor with (A) and without (B) ACMF [230]. Fig. 11 (b) shows the real time temperature in vivo measurements from the thermal infrared camera (surface) and optical fiber (surface or intratumor) [231]. Ahmed et al. [232] investigated in vivo MHT therapy on three PC3 xenograft tumor bearing mice injected with SPIONs exposed to an ACMF for 20 min. HPT temperature profiles [Fig. 11 (c)] of three mice for control, MNP alone(+MNP/-AMF), and treatment (+MNP/+AMF) groups of MNPs with MHT were obtained. It was observed that the required hyperthermic temperature of 48 °C was achieved for all three mice within 3 min and remained constant for the remaining 17 min. The tumor volume was continuously evaluated for 22 days and exhibited 85 % decrement in tumor volume compared to untreated mice [Fig. 11 (d)]. Time-lapse photographs of tumor bearing mice taken on day 0, 12, and 20 were shown in Fig. 11 (e). No tumor was seen in the treatment group whereas tumor volume increases over time for the mice treated with control and MNPs alone. Size dependent heating potentiality of IONPs has been explored in tumor bearing mice where nanocrystals of varying sizes (6, 9 and 40 nm) injected intratumorally under an ACMF of 9.35

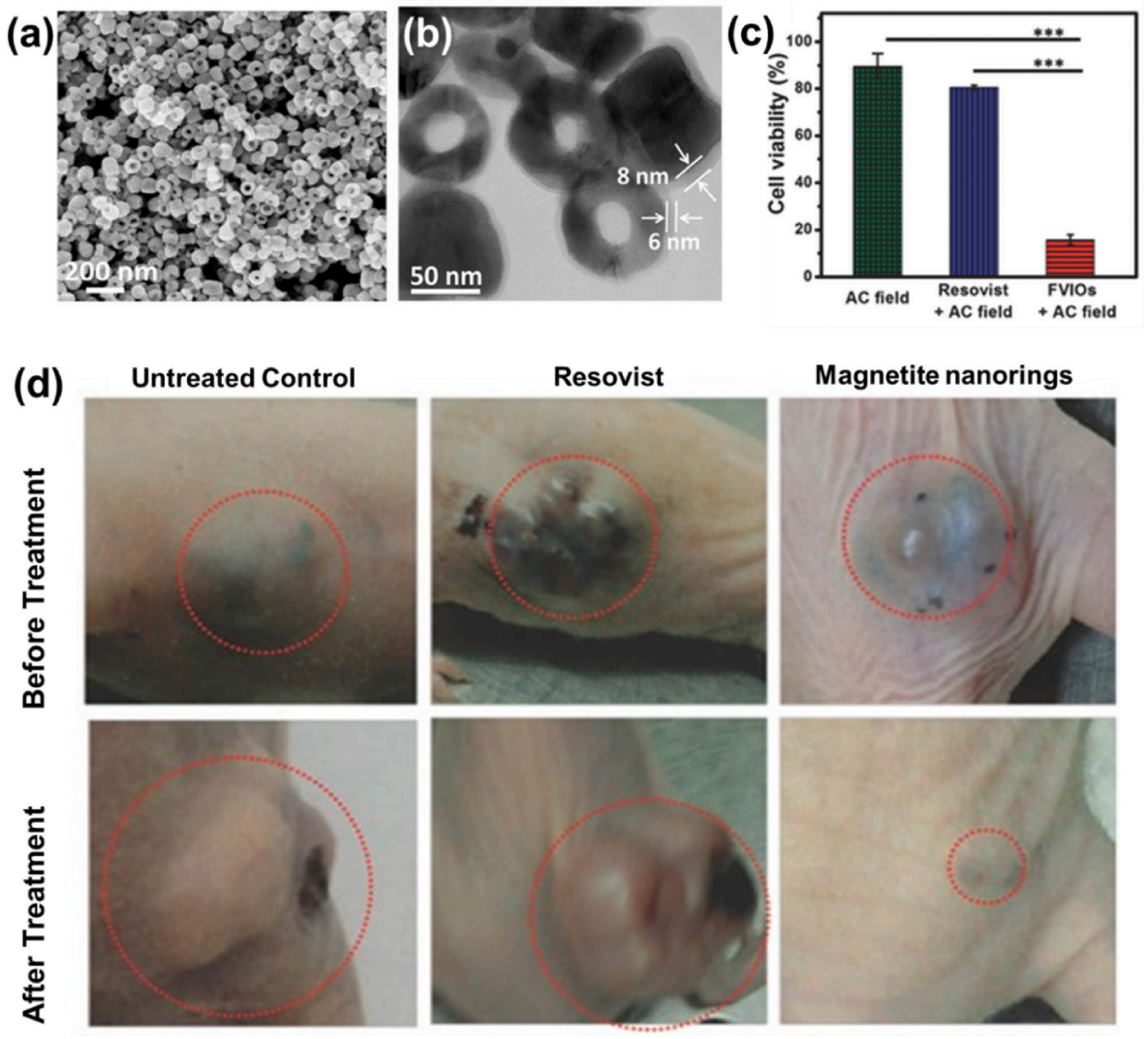

Fig. 10. (a, b) SEM and TEM image of magnetite nanorings, (c) cell viability of MCF-7 cancer cells subjected to MHT with ACMF alone, Resovist + ACMF and magnetite nanorings + ACMF and (d) nude mice xenografted with MCF-7 breast cancer cells before (upper row, dotted circle) and 40 days after MHT treatment (lower row) with control, Resovist and magnetite nanorings (reprinted with permission from Ref. [226]).

kA/m and 325 kHz for 60 min [71]. Negligible temperature rise was evidenced for 6 nm IONPs whereas significant hyperthermic temperature of 43 °C was observed for 40 nm sized IONPs [Fig. 12 (a)]. In vivo MHT study [Fig. 12 (b)] proved 40 nm sized IONPs could effectively reach the hyperthermic temperature and selectively heat the tumor tissues with a minimal concentration of MNPs. Magnetic resonance imaging (MRI) on cross section of mouse before and after injection of IONPs shows sharp contrast of IONPs inside the tumor exhibiting the affected region [Fig. 12 (c)]. It has been inferred that the cellular uptake of IONPs is size dependent, which affects the intra-tumoral distribution and thereby vary the heating efficacy. Mohamed et al. [233] in a recent study assessed the cytotoxic effects of 10 nm sized spherical shaped rutin modified IONPs in rats. It was demonstrated that rutin modified IONPs minimizes the toxic mechanisms such as cellular oxidative stress, cellular inflammation and induce indirect damage to the DNA of the living systems due to its anti-oxidative, anti-inflammatory and anti-apoptotic properties. Table 2 provides relevant in vivo MHT studies using Fe_3O_4 NPs.

In addition, IONPs conjugated with anticancer drugs were exploited to achieve an effective chemo-thermal therapy. Several in vitro and in vivo experiments using IONPs with anticancer drug (doxorubicin) as potential nanocarrier to achieve chemo-thermal therapy has been reported [234–237]. For instance, Mai et al. designed a nanocarrier of DOX loaded IONPs with cubic morphology for a combined MHT-mediated drug delivery [238]. In vitro studies on A431 epidermoid carcinoma cells revealed significant cytotoxic effects due to the accumulation of DOX conjugated IONPs together with MHT application [Fig. 12 (d, e, f)]. In vivo studies exhibited a complete tumor suppression by day 90 and significant survival rate of xenograft mouse model induced with A431 cells, under an ACMF of 11 kA/m and 110 kHz [Fig. 12 (g)]. Confocal images given in Fig. 12 (h, i, j) also showed the difference in tumor cell density and morphology when exposed with DOX conjugated IONPs + MHT. It was inferred that MHT along with drug delivery employing DOX loaded IONPs attains the highest therapeutic impact. These results confirm the therapeutic effectiveness of SPIONs-mediated MHT treatment to eradicate tumors.

6.3. *Clinical studies*

In vitro and in vivo studies have proved the potentiality of MHT-mediated tumor cell death, paving the way for clinical trials. Clinical trials of MHT by the direct intra tumoral injection of IONPs were carried out in Germany in patients with brain and prostate cancer [69]. Several preclinical studies are being performed to assess the efficacy of MNPs

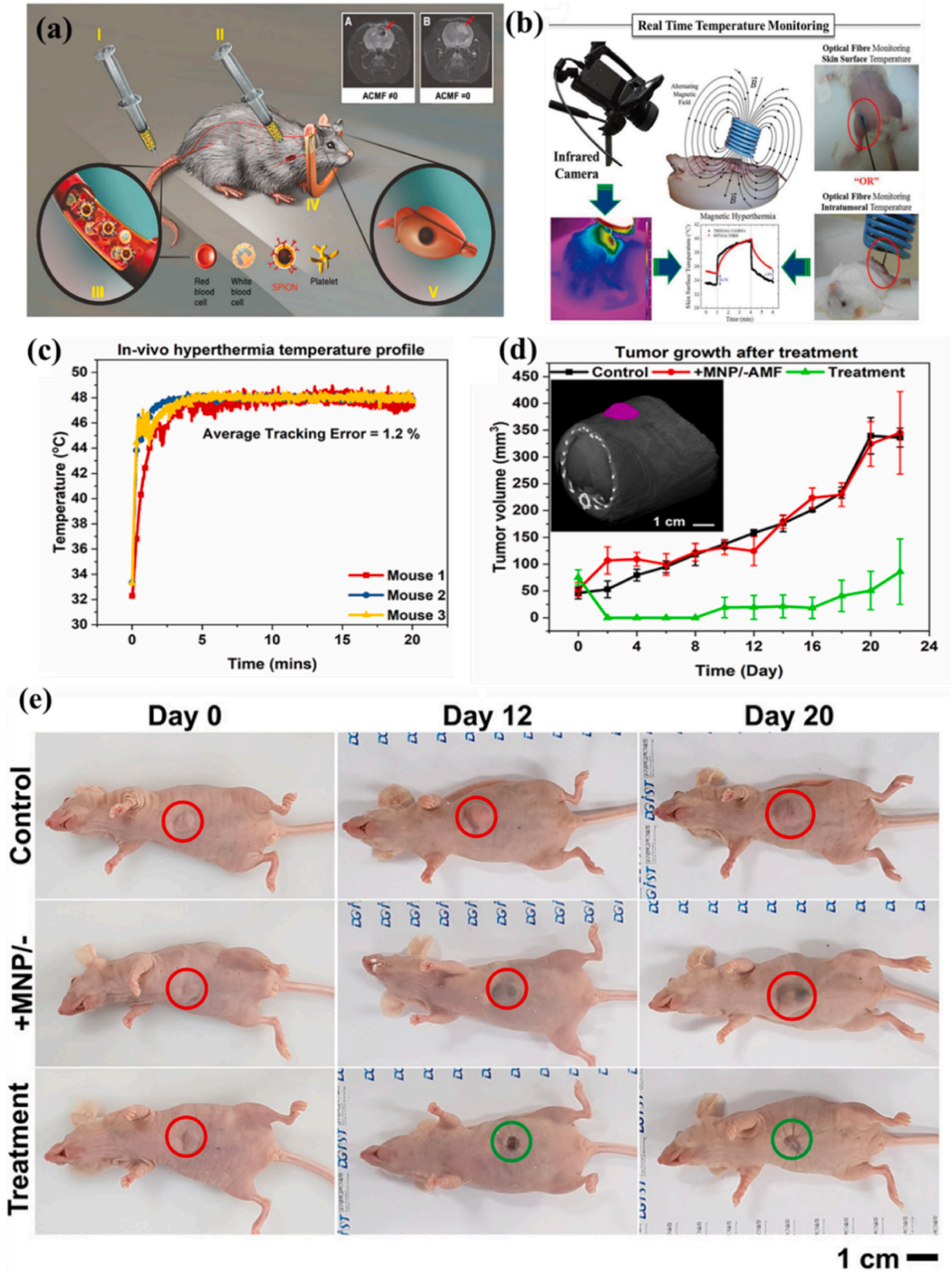

Fig. 11. Schematic illustration of (a) in vivo MHT using SPIONs (reprinted with permission from Ref. [230]), (b) real time temperature measurements from the thermal infrared camera (surface) and optical fiber (surface or intratumor) (reprinted with permission from Ref. [231]), (c) in vivo HPT temperature profiles of three mice from the treatment group, (d) tumor growth after MHT treatment over 22 days (inset exhibiting CT image of tumor bearing mouse prior to treatment) and (e) time-lapse images of tumor-bearing mice taken on day 0, 12, and 20 (red circles indicate tumor growth; green circles indicate scarring caused by MHT) (c, d and e reprinted with permission from Ref. [232]). (For interpretation of the references to color in this figure legend, the reader is referred to the Web version of this article.)

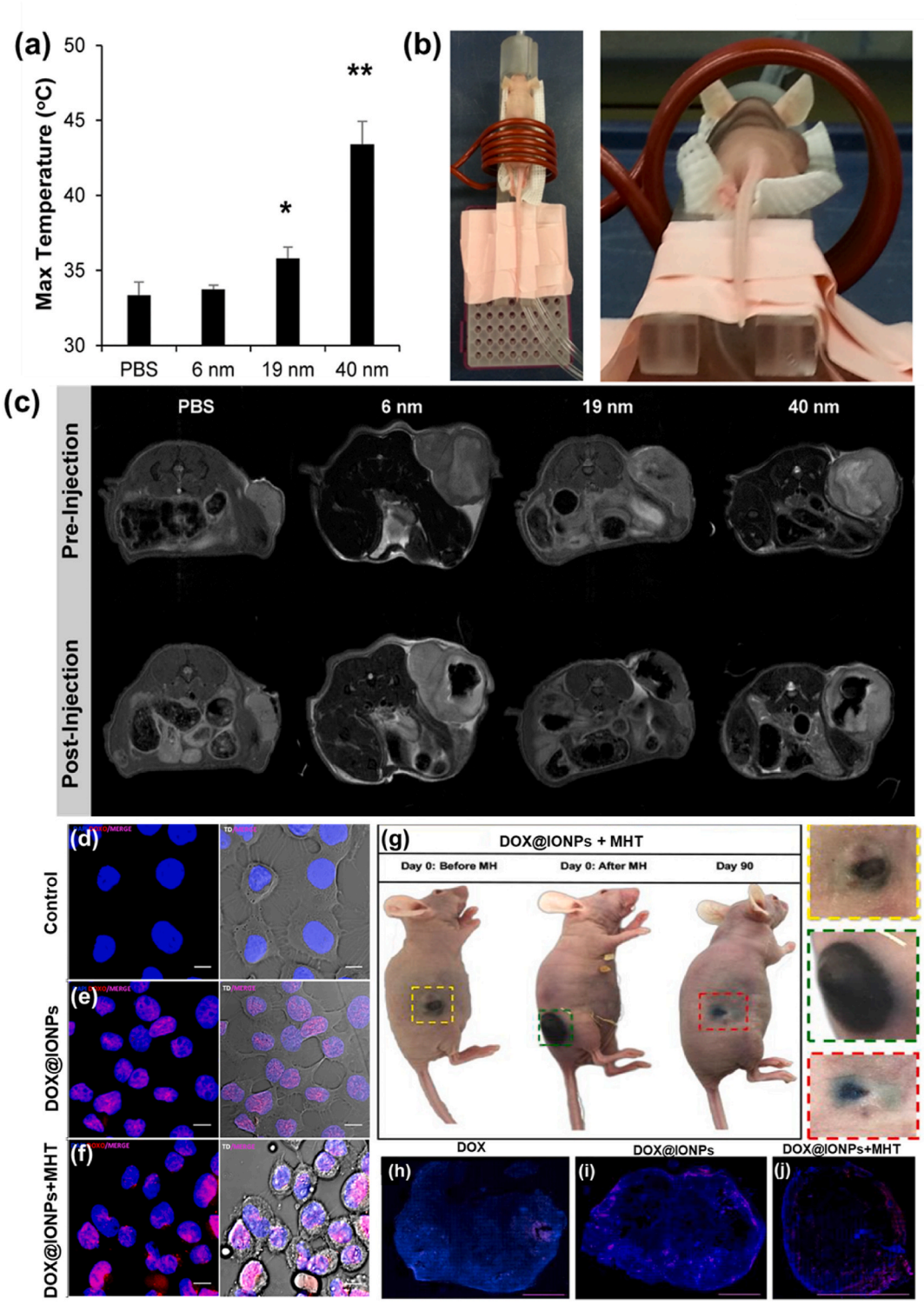

Fig. 12. In vivo MHT therapy experimented in tumor bearing mouse (a) Maximum temperature achieved during 1 h of heating at 9.35 kA/m and 325 kHz for varying sizes of IONPs, (b) in vivo MHT set up where mouse was placed in 5 cm diameter coil where the tumor was centered inside the coil and (c) MRI images of the cross section of the mouse before and after IONPs injection (reprinted with permission from Ref. [71]); confocal microscopic images (d, e, f) taken after 4 h of incubation for control untreated A431 cells, DOX@IONPs and DOX@IONPs + MHT respectively displaying distinct signs of cell stress and an improved DOX uptake (intense violet signal), (g) photographs of mouse after therapy; complete tumor suppression by day 90 post-treatment with DOX@IONPs + MHT (color coded inserts exhibit enlarged images of the tumor) and confocal images of the whole tumor slice, sacrificed 30 days post treatment, exhibiting the presence of viable cancer cells (DAPI blue staining) and DOX (red signal, shown in pink due to the merge with DAPI) for (h) DOX, (i) DOX@IONPs and (j) DOX@IONPs + MHT(reprinted with permission from Ref. [238]). (For interpretation of the references to color in this figure legend, the reader is referred to the Web version of this article.)

Table 2
Relevant in vivo studies using iron oxide (Fe_3O_4) nanoparticles for MHT-mediated cancer therapy.

Size (nm) of IONPs	Surface coatings	Injection dose	ACMF condition and time	Tumor nature and targeted animal	Tumor temperature	Therapeutic outcome	Ref
70–110	Chitosan	600–1000 μg per tumor	335 kHz, 14 kA/m, for 20 min	C6 glioblastoma tumor in rat	42 °C-44 °C	rapid tumor inhibition rate of 69.4 % within 8 days, with complete inhibition within 32 days, and no recurrence recorded over a 5-month follow-up	[209]
97.85 ± 0.74	–	100 μL of 30 % Fe_3O_4	423 kHz, 10 kA/m for 30 min	MCF-7 cells in mice	42 °C	DOX conjugated IONPs under MHT displayed superior antitumor efficacy and targeted delivery efficiency	[239]
149	Dextran	0.5 mg Fe/100 mm^3 tumor volume	1.048 MHz, 8.49 kA/m for 60 min	Panc-1 pancreatic cancer cells in mice	43–44 °C	Controlled heat distribution, gradual and persistent tumor growth inhibition over time and non-occurrence of tumor regrowth	[240]
519 ± 141	PEG	2.9 μgFe/μL	366 kHz, 13.3 kA/m for 60 min	Human glioblastomaU87MG in mice	43 ± 1 °C	Significant tumor growth inhibition after 2 cycles and inferred100 % survival rate	[241]
225 ± 45	Dextran	1 mg and 2 mg for single and double dose respectively	250 kHz, 27.9 kA/m for 30 min	Human fibrosarcoma in mice	42.5 °C	Tumor growth reduction by 3.6-fold and 2.5-fold for double dose and single dose treatment respectively	[242]
83.6	Polypyrrole and hyaluronic acid	18.64 mg Fe/kg	635 kHz, 30 A for 15 min	4T1 breast cancer in mice	45 °C	Effective elimination of cancer cells and inhibit tumor growth when MHT combined with drug release	[243]
30–45	PEG	0.25 mg Fe/100 mm^3	480 kHz, 10 kA/m for 15 min	4T1 breast cancer in mice	43 °C	88 % tumor inhibition when MNPs conjugated with DOX under MHT	[244]
145.9 ± 10.2	PEG	8 mg/kg	389 kHz, 19.5 kA/m for 30 min	SCC7 tumor in mice	45 °C	Exhibited the presence of necrotic areas and a higher expression of HSP 70	[225]
–	PEG	2 mg Fe/mL	312 kH, 30 kA/m for 10 min	4T1 cells in BALB/c mice	46.1 °C	59 % tumor inhibition under MHT and observed a concentration dependent therapeutic efficiency	[245]
160	PEG -silica	182 μg Fe/tumor	105 kHz, 18 kA/m for 30 min	xenograft tumor in C57/BL6 mouse	–	On MHT application, drug release along with thermal effects synergistically exhibit significant tumor growth inhibition, after 48 h of treatment	[246]
140	Dextran	1.8 mg Fe/100 mm^3	300 kHz, 4 kA/m for 3 min	BxPC3 pancreatic human cancer cells in mice	40–70 °C	Elevated temperature beyond the hyperthermic temperature could be controlled by modulating the field intensity during in vivo MHT protocols	[26]
72.4	3,4-dihydroxyhydrocinnamic acid	1 mg Fe/cm^3	365 kH, 300 Oe for 10 min	Hepa1–6 tumor model in C57BL/6 mice	–	Exhibited 95 % tumor inhibitory rate; absence of histopathological changes in major organs confirms the safety	[247]
200	Carboxy methyldextran	5 mg Fe/cm^3	245 kHz, 23 kA/m for 30 min	HeyA8 or A2780cp cells in Athymic nude mice	43 °C	Enhancement in tumor growth reduction due to multiple MHT treatments	[248]
19.5 ± 2.2 nm	PEG	10 mg Fe/kg	192 kHz, 220 G for 60 min	C6 xenografts in Male SCID mice	–	Potential tissue damage due to MHT; significant delay in tumor growth	[249]
100 nm	Aminosilane	–	309 kHz, 300 G for	Glioblastoma tumor in rats	43 °C	94.9 % reduction in tumor after 3 MHT exposure	[227]

injected in human patients. Preliminary clinical investigations using MNPs for the treatment of human brain tumors performed in 25 patients are reported [250]. A response rate of 34 % was observed with sufficient thermal responsiveness of brain metastasis. A novel HPT treatment modality employing IONPs for treating with 16 metastatic bone lesions in 15 patients was developed and achieved an optimum control of bone lesion metastasis [30]. Johannsen et al. [28] performed thermotherapy studies on IONPs using an external magnetic field applicator for the treatment of prostate cancer in 10 patients. NPs used in this trial were coated with an aminosilane-type shell with a core diameter of 15 nm, enough to elevate the HPT temperature under the applied ACMF parameters. The HPT temperature was tolerated by all patients indicating better clinical outcomes. However homogenous distribution of NPs in the prostrate was not observed in this initial trial. Another clinical trial was headed by Johannsen to study the treatment-related morbidity and quality of life associated with MHT employing IONPs in patients with locally recurrent prostate cancer [251]. Temperature upto 55 °C was obtained in prostrates with neither side effects nor toxicity levels. Oncological outcomes implied potential efficacy of the procedure. Morbidity related to treatment was found to be moderate and quality of life was transiently impaired by MHT. Maier-Hauff et al. [69] investigated the feasibility of phase I analysis on 14 patients for the MHT treatment of glioblastoma multiforme, one of the most aggressive forms of brain cancer. 14 patients were intratumorally administrated with aminosilane coated IONPs of core diameter 15 nm and subjected to HPT. This treatment modality was found to be safe and well tolerated by all patients with no side effects and local tumor control was observed. Following this, a prospective phase II analysis on 66 patients was experimented [29]. This clinical trial also demonstrated the safety of MHT when performed with similar aminosilane coated IONPs of core diameter 12 nm. This clinical trial associated with an improved survival rate of up to 12 months proved the efficacy of MHT in the treatment of brain cancer. These promising results led to the development of a new prototype magnetic field applicator for MHT therapy termed as NanoTherm [29]. The success of these clinical trials led to the commercialization of NanoTherm therapy. At present, clinically available MHT applicator in the world is NanoActivator® (MagForce AG, Germany), which operates at a frequency of 100 kHz with a varying field up to 18

kA/m. SPIONs-mediated MHT thermal therapy of the pelvic region with the aid of NanoActivator® applicator [124]. NanoTherm therapy as a medical device has received European Medicines Agency (EMA) approval for treating brain tumors since 2010 [252]. The effectiveness of the therapy has already been clinically tested on approximately 90 brain tumor patients and in pilot studies on approximately 80 patients with inter alia, pancreatic, prostate, breast, and esophageal cancer. Grauer et al. [253] implanted IONPs into six recurrent glioblastoma patients which then treated with intracavitary thermotherapy. Thermotherapy was experimented in the NanoActivator® at a frequency of 100 kHz and with variable magnetic field strengths of 2.5–15 kA/m. Patients underwent six 1-h HPT sessions in an ACMF along with radiotherapy at a dose of 39.6 Gy, have evidenced no major side effects during active therapy. Two patients were observed to have long-lasting treatment responses (>23 months) without receiving any further therapy. Clinical HPT utilizes the widely accepted human safe limit, i.e., $H.f \leq 5 \times 10^9$ A/ms (Brezovich limit) for the applied magnetic field parameters [254]. In a recent report, a new limit of $H.f = 9.46 \times 10^9$ A/ms was found to be safe and acceptable when performed in vivo MHT [255]. Translation of MHT from bench to the bed side clinic is still a challenging problem to address many of the limitations such as therapy-related NP toxicities, accumulation of NPs during heating, need of monitoring temperature changes in patients, uniform heating of target tissues sparing healthy surrounding tissues and standardizing treatment protocols to establish safety and efficacy. Fig. 13 depicts a schematic representation summarizing the major MHT clinical trials conducted using amino-silane coated IONPs of particle size of 15–16 nm on pancreatic and glioblastoma cancer patients using NanoActivator®.

7. Combinational therapy – MHT with PTT, CST and SDT

In view of the benefits of MHT, researchers are focusing on integrating MHT with chemotherapy for a combined magneto-chemo therapy to achieve an enhanced therapeutic effect. In spite of the evolving research progress during past three decades, the widespread success of combined magneto-chemo therapy is still hampered by limitations such as high particle concentration rate, lack of selectivity which affects surrounding normal healthy cells and adverse toxicity concerns associated with prolonged administration [23]. Photothermal therapy (PTT) has received immense research interest due to enhanced tumor ablation and minimal damage to surrounding healthy tissues, however limited tissue penetration of laser light limits its individual application [256, 257]. MHT shows excellent properties such as molecular-level specificity, long-range control, no depth penetration limit and nanoscale spatial resolution in comparison with PTT. Synergistic application of these multiple treatments can serve as a powerful enhancer for cancer cell death. Developing effective magnetic-based nanostructures which effectively produce heat with great potential both in MHT and PTT with meagre side effects remain a challenging platform for magneto-photo thermal therapy [Fig. 14 (a)]. Plasmonic NPs such as gold (Au) and magnetic IONPs are the prime choice for these heating-based applications [258–260]. Au exhibits outstanding optical properties such as localized surface plasmon resonance along with high light absorption and photothermal transduction, chemical stability and biocompatibility, which makes them promising candidates for PTT [261]. Fabrication of Au-IONPs nanohybrid platforms provides a dual MHT-PTT thermal therapy, opening new research arena towards advanced thermal-based therapies. Au coated polyethylenimine (PEI)-Fe_3O_4 NPs were reported to exhibit excellent magneto-thermal and photo-thermal properties when exposed to ACMF (110 kHz and 20 kA/m) and to light of suitable wavelength (850 nm) [262]. Temperature increment in bare and Au-coated PEI-Fe_3O_4 NPs of particle concentration rate of 10 mg/mL upon MHT and PTT and the corresponding SAR values obtained are shown in Fig. 14 (b and c). Such nanohybrids are proved to be efficient for achieving a synergized MHT -PTT induced cancer therapy. Similarly, Espinosa et al. [263] investigated the combined magnetic and plasmonic properties of IONPs decorated with gold for enhanced heat generation on PC3 xenografts. MNPs were intratumorally injected and exposed to MHT with an ACMF of 110 kHz and 25 mT and laser irradiation (680 nm and 0.3 W/cm^2) for a duration of 5 min. The infrared thermal imaging photographs of IONPs decorated with gold nanohybrid injected on tumor bearing mouse after 5 min heating under MHT alone, PTT alone

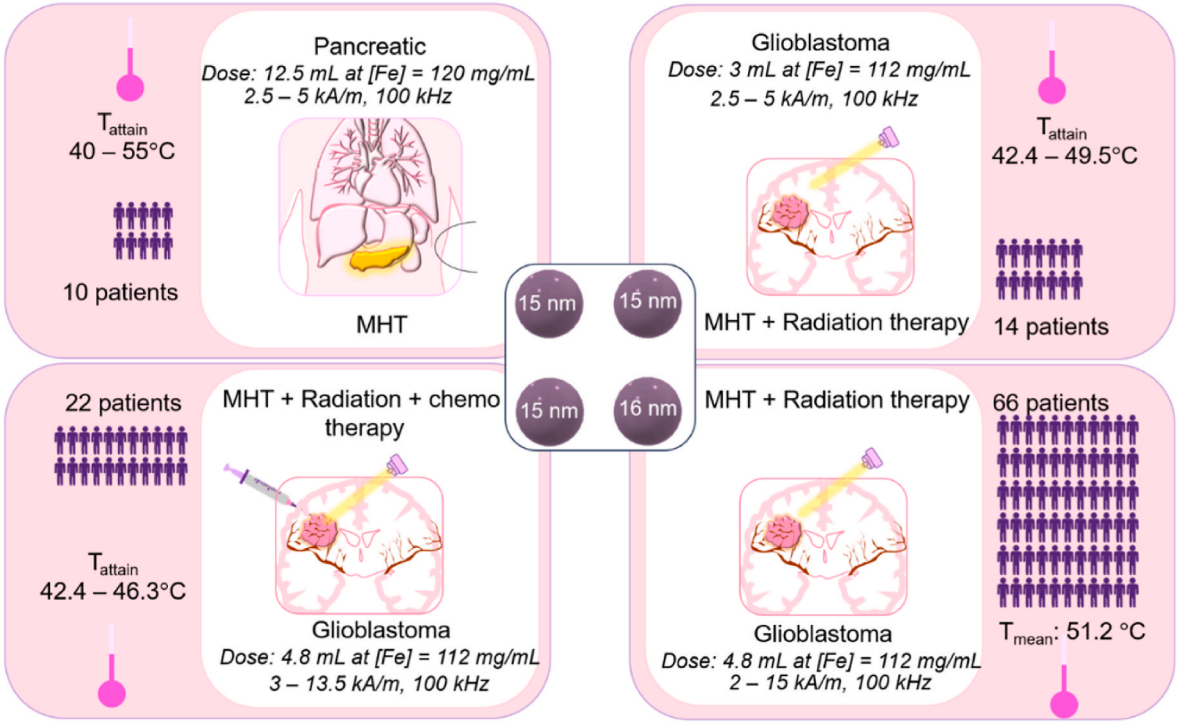

Fig. 13. Major MHT clinical trials performed using amino-silane coated IONPs of particle size of 15–16 nm on pancreatic and glioblastoma cancer patients using NanoActivator®(adapted from Ref. [25]).

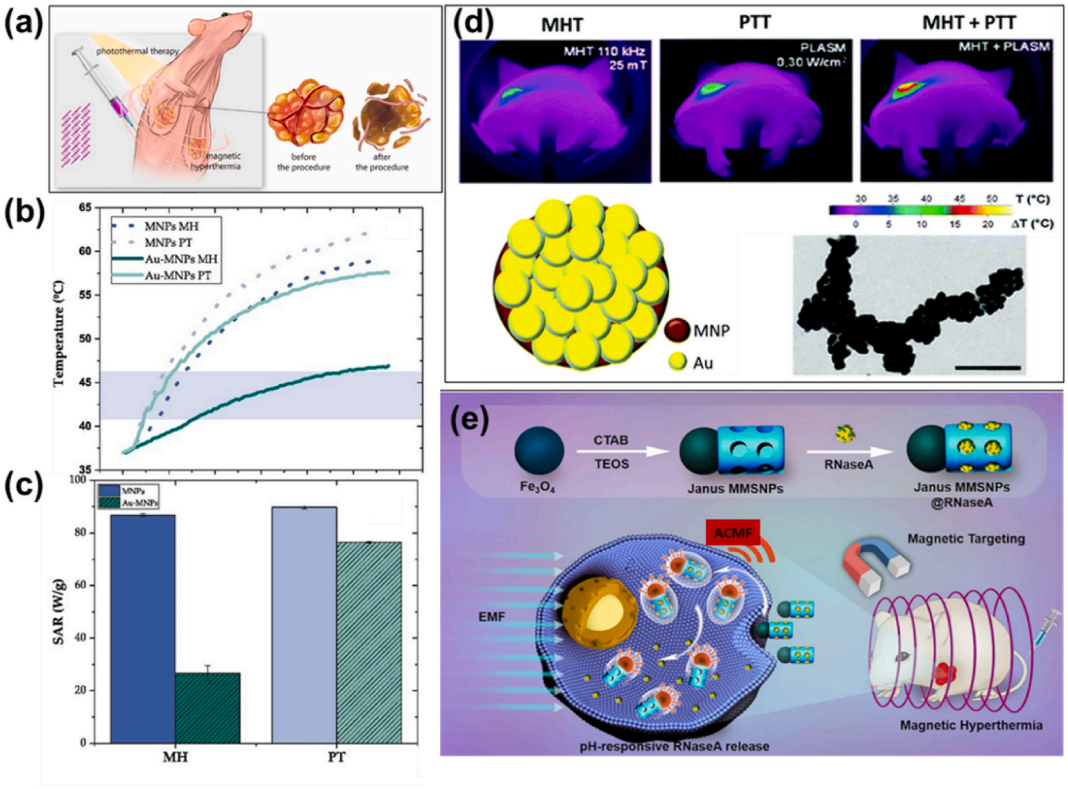

Fig. 14. (a) Schematic showing synergized photothermal therapy and magnetic field induced hyperthermia (reprinted with permission from Ref. [269]), (b) temperature increment of PEI-Fe_3O_4 (MNPs) and Au coated PEI-Fe_3O_4 (Au-MNPs) using magnetic hyperthermia (MH) under the application of 110 kHz and 20 kA/m ACMF and photothermia (PT) by laser irradiation of 850 nm (1 W/cm^2) power and (c) corresponding SAR values for the colloidal dispersion of 10 mg/mL PEI-Fe_3O_4 and Au-MNPs under an ACMF of 110 kHz and 20 kA/m and laser irradiation of 850 nm (1 W/cm^2) power (reprinted with permission from Ref. [262]), (d) infrared thermal imaging photographs of multi-functional single nanohybrid of gold (Au) decorated on IONPs (MNP) injected on tumor bearing mouse after 5 min heating under MHT alone, PTT alone and combined MHT + PTT (reprinted with permission from Ref. [263]) and (e) schematic illustration of the preparation of Fe_3O_4 based Janus NPs (MMSNPs) and loaded with ribonuclease A (RNaseA) for MHT (reprinted with permission from Ref. [270]). (For interpretation of the references to color in this figure legend, the reader is referred to the Web version of this article.)

and combined MHT + PTT were shown in Fig. 14 (d). The combined therapy resulted with rise in temperature by 20 °C within 2 min whereas individual modes resulted only about 9–10 °C with the same experimental conditions. A significant tumor regression was observed for the synergized treatment compared to individual mode. Such multifunctional nanohybrids impressively enhance the heating efficacy thereby opening up exciting new cancer therapeutic perspectives. Owing to the nano-amphiphilicity and binary asymmetric bio-functionalization, anisotropic-structured magnetic Janus NPs [Fig. 14 (e)] integrated with components of distinct physico-chemical and excellent magneto-thermal properties have emerged very recently for synergistic chemo-PTT-MHT thermal therapy [259,264]. The distinct compartments of Janus NPs can be surface modified with specific functional biomolecules for a separate control over the drug release thereby effectuating multidrug loading which can serve as an ideal drug carrier. Such NPs are characterized with (a) high drug loading capacity, (b) magnetic field assisted thermal dissipation with drug release and (c) photothermal cellular damage. Serea et al. [265] designed Janus Au: Fe_3O_4 NPs for evaluating MHT -PTT therapy with the aid of ACMF (frequencies of 143, 350 and 732 kHz and magnetic field upto 80 mT) and NIR-laser irradiation (785 nm). SAR value was found to be 8.3 kW/g/W/cm^2 and hence proved the nanosystem as efficient magnetic-plasmonic hybrid agent. Similarly, several recent works have been reported on Fe_3O_4 based Janus nanosystem for testing towards MHT-PTT combined therapy [259,266–268]. The intracellular heating mechanism of the developed Janus NPs as well as inhibition of toxicity related to ROS generation is another broad research arena which can be explored to design an effective heating power agent for cancer thermal therapies.

For designing a nanoplatform to relieve the tumor heat resistance induced by HSPs and to amplify the efficacy of MHT, intratumoral glucose levels in cancer sites have to be reduced. Increased glucose consumption and enhanced glycolysis covering the metabolic profile of cancer cells result in decrease in ATP generation thereby down-regulating the HSP expression. Cancer starvation therapy is one such technique for blocking the glucose supply leading to cell death. Glucose oxidase (GO_x)-mediated CST has been proved as a promising therapeutic approach with the potentiality to suppress tumor cell growth via catalyzing glucose oxidation. GO_x immobilized into IONPs exhibits controllable enzyme activity along with high therapeutic efficacy, self-supply oxygen, and nontoxicity, hence can be used as a potential platform to elevate cancer-starving therapy efficacy in solid tumors [172]. GO_x converts intratumoral glucose and oxygen into gluconic acid and hydrogen peroxide (H_2O_2). Cancer cells in comparison to normal cells rely heavily on glucose for cell survival and proliferation according to Warburg effect [271]. GO_x acts as a starvation therapy mediator which depletes the supply of glucose to tumor cells. This starvation therapy has proven effective in supplying abundant H_2O_2 and providing accumulation of gluconic acid which intensifies tumoral acidity. The combination of CST and MHT provides synergistic effects by targeting both the tumor vasculature and cancer cells directly, which enhances the overall therapeutic outcomes. Ying et al. [272] designed a magnetic hollow GO_x loaded hollow iron oxide nanosystem to drive starvation-chemo- MHT synergistic therapy for tumor treatment. It was observed that the synergistic therapy was accomplished via ROS and oxygen modulation for prostate tumor treatment. The excessive production and accumulation

of H_2O_2 leads to the Fenton reaction for generating ROS to achieve a chemodynamic therapy. Here, GO_x acts as an antitumor drug playing a tumor killing role and reduce the impact on surrounding normal cells through controlled release. ROS generation and glucose consumption additionally suppress the HSP expression and enhance the MHT efficacy. The synergistic effects induced by integrated therapeutic modalities provide a way for clinical translation of multimodal therapy. Yu et al. [273] synthesized a muti-functional GO_x-IONPs based magnetic

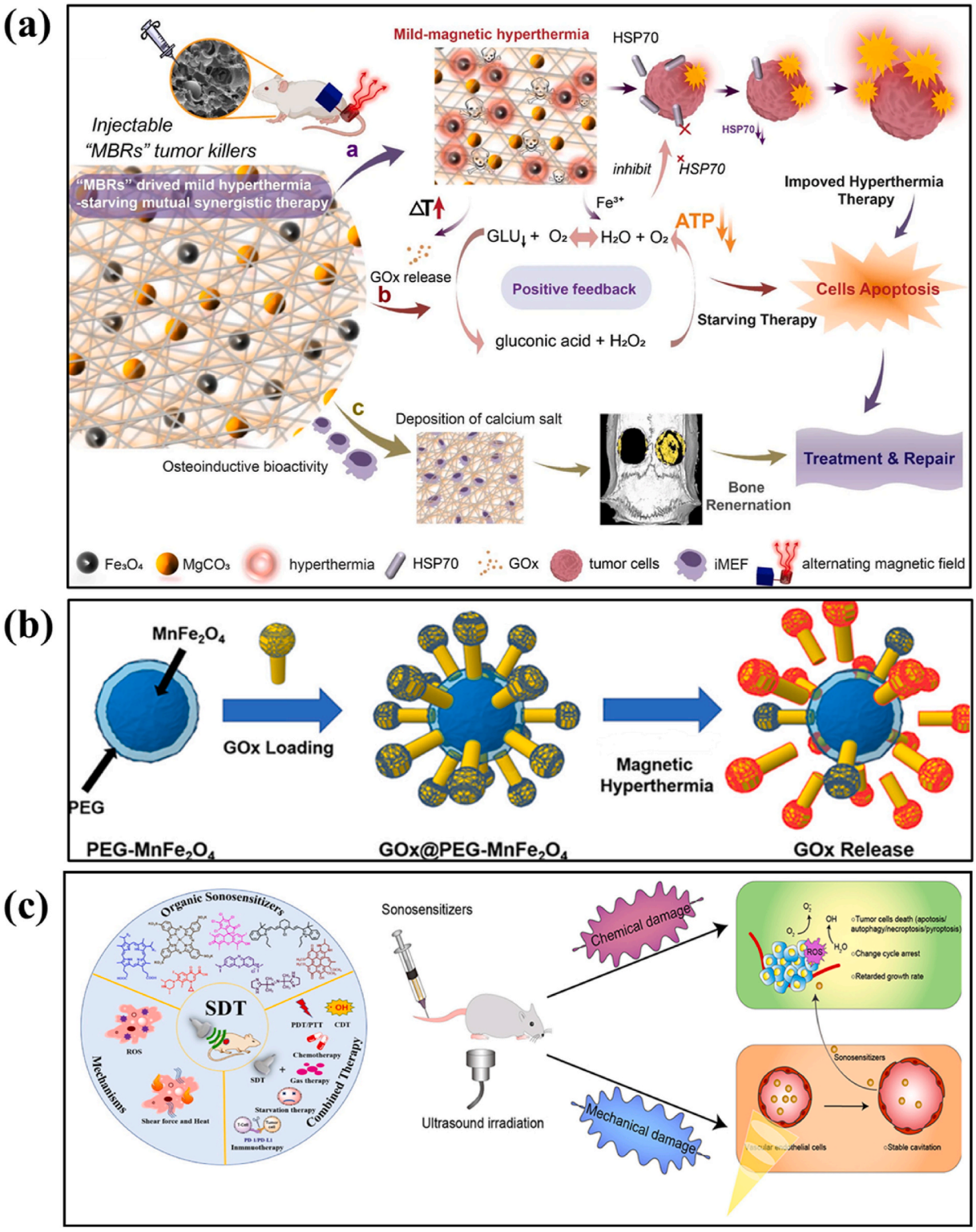

Fig. 15. (a) MHT triggered GOx release to induce starvation-magnetic synergistic therapy in 143B bone tumor. The enzymatic activity of GOx was reserved under mild thermal conditions and accelerated the enzyme-promoting reaction, and HSP70 was inhibited by simultaneously decreasing ATP for enhanced MHT ((reprinted with permission from Ref. [273]), (b) therapeutic nanosystem composed of glucose oxidase (GOx) loaded in polyethylene glycol (PEG) modified manganese ferrite ($MnFe_2O_4$) NPs for CST using MHT (reprinted with permission from Ref. [172]) and (c) SDT-based combined therapy and the possible mechanisms of SDT (reprinted with permission from Ref. [274]).

nano-system to drive MHT - starvation effects achieving synergistic therapy for osteosarcoma treatment [Fig. 15 (a)]. It was observed that MHT enhances the effect of starvation therapy in the hypoxic microenvironment simultaneously triggering GO_x release and inhibiting ATP production consequently reducing HSP expression. MHT aids in GO_x release to accelerate the transformation of glucose into gluconic acid and H_2O_2 and further transforms to O_2 and H_2O in the thermal environment. Hence, the system offers a minimally invasive therapy for osteosarcoma and a propitious platform for further clinical translation. A combinatorial effect of MHT with starvation therapy employing GOx loaded Mn-ferrite based nanosystem has been reported [172] as shown in Fig. 15 (b). 82 % release of GOx in the cancer cell-mimicking environment under an ACMF of 250 kHz and 450 Oe for 25 min was observed along with an enhanced tumoricidal effect. Although MHT along with cancer starvation therapy is considered to be an effectual cancer treatment, clinical studies are needed to further evaluate the safety and efficacy of this multi-modal approach in cancer patients.

The MHT efficacy is still limited with the thermal tolerance rising from overexpressed HSPs. ROS generation is one method for reducing HSP expression and subsequently leading to an enhanced cellular apoptosis. Sonodynamic therapy (SDT) employing nano sonosensitizers under acoustic irradiation (ultrasound) has been confirmed to be effective for ROS generation to ablate tumors [Fig. 15 (c)]. Commonly used sonosensitizers are porphyrins and their derivatives, phthalocyanines, TiO_2 NPs, mesoporous silica NPs, lipid-based NPs, polymeric NPs, albumin NPs, Au NPs, carbon-based NPs [275–279]. Ultrasound triggered SDT exhibits desirable merits of minimal invasiveness and increased tissue penetration depth. SDT consumes greater amount of tissue oxygen to generate ROS via sonoluminescence inducing cancer cell death. SDT in combination with MHT facilitates the therapeutic effects such as increased ROS generation for enhanced cell death, improved drug delivery, enhanced tumor penetration and combined cytotoxic effects. Zhang et al. [280] constructed a synergistic multifunctional HP-HIONs@PDA-PEG nanosystem comprising hollow IONPs, hematoporphyrin, polydopamine and PEG for evaluating synergistic efficacy of MHT-SDT for tumor therapy. In vitro and in vivo results revealed that IONPs loaded with hematoporphyrin efficiently respond to ultrasonic irradiation for enhanced ROS production, facilitating thermal tolerance via the cleavage of HSPs thereby enhancing magnetic performance. It was inferred that increased tissue penetration was achieved in case of MHT-SDT therapy in comparison with MHT-PTT and chemo MHT therapy. This nanosystem simultaneously overcomes the limitations associated with MHT and SDT alone and hence revealed the synergistic therapeutic efficacy. The ingenious combination SDT-assisted starvation therapy and SDT-assisted PTT therapy have also exhibited superiority in the therapeutical effect [281,282]. Though the combined MHT and SDT effect offers improved therapeutic outcomes for cancer treatment, further research is required to optimize the treatment parameters and understand the underlying mechanisms of synergy on various cancer types.

8. Concluding remarks and outlook

Despite a plethora of studies being conducted over the past few decades involving IONP-based cancer MHT, research translation into clinical trials still faces critical challenges and shortcomings. Factors such as non-selective heating, excessive local heating, and unwanted particle accumulation in vital organs of the body (post-MHT) are some of the major drawbacks of clinical HPT [16,47,283,284]. Therefore, sub-local tumoral temperature monitoring and precise control are prerequisites for an efficient and productive bench-to-bedside transition. The duration of heat exposure and the intensity of applied magnetic field are critical. A controlled increase in temperature over time can elicit selective damage to cancer cells. Repeated sessions of HPT may increase the efficacy of treatment while allowing healthy cells sufficient time to recover. The temperature of MNPs is controlled during MHT by adjusting the externally guided magnetic field parameters such as strength and frequency where the product of both should be within the biological tolerance limit known as Brezovich criterion [254] without harming any healthy cells. Optimal power dissipation in terms of heat energy in MHT determines the appropriate concentration of IONPs to be used.

Selecting appropriate MNPs with proper surface functionality, morphology control, biocompatibility/biodegradability are key parameters that strongly determine the therapeutic effectiveness. Recently, shape-anisotropic iron oxide nanostructures exhibiting exciting magneto-thermal properties have received significant attention due to their applications in cancer nanomedicine. Various morphologies of IONPs such as rods, rings, cubes, wire, tubes, ellipsoids and core-shell nanostructures can optimize the magnetic features owing to their shape anisotropy thereby enhancing the heating efficiency beneficial for MHT. For instance, iron oxide nanorings exhibited extraordinary SAR values (~2346 W/g), owing to their exciting shape-induced vortex-domain structure and improved magnetic properties [226]. These nanorings exhibited enhanced therapeutic efficiency for MHT treatment of a breast tumor in vivo without any conjugation of drugs or other combined therapies. Recent studies have contributed immensely, posing these shape- and surface-modified nanostructures as promising agents for MHT applications. Efforts need to be directed to fabricate this kind of smart nanostructures with exciting magnetic properties. Additionally, incorporating certain elements, like a nominal inclusion of rare earth (RE) ions such as gadolinium, cerium, erbium or yttrium into iron oxide spinel structure, could potentially upgrade the heating efficiency of these nanostructures [122]. Besides implementing sophisticated surface functionalization strategies or incorporating RE ions into MNPs to further boost their biomedical abilities, researchers must address toxicity concerns regarding ferrite-based nanocomposites and develop novel and innovative approaches to minimize potential harm. Consequently, much more advanced scientific research has to be administered further to explore the fundamental structure-property relationships of these nanostructures to better understand and utilize them for futuristic applications.

Sometimes, combinatorial therapy approaches such as MHT with conventional cancer therapies (radiation or chemotherapy) have been implemented to completely annihilate malignant tissues. Surface functionalization of IONPs with anticancer drugs to achieve a chemo-thermal therapy is an important aspect that needs special attention. The emerging therapies such as photothermal, starvation and sonodynamic therapy in conjunction with MHT have exhibited high feasibility and therapeutic effectiveness with meagre side effects. The intracellular heating mechanism as well as inhibition of toxicity related to ROS generation has to be explored for designing an effective heating power agent of magnetic nanostructures for such synergistic therapies. Fundamental cell (in vitro) studies/animal (in vivo) models must be conducted to analyze the endosomal escape efficiency of these nanostructures, which plays a pivotal role in the advanced stages of combinatorial clinical MHT [190,285]. In addition to the above-said combinational therapies, MHT can be used as an adjuvant treatment along with immunotherapy, gene therapy and personalized medicine which hold great promise in improving cancer treatment outcomes limiting its toxicity and side effects. Apart from cancer cell killing using heat, MNPs mediated MHT can also trigger an anti-tumor immune response thereby releasing tumor antigens and endogenous adjuvants such as HSPs and damage-associated molecular patterns, thereby aiding potential cancer therapy [286]. Immunotherapies are capable of preventing tumor recurrence and metastasis by stimulating and activating the antitumor immune system to attack tumor cells. However, the durable response due to this therapy is too low. It was reported that MHT with immunotherapy could result in systemic therapeutic responses for tumor metastasis inhibition [23]. Chao et al. [287] demonstrated that the combination of iron-based NPs mediated MHT with local injection of nano-adjuvant and systemic injection of anti-cytotoxic T lymphocyte

antigen-4 checkpoint blockade revealed tumor metastasis inhibition. Similarly, MHT in combination with gene therapy can complement their individual advantages to achieve a significant synergistic effect for an improved cancer therapeutic efficacy. MNPs are excellent candidates for gene delivery where MNPs are accumulated in the tumor cell and release the genes to improve the effectiveness by controlling gene expression through genetic editing. Yin et al. [288] reported core-shell structured MNPs to deliver and activate a heat-inducible gene vector which encodes tumor necrosis factor-related apoptosis-inducing ligand (TRAIL) in adipose-derived mesenchymal stem cells (AD-MSCs). These MNPs generate heat under the application of ACMF and TRAIL was selectively expressed thereby inducing significant ovarian cancer cell apoptosis in vitro and in vivo. Personalized medicine based MHT maximize cancer therapeutic effects while minimizing risks based on individual patient characteristics and specific tumor properties. Optimizing structural parameters of MNPs such as size, shape, composition and surface modification depending on specific tumor type, size, and location can enhance MHT efficacy and improve their targeting ability. Moreover, focus should be directed towards understanding specific biomarkers, thermal dose optimization and selection of suitable combination therapies (MHT + chemo/radiation/immunotherapy) for personalized medicine. Ongoing research and clinical trials are essential for validating such strategies and improving their implementation in clinical practice.

While IONPs hold great promise for MHT, thorough investigations into their safety profile, biodegradability, and long-term effects are essential. Safety of IONPs can vary based on size, surface coatings, and concentration of NPs used for MHT. Ongoing research will help establish protocols for their safe application in clinical settings. While optimizing IONPs for heating efficacy, it is imperative to address potential toxicity risks associated with these MNPs. In vitro and in vivo studies are essential to provide an initial assessment about the cytotoxicity and inflammatory responses of IONPs to determine its safety. Understanding the property of generating ROS to induce oxidative stress in biological systems is important for assessing safety of IONPs. IONPs are capable of degrading into non-toxic iron ions, which are naturally processed by the body. However, the rate of degradation can vary based on particle size and surface modification. Human body can eliminate IONPs via the RES, primarily through the liver and spleen. Research into the biodistribution and clearance of these particles helps inform their long-term safety. Although IONPs can degrade, there is still a risk of accumulation in organs, particularly if large doses are used. Long-term studies are needed to assess whether such chronic exposure leads to harmful effects. Prolonged interaction with tissues could result in fibrosis or other adverse conditions. Long-term biocompatibility studies can help elucidate these risks. Advancements in technology and regulatory frameworks are crucial for the successful clinical translation of MHT. Research efforts focused on understanding the biological mechanisms involved, optimizing treatment protocols, and enhancing safety profiles will be essential in establishing this technique as a mainstay in cancer therapy. Collaboration between researchers, clinicians, and regulatory bodies will play a key role in driving innovation and ensuring patient safety. Although randomized human clinical trials for the treatment of glioblastoma and prostate cancer have been conducted [28,69], factors such as uniform heating, temperature control, biocompatibility and clearance and depth of penetration to deep seated tumors have to be addressed via further research and development, which will be critical for advancing MHT as a feasible therapeutic option in clinical practice. To overcome these challenges, innovative advancements have to be made involving comprehensive cancer MHT studies, including those of scientists and medical professionals, which can make the clinical application of MNPs a viable option soon. Addressing the above-said limitations will assist in achieving efficient clinical translation of MNP-mediated cancer HPT to combat the global burden of cancer.

Funding

This research did not receive any specific grant from funding agencies in the public, commercial, or not-for-profit sectors.

CRediT authorship contribution statement

Arunima Rajan: Writing – original draft, Visualization, Conceptualization. **Suvra S. Laha:** Writing – review & editing. **Niroj Kumar Sahu:** Writing – review & editing. **Nanasaheb D. Thorat:** Writing – review & editing, Supervision. **Balakrishnan Shankar:** Writing – review & editing, Supervision.

Declaration of competing interest

The authors declare that they have no known competing financial interests or personal relationships that could have appeared to influence the work reported in this paper.

Acknowledgements

A.R. and B.S. would like to gratefully acknowledge the support and encouragement received from Amrita Vishwa Vidyapeetham, Amritapuri Campus.

Data availability

Data will be made available on request.

References

[1] H. Sung, J. Ferlay, R.L. Siegel, M. Laversanne, I. Soerjomataram, A. Jemal, F. Bray, Global cancer statistics 2020: GLOBOCAN estimates of incidence and mortality worldwide for 36 cancers in 185 countries, CA A Cancer J. Clin. 71 (3) (2021) 209–249.
[2] A.E. Yuzhalin, Redefining cancer research for therapeutic breakthroughs, Br. J. Cancer 130 (7) (2024) 1078–1082.
[3] Chapter 10 - cell cycle and cancer, in: S.R. Goodman (Ed.), Goodman's Medical Cell Biology, fourth ed., Academic Press, 2021, pp. 295–313.
[4] G.M. Cooper, The Cell: A Molecular Approach, second ed., 2000. Sinauer Associates 2000.
[5] R. Lugano, M. Ramachandran, A. Dimberg, Tumor angiogenesis: causes, consequences, challenges and opportunities, Cell. Mol. Life Sci. 77 (9) (2020) 1745–1770.
[6] M. Egeblad, E.S. Nakasone, Z. Werb, Tumors as organs: complex tissues that interface with the entire organism, Dev. Cell 18 (6) (2010) 884–901.
[7] R. Baskar, K.A. Lee, R. Yeo, K.-W. Yeoh, Cancer and radiation therapy: current advances and future directions, Int. J. Med. Sci. 9 (3) (2012) 193–199.
[8] D.T. Debela, S.G.Y. Muzazu, K.D. Heraro, M.T. Ndalama, B.W. Mesele, D.C. Haile, S.K. Kitui, T. Manyazewal, New Approaches and Procedures for Cancer Treatment: Current Perspectives, vol. 9, SAGE Open Medicine, 2021 20503121211034366.
[9] M. Eslami, O. Memarsadeghi, A. Davarpanah, A. Arti, K. Nayernia, B. Behnam, Overcoming chemotherapy resistance in metastatic cancer: a comprehensive review, Biomedicines 12 (1) (2024) 183.
[10] M. Tangsiri, A. Hheidari, M. Liaghat, M. Razlansari, N. Ebrahimi, A. Akbari, S.M. N. Varnosfaderani, F. Maleki-Sheikhabadi, A. Norouzi, M. Bakhtiyari, H. Zalpoor, M. Nabi-Afjadi, A. Rahdar, Promising applications of nanotechnology in inhibiting chemo-resistance in solid tumors by targeting epithelial-mesenchymal transition (EMT), Biomed. Pharmacother. 170 (2024) 115973.
[11] A. Rismanbaf, Improving targeted small molecule drugs to overcome chemotherapy resistance, Cancer Reports 7 (1) (2024) e1945.
[12] S. Kumar, A. Daverey, N.K. Sahu, D. Bahadur, In vitro evaluation of PEGylated mesoporous MgFe2O4 magnetic nanoassemblies (MMNs) for chemo-thermal therapy, J. Mater. Chem. B 1 (30) (2013) 3652–3660.
[13] N. Taefehshokr, B. Baradaran, A. Baghbanzadeh, S. Taefehshokr, Promising approaches in cancer immunotherapy, Immunobiology 225 (2) (2020) 151875.
[14] M.A. Cheever, C.S. Higano, PROVENGE (Sipuleucel-T) in prostate cancer: the first FDA-approved therapeutic cancer vaccine, Clin. Cancer Res. 17 (11) (2011) 3520–3526.
[15] A. Baeza, Tumor targeted nanocarriers for immunotherapy, Molecules 25 (7) (2020) 1508.
[16] M. Mallory, E. Gogineni, G.C. Jones, L. Greer, C.B. Simone, Therapeutic hyperthermia: the old, the new, and the upcoming, Crit. Rev. Oncol. Hematol. 97 (2016) 56–64.
[17] J. Crezee, N.A.P. Franken, A.L. Oei, Hyperthermia-based anti-cancer treatments, Cancers 13 (6) (2021) 1240.

[18] X. Tang, F. Cao, W. Ma, Y. Tang, B. Aljahdali, M. Alasir, i.E. Salih, S. Dibart, Cancer cells resist hyperthermia due to its obstructed activation of caspase 3, Rep. Practical Oncol. Radiother. 25 (3) (2020) 323–326.

[19] G.Y. Yi, M.J. Kim, H.I. Kim, J. Park, S.H. Baek, Hyperthermia treatment as a promising anti-cancer strategy: therapeutic targets, perspective mechanisms and synergistic combinations in experimental approaches, Antioxidants 11 (4) (2022) 625.

[20] Y. Yang, L. Huangfu, H. Li, D. Yang, Research progress of hyperthermia in tumor therapy by influencing metabolic reprogramming of tumor cells, Int. J. Hyperther. 40 (1) (2023) 2270654.

[21] G. Hegyi, G.P. Szigeti, A. Szász, Hyperthermia versus oncothermia: cellular effects in complementary cancer therapy, Evid. base Compl. Alternative Med. 2013 (1) (2013) 672873.

[22] A. Szasz, Heterogeneous heat absorption is complementary to radiotherapy, Cancers 14 (4) (2022) 901.

[23] X. Liu, Y. Zhang, Y. Wang, W. Zhu, G. Li, X. Ma, Y. Zhang, S. Chen, S. Tiwari, K. Shi, S. Zhang, H.M. Fan, Y.X. Zhao, X.-J. Liang, Comprehensive understanding of magnetic hyperthermia for improving antitumor therapeutic efficacy, Theranostics 10 (8) (2020) 3793–3815.

[24] I. Rubia-Rodríguez, A. Santana-Otero, S. Spassov, E. Tombácz, C. Johansson, P. De La Presa, F.J. Teran, M.D. Morales, S. Veintemillas-Verdaguer, N.T. K. Thanh, M.O. Besenhard, C. Wilhelm, F. Gazeau, Q. Harmer, E. Mayes, B. B. Manshian, S.J. Soenen, Y. Gu, Á. Millán, E.K. Efthimiadou, J. Gaudet, P. Goodwill, J. Mansfield, U. Steinhoff, J. Wells, F. Wiekhorst, D. Ortega, Whither magnetic hyperthermia? A tentative roadmap, Materials 14 (4) (2021) 706.

[25] H. Gavilán, S.K. Avugadda, T. Fernández-Cabada, N. Soni, M. Cassani, B.T. Mai, R. Chantrell, T. Pellegrino, Magnetic nanoparticles and clusters for magnetic hyperthermia: optimizing their heat performance and developing combinatorial therapies to tackle cancer, Chem. Soc. Rev. 50 (20) (2021) 11614–11667.

[26] Y. Luengo, Z.V. Díaz-Riascos, D. García-Soriano, F.J. Teran, E.J. Artés-Ibáñez, O. Ibarrola, Á. Somoza, R. Miranda, S. Schwartz, I. Abasolo, G. Salas, Fine control of in vivo magnetic hyperthermia using iron oxide nanoparticles with different coatings and degree of aggregation, Pharmaceutics 14 (8) (2022) 1526.

[27] S. Healy, A.F. Bakuzis, P.W. Goodwill, A. Attaluri, J.W.M. Bulte, R. Ivkov, Clinical magnetic hyperthermia requires integrated magnetic particle imaging, WIREs Nanomedicine and Nanobiotechnology 14 (3) (2022) e1779.

[28] M. Johannsen, U. Gneveckow, B. Thiesen, K. Taymoorian, C.H. Cho, N. Waldöfner, R. Scholz, A. Jordan, S.A. Loening, P. Wust, Thermotherapy of prostate cancer using magnetic nanoparticles: feasibility, imaging, and three-dimensional temperature distribution, Eur. Urol. 52 (6) (2007) 1653–1662.

[29] K. Maier-Hauff, F. Ulrich, D. Nestler, H. Niehoff, P. Wust, B. Thiesen, H. Orawa, V. Budach, A. Jordan, Efficacy and safety of intratumoral thermotherapy using magnetic iron-oxide nanoparticles combined with external beam radiotherapy on patients with recurrent glioblastoma multiforme, J. Neuro Oncol. 103 (2) (2011) 317–324.

[30] A. Matsumine, K. Kusuzaki, T. Matsubara, K. Shintani, H. Satonaka, T. Wakabayashi, S. Miyazaki, K. Morita, K. Takegami, A. Uchida, Novel hyperthermia for metastatic bone tumors with magnetic materials by generating an alternating electromagnetic field, Clin. Exp. Metastasis 24 (3) (2007) 191–200.

[31] Z. Hedayatnasab, F. Abnisa, W.M.A.W. Daud, Review on magnetic nanoparticles for magnetic nanofluid hyperthermia application, Mater. Des. 123 (2017) 174–196.

[32] S. Zhao, X. Yu, Y. Qian, W. Chen, J. Shen, Multifunctional magnetic iron oxide nanoparticles: an advanced platform for cancer theranostics, Theranostics 10 (14) (2020) 6278–6309.

[33] T.I. Shabatina, O.I. Vernaya, N.L. Shimanovskiy, M.Y. Melnikov, Metal and metal oxides nanoparticles and nanosystems in anticancer and antiviral theragnostic agents, Pharmaceutics 15 (4) (2023) 1181.

[34] M.E. Lorkowski, P.U. Atukorale, K.B. Ghaghada, E. Karathanasis, Stimuli-Responsive iron oxide nanotheranostics: a versatile and powerful approach for cancer therapy, Adv. Healthcare Mater. 10 (5) (2021) 2001044.

[35] J. Nowak-Jary, B. Machnicka, Pharmacokinetics of magnetic iron oxide nanoparticles for medical applications, J. Nanobiotechnol. 20 (1) (2022) 305.

[36] N. Zhu, H. Ji, P. Yu, J. Niu, M.U. Farooq, M.W. Akram, I.O. Udego, H. Li, X. Niu, Surface modification of magnetic iron oxide nanoparticles, Nanomaterials 8 (10) (2018) 810.

[37] P. Kush, P. Kumar, R. Singh, A. Kaushik, Aspects of high-performance and bio-acceptable magnetic nanoparticles for biomedical application, Asian J. Pharm. Sci. 16 (6) (2021) 704–737.

[38] A. Rajan, N.K. Sahu, Review on magnetic nanoparticle-mediated hyperthermia for cancer therapy, J. Nanoparticle Res. 22 (11) (2020) 319.

[39] B. Rezaei, A. Harun, X. Wu, P.R. Iyer, S. Mostufa, S. Ciannella, I.H. Karampelas, J. Chalmers, I. Srivastava, J. Gómez-Pastora, K. Wu, Effect of polymer and cell membrane coatings on theranostic applications of nanoparticles: a review, Advanced Healthcare Materials n/a (n/a) (2024) 2401213.

[40] P. Das, M. Colombo, D. Prosperi, Recent advances in magnetic fluid hyperthermia for cancer therapy, Colloids Surf. B Biointerfaces 174 (2019) 42–55.

[41] M.J. Molaei, Magnetic hyperthermia in cancer therapy, mechanisms, and recent advances: a review, J. Biomater. Appl. 39 (1) (2024) 3–23.

[42] M. Kacem, A. Essoumhi, M. Dib, Magnetic iron oxide-based materials and their hyperthermia application: a review, Inorg. Chem. Commun. 166 (2024) 112510.

[43] L. Zhang, Q. Li, J. Liu, Z. Deng, X. Zhang, N. Alifu, X. Zhang, Z. Yu, Y. Liu, Z. Lan, T. Wen, K. Sun, Recent advances in functionalized ferrite nanoparticles: from fundamentals to magnetic hyperthermia cancer therapy, Colloids Surf. B Biointerfaces 234 (2024) 113754.

[44] V. Vijayakanth, K. Chintagumpala, A review on an effect of dispersant type and medium viscosity on magnetic hyperthermia of nanoparticles, Polym. Bull. 80 (5) (2023) 4737–4781.

[45] J. van der Zee, Heating the patient: a promising approach? Ann. Oncol. 13 (8) (2002) 1173–1184.

[46] N. Papavramidou, T. Papavramidis, T. Demetriou, Ancient Greek and greco–roman methods in modern surgical treatment of cancer, Ann. Surg Oncol. 17 (3) (2010) 665–667.

[47] A. Markota, Ž. Kalamar, J. Fluher, S. Pirkmajer, Therapeutic hyperthermia for the treatment of infection—a narrative review, Front. Physiol. 14 (2023).

[48] I.J. Spiro, D.L. Denman, W.C. Dewey, Effect of hyperthermia on isolated DNA polymerase-β, Radiat. Res. 95 (1) (1983) 68–77.

[49] H.K. Matthews, C. Bertoli, R.A.M. de Bruin, Cell cycle control in cancer, Nat. Rev. Mol. Cell Biol. 23 (1) (2022) 74–88.

[50] K. Collins, T. Jacks, N.P. Pavletich, The cell cycle and cancer, Proc. Natl. Acad. Sci. USA 94 (7) (1997) 2776–2778.

[51] N.M. Kühl, L. Rensing, Heat shock effects on cell cycle progression, Cellular and Molecular Life Sciences CMLS 57 (3) (2000) 450–463.

[52] N.R. Datta, S.G. Ordóñez, U.S. Gaipl, M.M. Paulides, H. Crezee, J. Gellermann, D. Marder, E. Puric, S. Bodis, Local hyperthermia combined with radiotherapy and-/or chemotherapy: recent advances and promises for the future, Cancer Treat Rev. 41 (9) (2015) 742–753.

[53] Y. Cheng, S. Weng, L. Yu, N. Zhu, M. Yang, Y. Yuan, The role of hyperthermia in the multidisciplinary treatment of malignant tumors, Integr. Cancer Ther. 18 (2019) 1534735419876345.

[54] T.-M. Liu, J. Conde, T. Lipiński, A. Bednarkiewicz, C.-C. Huang, Revisiting the classification of NIR-absorbing/emitting nanomaterials for in vivo bioapplications, NPG Asia Mater. 8 (8) (2016), 295-e295.

[55] X. Huang, I.H. El-Sayed, W. Qian, M.A. El-Sayed, Cancer cell imaging and photothermal therapy in the near-infrared region by using gold nanorods, J. Am. Chem. Soc. 128 (6) (2006) 2115–2120.

[56] D. Kim, H. Kim, Optimization of photothermal therapy treatment effect under various laser irradiation conditions, Int. J. Mol. Sci. 23 (11) (2022) 5928.

[57] L.A. Dombrovsky, Laser-induced thermal treatment of superficial human tumors: an advanced heating strategy and non-arrhenius law for living tissues, Frontiers in Thermal Engineering 1 (2022).

[58] A.J. Schupper, T. Chanenchuk, A. Racanelli, G. Price, C.G. Hadjipanayis, Laser hyperthermia: past, present, and future, Neuro Oncol. 24 (Supplement_6) (2022) S42–S51.

[59] B. Prasad, J.K. Kim, S. Kim, Role of simulations in the treatment planning of radiofrequency hyperthermia therapy in clinics, Journal of Oncology 2019 (1) (2019) 9685476.

[60] J.R.J. Paré, J.M.R. Bélanger, G. Cormier, D. Foucher, A. Thériault, J.-C. Savoie, J.-F. Rochas, Microwave-assisted chemical ablation (MA-CA): a novel microwave-assisted tissue ablation procedure—preliminary assessment of efficiency, Appl. Sci. 13 (12) (2023) 7177.

[61] N.S. Awad, V. Paul, N.M. AlSawaftah, G. ter Haar, T.M. Allen, W.G. Pitt, G. A. Husseini, Ultrasound-Responsive nanocarriers in cancer treatment: a review, ACS Pharmacol. Transl. Sci. 4 (2) (2021) 589–612.

[62] Y. Liang, S. Zhang, D. Wang, P. Ji, B. Zhang, P. Wu, L. Wang, Z. Liu, J. Wang, Y. Duan, L. Yuan, Dual-functional nanodroplet for tumor vasculature ultrasound imaging and tumor immunosuppressive microenvironment remodeling, Advanced Healthcare Materials n/a (n/a) (2024) 2401274.

[63] H. Chen, J. Burnett, F. Zhang, J. Zhang, H. Paholak, D. Sun, Highly crystallized iron oxide nanoparticles as effective and biodegradable mediators for photothermal cancer therapy, J. Mater. Chem. B 2 (7) (2014) 757–765.

[64] P. Liang, L. Mao, Y. Dong, Z. Zhao, Q. Sun, M. Mazhar, Y. Ma, S. Yang, W. Ren, Design and application of near-infrared nanomaterial-liposome hybrid nanocarriers for cancer photothermal therapy, Pharmaceutics 13 (12) (2021) 2070.

[65] P. Zhou, H. Zhao, Q. Wang, Z. Zhou, J. Wang, G. Deng, X. Wang, Q. Liu, H. Yang, S. Yang, Photoacoustic-enabled self-guidance in magnetic-hyperthermia Fe@Fe3O4 nanoparticles for theranostics in vivo, Adv. Healthcare Mater. 7 (9) (2018) 1701201.

[66] Z. Zhou, Y. Sun, J. Shen, J. Wei, C. Yu, B. Kong, W. Liu, H. Yang, S. Yang, W. Wang, Iron/iron oxide core/shell nanoparticles for magnetic targeting MRI and near-infrared photothermal therapy, Biomaterials 35 (26) (2014) 7470–7478.

[67] S. Cabana, A. Curcio, A. Michel, C. Wilhelm, A. Abou-Hassan, Iron oxide mediated photothermal therapy in the second biological window: a comparative study between magnetite/maghemite nanospheres and nanoflowers, Nanomaterials 10 (8) (2020) 1548.

[68] M. Peiravi, H. Eslami, M. Ansari, H. Zare-Zardini, Magnetic hyperthermia: potentials and limitations, J. Indian Chem. Soc. 99 (1) (2022) 100269.

[69] K. Maier-Hauff, R. Rothe, R. Scholz, U. Gneveckow, P. Wust, B. Thiesen, A. Feussner, A. von Deimling, N. Waldoefner, R. Felix, A. Jordan, Intracranial thermotherapy using magnetic nanoparticles combined with external beam radiotherapy: results of a feasibility study on patients with glioblastoma multiforme, J. Neuro Oncol. 81 (1) (2007) 53–60.

[70] R.K. Gilchrist, R. Medal, W.D. Shorey, R.C. Hanselman, J.C. Parrott, C.B. Taylor, Selective inductive heating of lymph nodes, Ann. Surg. 146 (4) (1957).

[71] S. Tong, C.A. Quinto, L. Zhang, P. Mohindra, G. Bao, Size-dependent heating of magnetic iron oxide nanoparticles, ACS Nano 11 (7) (2017) 6808–6816.

[72] A. Jordan, P. Wust, H. Fähling, W. John, A. Hinz, R. Felix, Inductive heating of ferrimagnetic particles and magnetic fluids: physical evaluation of their potential for hyperthermia, Int. J. Hyperther. 9 (1) (1993) 51–68.

[73] D.C.F. Chan, D.B. Kirpotin, P.A. Bunn, Synthesis and evaluation of colloidal magnetic iron oxides for the site-specific radiofrequency-induced hyperthermia of cancer, J. Magn. Magn Mater. 122 (1) (1993) 374–378.
[74] R. Bushra, M. Ahmad, K. Alam, F. Seidi, Qurtulen, S. Shakeel, J. Song, Y. Jin, H. Xiao, Recent advances in magnetic nanoparticles: key applications, environmental insights, and future strategies, Sustainable Materials and Technologies (2024) e00985.
[75] M. Szwed, A. Marczak, Application of nanoparticles for magnetic hyperthermia for cancer treatment—the current state of knowledge, Cancers 16 (6) (2024) 1156.
[76] V. Vijayan, A. Sundaram, A. Vasukutty, R. Bardhan, S. Uthaman, I.-K. Park, Tumor-targeting cell membrane-coated nanorings for magnetic-hyperthermia-induced tumor ablation, Biomater. Sci. 11 (21) (2023) 7188–7202.
[77] A.I. Rezk, Y.-H. Kim, S. Chun, C.H. Park, C.S. Kim, Thermo-responsive-polymeric-gates of poly(N-isopropylacrylamide)/N-(hydroxymethyl)acrylamide coated magnetic nanoparticles as a synergistic approach to cancer therapy: drug release and kinetics models of chemothermal magnetic nanoparticles, Mater. Des. 234 (2023) 112350.
[78] I.M. Obaidat, B. Issa, Y. Haik, Magnetic properties of magnetic nanoparticles for efficient hyperthermia, Nanomaterials (2015) 63–89.
[79] A.C. Horta, P. André, J.S. Amaral, C.O. Amorim, Curie temperature control in Zn-Fe ferrite superparamagnetic nanoparticles, J. Magn. Magn Mater. 610 (2024) 172497.
[80] G. Niraula, C. Wu, X. Yu, S. Malik, D.S. Verma, R. Yang, B. Zhao, S. Ding, W. Zhang, S.K. Sharma, The Curie temperature: a key playmaker in self-regulated temperature hyperthermia, J. Mater. Chem. B 12 (2) (2024) 286–331.
[81] J. Giri, A. Ray, S. Dasgupta, D. Datta, D. Bahadur, Investigation on T c tuned nano particles of magnetic oxides for hyperthermia applications, Bio Med. Mater. Eng. 13 (2003) 387–399.
[82] V. Reichel, A. Kovács, M. Kumari, É. Bereczk-Tompa, E. Schneck, P. Diehle, M. Pósfai, A.M. Hirt, M. Duchamp, R.E. Dunin-Borkowski, D. Faivre, Single crystalline superstructured stable single domain magnetite nanoparticles, Sci. Rep. 7 (1) (2017) 45484.
[83] Y.-w. Jun, Y.-M. Huh, J.-s. Choi, J.-H. Lee, H.-T. Song, S. Kim, S. Yoon, K.-S. Kim, J.-S. Shin, J.-S. Suh, J. Cheon, Nanoscale size effect of magnetic nanocrystals and their utilization for cancer diagnosis via magnetic resonance imaging, J. Am. Chem. Soc. 127 (16) (2005) 5732–5733.
[84] Q. Li, C.W. Kartikowati, S. Horie, T. Ogi, T. Iwaki, K. Okuyama, Correlation between particle size/domain structure and magnetic properties of highly crystalline Fe3O4 nanoparticles, Sci. Rep. 7 (1) (2017) 9894.
[85] B. Issa, I.M. Obaidat, B.A. Albiss, Y. Haik, Magnetic nanoparticles: surface effects and properties related to biomedicine applications, Int. J. Mol. Sci. (2013) 21266–21305.
[86] N. Sezer, İ. Arı, Y. Biçer, M. Koç, Superparamagnetic nanoarchitectures: multimodal functionalities and applications, J. Magn. Magn Mater. 538 (2021) 168300.
[87] B. Mehdaoui, A. Meffre, J. Carrey, S. Lachaize, L.-M. Lacroix, M. Gougeon, B. Chaudret, M. Respaud, Optimal size of nanoparticles for magnetic hyperthermia: a combined theoretical and experimental study, Adv. Funct. Mater. 21 (23) (2011) 4573–4581.
[88] D. Chenthamara, S. Subramaniam, S.G. Ramakrishnan, S. Krishnaswamy, M. M. Essa, F.-H. Lin, M.W. Qoronfleh, Therapeutic efficacy of nanoparticles and routes of administration, Biomater. Res. 23 (1) (2019) 20.
[89] S. Barua, S. Mitragotri, Challenges associated with penetration of nanoparticles across cell and tissue barriers: a review of current status and future prospects, Nano Today 9 (2) (2014) 223–243.
[90] H.H. Gustafson, D. Holt-Casper, D.W. Grainger, H. Ghandehari, Nanoparticle uptake: the phagocyte problem, Nano Today 10 (4) (2015) 487–510.
[91] N. Hoshyar, S. Gray, H. Han, G. Bao, The effect of nanoparticle size on in vivo pharmacokinetics and cellular interaction, Nanomedicine 11 (6) (2016) 673–692.
[92] S.V. Spirou, S.A. Costa Lima, P. Bouziotis, S. Vranješ-Djurić, E.K. Efthimiadou, A. Laurenzana, A.I. Barbosa, I. Garcia-Alonso, C. Jones, D. Jankovic, O.L. Gobbo, Recommendations for in vitro and in vivo testing of magnetic nanoparticle hyperthermia combined with radiation therapy, Nanomaterials 8 (5) (2018) 306.
[93] F. Reyes-Ortega, Á.V. Delgado, G.R. Iglesias, Modulation of the magnetic hyperthermia response using different superparamagnetic iron oxide nanoparticle morphologies, Nanomaterials 11 (3) (2021) 627.
[94] R.E. Rosensweig, Heating magnetic fluid with alternating magnetic field, J. Magn. Magn Mater. 252 (2002) 370–374.
[95] P.C. Fannin, An experimental observation of the dynamic behaviour of ferrofluids, J. Magn. Magn Mater. 136 (1) (1994) 49–58.
[96] S. Laurent, S. Dutz, U.O. Häfeli, M. Mahmoudi, Magnetic fluid hyperthermia: focus on superparamagnetic iron oxide nanoparticles, Adv. Colloid Interface Sci. 166 (1) (2011) 8–23.
[97] Y. Song, D. Li, Y. Lu, K. Jiang, Y. Yang, Y. Xu, L. Dong, X. Yan, D. Ling, X. Yang, S.-H. Yu, Ferrimagnetic mPEG-b-PHEP copolymer micelles loaded with iron oxide nanocubes and emodin for enhanced magnetic hyperthermia–chemotherapy, Natl. Sci. Rev. 7 (4) (2020) 723–736.
[98] J. Sung Lee, J. Myung Cha, H. Young Yoon, J.-K. Lee, Y. Keun Kim, Magnetic multi-granule nanoclusters: a model system that exhibits universal size effect of magnetic coercivity, Sci. Rep. 5 (1) (2015) 12135.
[99] P.B. Kharat, S.B. Somvanshi, P.P. Khirade, K.M. Jadhav, Induction heating analysis of surface-functionalized nanoscale CoFe2O4 for magnetic fluid hyperthermia toward noninvasive cancer treatment, ACS Omega 5 (36) (2020) 23378–23384.
[100] S.J. Salih, W.M. Mahmood, Review on magnetic spinel ferrite (MFe2O4) nanoparticles: from synthesis to application, Heliyon 9 (6) (2023) e16601.
[101] M.P. Ghosh, N.J. Mondal, R. Sonkar, B. Boro, J.P. Borah, D. Chowdhury, Sm doped Cu–Ni spinel ferrite nanoparticles for hyperthermia and photocatalytic applications, ACS Appl. Nano Mater. 7 (7) (2024) 7028–7042.
[102] P.K. Baruah, N. Mukherjee, B. Bhagat, K. Mukherjee, Wet chemical synthesis of cubic spinel ferrites: a review addressing phase formation behavior and nanostructuring, Cryst. Growth Des. 24 (3) (2024) 1504–1528.
[103] A. Rajan, R.K. Chandunika, F. Raju, R. Joshi, N.K. Sahu, R.S. Ningthoujam, Synthesis and processing of magnetic-based nanomaterials for biomedical applications, in: A.K. Tyagi, R.S. Ningthoujam (Eds.), Handbook on Synthesis Strategies for Advanced Materials: Volume-II: Processing and Functionalization of Materials, Springer Nature Singapore, Singapore, 2022, pp. 659–714.
[104] A.G. Leonel, A.A.P. Mansur, H.S. Mansur, Advanced functional nanostructures based on magnetic iron oxide nanomaterials for water remediation: a review, Water Res. 190 (2021) 116693.
[105] J. de Oliveira, M.B. Denadai, D.L. Costa, Crosstalk between heme oxygenase-1 and iron metabolism in macrophages: implications for the modulation of inflammation and immunity, Antioxidants 11 (5) (2022) 861.
[106] A. Włodarczyk, S. Gorgoń, A. Radoń, K. Bajdak-Rusinek, Magnetite nanoparticles in magnetic hyperthermia and cancer therapies: challenges and perspectives, Nanomaterials 12 (11) (2022) 1807.
[107] R. Sun, H. Chen, J. Zheng, T. Yoshitomi, N. Kawazoe, Y. Yang, G. Chen, Composite scaffolds of gelatin and Fe3O4 nanoparticles for magnetic hyperthermia-based breast cancer treatment and adipose tissue regeneration, Adv. Healthcare Mater. 12 (9) (2023) 2202604.
[108] E. Bertuit, N. Menguy, C. Wilhelm, A.-L. Rollet, A. Abou-Hassan, Angular orientation between the cores of iron oxide nanoclusters controls their magneto–optical properties and magnetic heating functions, Commun. Chem. 5 (1) (2022) 164.
[109] E. Bertuit, E. Benassai, G. Mériguet, J.-M. Greneche, B. Baptiste, S. Neveu, C. Wilhelm, A. Abou-Hassan, Structure–property–function relationships of iron oxide multicore nanoflowers in magnetic hyperthermia and photothermia, ACS Nano 16 (1) (2022) 271–284.
[110] D.A. Rivani, I. Retnosari, Kusumandari, T.E. Saraswati, Influence of TiO2 addition on the magnetic properties of carbon-based iron oxide nanocomposites synthesized using submerged arc-discharge, IOP Conf. Ser. Mater. Sci. Eng. 509 (1) (2019) 012034.
[111] F. Arteaga-Cardona, K. Rojas-Rojas, R. Costo, M.A. Mendez-Rojas, A. Hernando, P. de la Presa, Improving the magnetic heating by disaggregating nanoparticles, J. Alloys Compd. 663 (2016) 636–644.
[112] A. Zeleňáková, Ľ. Nagy, P. Hrubovčák, M. Barutiak, M. Lisnichuk, V. Huntošová, A. Mrakovič, M. Gerina, D. Zákutná, Cobalt-ferrite nano-cubes for magnetic hyperthermia applications, J. Alloys Compd. 989 (2024) 174415.
[113] S.K. Paswan, P. Kumar, S. Kumari, S. Datta, M. Kar, J.P. Borah, L. Kumar, Temperature dependent magnetic and electrical transport properties of lanthanum and samarium substituted nanocrystalline nickel ferrite and their hyperthermia applications, J. Alloys Compd. 973 (2024) 172830.
[114] S.A. Patil, T.C. Gavandi, M.V. Londhe, A.B. Salunkhe, A.K. Jadhav, V.M. Khot, Manganese iron oxide nanoparticles for magnetic hyperthermia, antibacterial and ROS generation performance, J. Cluster Sci. 35 (5) (2024) 1405–1415.
[115] S. Mohana, S. Sumathi, Agaricus bisporus mediated synthesis of cobalt ferrite, copper ferrite and zinc ferrite nanoparticles for hyperthermia treatment and drug delivery, J. Cluster Sci. 35 (1) (2024) 129–142.
[116] G. Nandhini, M.K. Shobana, Effect of moringa oleifera with pure and Zn-doped Mn and Ni nanoferrites for hyperthermia applications, Mater. Today Commun. 39 (2024) 109046.
[117] K.P. Hazarika, C. Borgohain, J.P. Borah, Influence of controlled dipolar interaction for polymer-coated Gd-doped magnetite nanoparticles toward magnetic hyperthermia application, ACS Omega 9 (6) (2024) 6696–6708.
[118] P. Sahoo, P. Choudhary, S.S. Laha, A. Dixit, O.T. Mefford, Recent advances in zinc ferrite (ZnFe2O4) based nanostructures for magnetic hyperthermia applications, Chem. Commun. 59 (81) (2023) 12065–12090.
[119] S.K. Shaw, S.K. Alla, S.S. Meena, R.K. Mandal, N.K. Prasad, Stabilization of temperature during magnetic hyperthermia by Ce substituted magnetite nanoparticles, J. Magn. Magn Mater. 434 (2017) 181–186.
[120] J. de Jesús Ibarra–Sánchez, T. López–Luke, G. Ramírez–García, S. Sidhik, T. Córdova–Fraga, J. de Jesús Bernal–Alvarado, M.E. Cano, A. Torres–Castro, E. de la Rosa, Synthesis and characterization of Fe3O4:Yb3+:Er3+ nanoparticles with magnetic and optical properties for hyperthermia applications, J. Magn. Magn Mater. 465 (2018) 406–411.
[121] P. Kowalik, J. Mikulski, A. Borodziuk, M. Duda, I. Kamińska, K. Zajdel, J. Rybusinski, J. Szczytko, T. Wojciechowski, K. Sobczak, R. Minikayev, M. Kulpa-Greszta, R. Pazik, P. Grzaczkowska, K. Fronc, M. Lapinski, M. Frontczak-Baniewicz, B. Sikora, Yttrium-doped iron oxide nanoparticles for magnetic hyperthermia applications, J. Phys. Chem. C 124 (12) (2020) 6871–6883.
[122] S.S. Laha, N.D. Thorat, G. Singh, C.I. Sathish, J. Yi, A. Dixit, A. Vinu, Rare-earth doped iron oxide nanostructures for cancer theranostics: magnetic hyperthermia and magnetic resonance imaging, Small 18 (11) (2022) 2104855.
[123] K.K. Kefeni, T.A.M. Msagati, T.T.I. Nkambule, B.B. Mamba, Spinel ferrite nanoparticles and nanocomposites for biomedical applications and their toxicity, Mater. Sci. Eng. C 107 (2020) 110314.
[124] B. Thiesen, A. Jordan, Clinical applications of magnetic nanoparticles for hyperthermia, Int. J. Hyperther. 24 (6) (2008) 467–474.
[125] X.L. Liu, C.T. Ng, P. Chandrasekharan, H.T. Yang, L.Y. Zhao, E. Peng, Y.B. Lv, W. Xiao, J. Fang, J.B. Yi, H. Zhang, K.-H. Chuang, B.H. Bay, J. Ding, H.M. Fan,

Synthesis of ferromagnetic Fe0.6Mn0.4O nanoflowers as a new class of magnetic theranostic platform for in vivo T1-T2 dual-mode magnetic resonance imaging and magnetic hyperthermia therapy, Adv. Healthcare Mater. 5 (16) (2016) 2092–2104.
[126] C. Caro, C. Guzzi, I. Moral-Sánchez, J.D. Urbano-Gámez, A.M. Beltrán, M. L. García-Martín, Smart design of ZnFe and ZnFe@Fe nanoparticles for MRI-tracked magnetic hyperthermia therapy: challenging classical theories of nanoparticles growth and nanomagnetism, Adv. Healthcare Mater. 13 (12) (2024) 2304044.
[127] C. He, Y. Hu, L. Yin, C. Tang, C. Yin, Effects of particle size and surface charge on cellular uptake and biodistribution of polymeric nanoparticles, Biomaterials 31 (13) (2010) 3657–3666.
[128] K. Malhotra, B. Kumar, P.A.E. Piunno, U.J. Krull, Cellular uptake of upconversion nanoparticles based on surface polymer coatings and protein corona, ACS Appl. Mater. Interfaces 16 (28) (2024) 35985–36001.
[129] D. Zhang, L. Wei, M. Zhong, L. Xiao, H.-W. Li, J. Wang, The morphology and surface charge-dependent cellular uptake efficiency of upconversion nanostructures revealed by single-particle optical microscopy, Chem. Sci. 9 (23) (2018) 5260–5269.
[130] Y. Portilla, Y. Fernández-Afonso, S. Pérez-Yagüe, V. Mulens-Arias, M.P. Morales, L. Gutiérrez, D.F. Barber, Different coatings on magnetic nanoparticles dictate their degradation kinetics in vivo for 15 months after intravenous administration in mice, J. Nanobiotechnol. 20 (1) (2022) 543.
[131] L.K. Bogart, A. Taylor, Y. Cesbron, P. Murray, R. Lévy, Photothermal microscopy of the core of dextran-coated iron oxide nanoparticles during cell uptake, ACS Nano 6 (7) (2012) 5961–5971.
[132] H. Khurshid, J. Alonso, Z. Nemati, M.H. Phan, P. Mukherjee, M.L. Fdez-Gubieda, J.M. Barandiarán, H. Srikanth, Anisotropy effects in magnetic hyperthermia: a comparison between spherical and cubic exchange-coupled FeO/Fe3O4 nanoparticles, J. Appl. Phys. 117 (17) (2015) 17A337.
[133] C. Martinez-Boubeta, K. Simeonidis, A. Makridis, M. Angelakeris, O. Iglesias, P. Guardia, A. Cabot, L. Yedra, S. Estradé, F. Peiró, Z. Saghi, P.A. Midgley, I. Conde-Leborán, D. Serantes, D. Baldomir, Learning from nature to improve the heat generation of iron-oxide nanoparticles for magnetic hyperthermia applications, Sci. Rep. 3 (1) (2013) 1652.
[134] P.B. Balakrishnan, N. Silvestri, T. Fernandez-Cabada, F. Marinaro, S. Fernandes, S. Fiorito, M. Miscuglio, D. Serantes, S. Ruta, K. Livesey, O. Hovorka, R. Chantrell, T. Pellegrino, Exploiting unique alignment of cobalt ferrite nanoparticles, mild hyperthermia, and controlled intrinsic cobalt toxicity for cancer therapy, Adv. Mater. 32 (45) (2020) 2003712.
[135] D. Serantes, K. Simeonidis, M. Angelakeris, O. Chubykalo-Fesenko, M. Marciello, M.d.P. Morales, D. Baldomir, C. Martinez-Boubeta, Multiplying magnetic hyperthermia response by nanoparticle assembling, J. Phys. Chem. C 118 (11) (2014) 5927–5934.
[136] R. Das, J. Alonso, Z. Nemati Porshokouh, V. Kalappattil, D. Torres, M.-H. Phan, E. Garaio, J.Á. García, J.L. Sanchez Llamazares, H. Srikanth, Tunable high aspect ratio iron oxide nanorods for enhanced hyperthermia, J. Phys. Chem. C 120 (18) (2016) 10086–10093.
[137] A. Rajan, N.K. Sahu, Hydrophobic-to-Hydrophilic transition of Fe3O4 nanorods for magnetically induced hyperthermia, ACS Appl. Nano Mater. 4 (5) (2021) 4642–4653.
[138] H. Gao, T. Zhang, Y. Zhang, Y. Chen, B. Liu, J. Wu, X. Liu, Y. Li, M. Peng, Y. Zhang, G. Xie, F. Zhao, H.M. Fan, Ellipsoidal magnetite nanoparticles: a new member of the magnetic-vortex nanoparticles family for efficient magnetic hyperthermia, J. Mater. Chem. B 8 (3) (2020) 515–522.
[139] J. Mohapatra, M. Xing, J. Beatty, J. Elkins, T. Seda, S.R. Mishra, J.P. Liu, Enhancing the magnetic and inductive heating properties of Fe3O4 nanoparticles via morphology control, Nanotechnology 31 (27) (2020) 275706.
[140] D. García-Soriano, P. Milán-Rois, N. Lafuente-Gómez, C. Rodríguez-Díaz, C. Navío, Á. Somoza, G. Salas, Multicore iron oxide nanoparticles for magnetic hyperthermia and combination therapy against cancer cells, J. Colloid Interface Sci. 670 (2024) 73–85.
[141] P. Guardia, R. Di Corato, L. Lartigue, C. Wilhelm, A. Espinosa, M. Garcia-Hernandez, F. Gazeau, L. Manna, T. Pellegrino, Water-soluble iron oxide nanocubes with high values of specific absorption rate for cancer cell hyperthermia treatment, ACS Nano 6 (4) (2012) 3080–3091.
[142] J.G. Ovejero, D. Cabrera, J. Carrey, T. Valdivielso, G. Salas, F.J. Teran, Effects of inter- and intra-aggregate magnetic dipolar interactions on the magnetic heating efficiency of iron oxide nanoparticles, Phys. Chem. Chem. Phys. 18 (16) (2016) 10954–10963.
[143] A. Rajan, M. Sharma, N.K. Sahu, Assessing magnetic and inductive thermal properties of various surfactants functionalised Fe3O4 nanoparticles for hyperthermia, Sci. Rep. 10 (1) (2020) 15045.
[144] A. Rajan S, N.K. Sahu, Inductive calorimetric assessment of iron oxide nano-octahedrons for magnetic fluid hyperthermia, Colloids Surf. A Physicochem. Eng. Asp. 603 (2020) 125210.
[145] C.R. Kalaiselvan, S.S. Laha, S.B. Somvanshi, T.A. Tabish, N.D. Thorat, N.K. Sahu, Manganese ferrite (MnFe2O4) nanostructures for cancer theranostics, Coord. Chem. Rev. 473 (2022) 214809.
[146] R.A. Bohara, N.D. Thorat, S.H. Pawar, Role of functionalization: strategies to explore potential nano-bio applications of magnetic nanoparticles, RSC Adv. 6 (50) (2016) 43989–44012.
[147] A. Barra, J.K. Wychowaniec, D. Winning, M.M. Cruz, L.P. Ferreira, B.J. Rodriguez, H. Oliveira, E. Ruiz-Hitzky, C. Nunes, D.F. Brougham, P. Ferreira, Magnetic chitosan bionanocomposite films as a versatile platform for biomedical hyperthermia, Adv. Healthcare Mater. 13 (11) (2024) 2303861.
[148] N.K. Sahu, J. Gupta, D. Bahadur, PEGylated FePt–Fe3O4 composite nanoassemblies (CNAs): in vitro hyperthermia, drug delivery and generation of reactive oxygen species (ROS), Dalton Trans. 44 (19) (2015) 9103–9113.
[149] I. Roy Kritika, Therapeutic applications of magnetic nanoparticles: recent advances, Materials Advances 3 (20) (2022) 7425–7444.
[150] R. Di Corato, A. Espinosa, L. Lartigue, M. Tharaud, S. Chat, T. Pellegrino, C. Ménager, F. Gazeau, C. Wilhelm, Magnetic hyperthermia efficiency in the cellular environment for different nanoparticle designs, Biomaterials 35 (24) (2014) 6400–6411.
[151] H. Arami, A. Khandhar, D. Liggitt, K.M. Krishnan, In vivo delivery, pharmacokinetics, biodistribution and toxicity of iron oxide nanoparticles, Chem. Soc. Rev. 44 (23) (2015) 8576–8607.
[152] J. Huang, L. Bu, J. Xie, K. Chen, Z. Cheng, X. Li, X. Chen, Effects of nanoparticle size on cellular uptake and liver MRI with polyvinylpyrrolidone-coated iron oxide nanoparticles, ACS Nano 4 (12) (2010) 7151–7160.
[153] M. Yu, J. Zheng, Clearance pathways and tumor targeting of imaging nanoparticles, ACS Nano 9 (7) (2015) 6655–6674.
[154] D. Cabrera, A. Coene, J. Leliaert, E.J. Artés-Ibáñez, L. Dupré, N.D. Telling, F. J. Teran, Dynamical magnetic response of iron oxide nanoparticles inside live cells, ACS Nano 12 (3) (2018) 2741–2752.
[155] A. Abushrida, I. Elhuni, V. Taresco, L. Marciani, S. Stolnik, M.C. Garnett, A simple and efficient method for polymer coating of iron oxide nanoparticles, J. Drug Deliv. Sci. Technol. 55 (2020) 101460.
[156] M. Jamir, R. Islam, L.M. Pandey, J.P. Borah, Effect of surface functionalization on the heating efficiency of magnetite nanoclusters for hyperthermia application, J. Alloys Compd. 854 (2021) 157248.
[157] M. Vassallo, D. Martella, G. Barrera, F. Celegato, M. Coïsson, R. Ferrero, E. S. Olivetti, A. Troia, H. Sözeri, C. Parmeggiani, D.S. Wiersma, P. Tiberto, A. Manzin, Improvement of hyperthermia properties of iron oxide nanoparticles by surface coating, ACS Omega 8 (2) (2023) 2143–2154.
[158] A. Radoń, A. Włodarczyk, Ł. Sieroń, M. Rost-Roszkowska, Ł. Chajec, D. Łukowiec, A. Ciuraszkiewicz, P. Gębara, S. Wacławek, A. Kolano-Burian, Influence of the modifiers in polyol method on magnetically induced hyperthermia and biocompatibility of ultrafine magnetite nanoparticles, Sci. Rep. 13 (1) (2023) 7860.
[159] P.J. Sugumaran, X.-L. Liu, T.S. Herng, E. Peng, J. Ding, GO-functionalized large magnetic iron oxide nanoparticles with enhanced colloidal stability and hyperthermia performance, ACS Appl. Mater. Interfaces 11 (25) (2019) 22703–22713.
[160] Z. Shaterabadi, Á. Delgado, G.R. Iglesias, Solvothermally synthesized magnetite nanorods for application in magnetic hyperthermia and photothermia, J. Magn. Magn Mater. 596 (2024) 171990.
[161] K. Rekha, R. Ezhil Vizhi, B.B. Lahiri, J. Philip, Synthesis, physico-chemical properties, and AC induction heating of polycaprolactone-coated bio-compatible Fe3O4 nanoparticles, Inorg. Chem. Commun. 165 (2024) 112466.
[162] V. Narayanaswamy, S. Sambasivam, A. Saj, S. Alaabed, B. Issa, I.A. Al-Omari, I. M. Obaidat, Role of magnetite nanoparticles size and concentration on hyperthermia under various field frequencies and strengths, Molecules 26 (4) (2021) 796.
[163] M. Jamir, C. Borgohain, J.P. Borah, Influence of structure and magnetic properties of surface modified nanoparticles for hyperthermia application, Phys. B Condens. Matter 648 (2023) 414405.
[164] N. Van Khien, C. Thi Anh Xuan, L.H. Nguyen, P.H. Nam, T. Thi Thao, Role of citric acid coating in enhancing applicability of CoFe2O4 nanoparticles in antibacterial and hyperthermia, Mater. Today Commun. 38 (2024) 107982.
[165] K. Duraisamy, M. Devaraj, A. Gangadharan, K.S. Martirosyan, N.K. Sahu, P. Manogaran, G.E. Kreedapathy, Single domain soft ferromagnetic ferrofluid suitable for intratumoural magnetic hyperthermia, Colloids Surf. A Physicochem. Eng. Asp. 684 (2024) 133049.
[166] M. Jamir, C. Borgohain, J.P. Borah, Dipolar and anisotropy effect on dextran coated Cu doped ferrite for magnetic hyperthermia applications, J. Magn. Magn Mater. 580 (2023) 170917.
[167] G. Phukan, M. Kar, J.P. Borah, Interplay of anisotropy energy barrier and self-heating efficiency of cobalt-substituted CuFe2O4 nanoparticles, ACS Appl. Mater. Interfaces 16 (1) (2024) 261–271.
[168] A. Gasser, W. Ramadan, Y. Getahun, M. Garcia, M. Karim, A.A. El-Gendy, Feasibility of superparamagnetic NiFe2O4 and GO-NiFe2O4 nanoparticles for magnetic hyperthermia, Mater. Sci. Eng., B 297 (2023) 116721.
[169] K. El-Boubbou, O.M. Lemine, S. Algessair, N. Madkhali, B. Al-Najar, E. AlMatri, R. Ali, M. Henini, Preparation and characterization of various PVPylated divalent metal-doped ferrite nanoparticles for magnetic hyperthermia, RSC Adv. 14 (22) (2024) 15664–15679.
[170] M.S. Nunes, M.A. Morales, A. Paesano, J.H. de Araújo, Synthesis and characterization of monophasic MnFe2O4 nanoparticles for potential application in magnetic hyperthermia, Ceram. Int. 50 (14) (2024) 25333–25341.
[171] A. Singh, P. Kumar, S. Pathak, K. Jain, P. Garg, M. Pant, A.K. Mahapatro, R. K. Singh, P. Rajput, S.-K. Kim, K.K. Maurya, R.P. Pant, Tailored nanoparticles for magnetic hyperthermia: highly stable aqueous dispersion of Mn-substituted magnetite superparamagnetic nanoparticles by double surfactant coating for improved heating efficiency, J. Alloys Compd. 976 (2024) 172999.
[172] M. Anithkumar, A. Rajan S, A. Khan, B. Kaczmarek, M. Michalska-Sionkowska, K. Łukowicz, A.M. Osyczka, J. Gupta, N.K. Sahu, Glucose oxidase-loaded MnFe2O4 nanoparticles for hyperthermia and cancer starvation therapy, ACS Appl. Nano Mater. 6 (4) (2023) 2605–2614.

[173] A.R. Al-Areqi, X. Yu, R. Yang, C. Wang, C. Wu, W. Zhang, Synthesis of zinc ferrite particles with high saturation magnetization for magnetic induction hyperthermia, J. Magn. Magn Mater. 579 (2023) 170839.
[174] M. Jamir, C. Borgohain, J.P. Borah, Study of chitosan coated copper substituted nano-ferrites for hyperthermia applications, Phys. E Low-dimens. Syst. Nanostruct. 146 (2023) 115560.
[175] S.B. Somvanshi, S.A. Jadhav, S.S. Gawali, K. Zakde, K.M. Jadhav, Core-shell structured superparamagnetic Zn-Mg ferrite nanoparticles for magnetic hyperthermia applications, J. Alloys Compd. 947 (2023) 169574.
[176] A. Manohar, V. Vijayakanth, K. Chintagumpala, P. Manivasagan, E.-S. Jang, K. H. Kim, Zn- doped MnFe2O4 nanoparticles for magnetic hyperthermia and their cytotoxicity study in normal and cancer cell lines, Colloids Surf. A Physicochem. Eng. Asp. 675 (2023) 132037.
[177] K. Shah, A. Bhardwaj, D. Bhadla, K. Parekh, N. Jain, Cytotoxicity and uptake analysis of Mn-Zn ferrite-based temperature-sensitive ferrofluid on cervical and bone cancer cells, J. Magn. Magn Mater. 589 (2024) 171534.
[178] A. Manohar, P. Manivasagan, E.-S. Jang, N. Mameda, A.A. Al-Kahtani, S. Kumar, A. Kumar, M. Ubaidullah, K.H. Kim, Tailored Zn1-xMg0.5CuxFe2O4 nanoparticles: optimizing magnetic hyperthermia for enhanced efficacy and investigating cytotoxicity in normal and cancer cell lines, Mater. Chem. Phys. 316 (2024) 129050.
[179] A. Manohar, V. Vijayakanth, M.R. Pallavolu, K.H. Kim, Effects of Ni - substitution on structural, magnetic hyperthermia, photocatalytic and cytotoxicity study of MgFe2O4 nanoparticles, J. Alloys Compd. 879 (2021) 160515.
[180] S.O. Aisida, T.C. Chibueze, M.H. Alnasir, O.E. Oyewande, A.T. Raji, C.E. Ekuma, I. Ahmad, T.k. Zhao, M. Maaza, F.I. Ezema, Microstructural and magneto-optical properties of Co1-xNix Fe2O4 nanocomposites for hyperthermia applications, Solid State Sci. 136 (2023) 107107.
[181] Z. Shaterabadi, G. Nabiyouni, Z.M. Asadi, G.R. Iglesias, M. Soleymani, Enhanced magnetic hyperthermia efficiency in poly vinyl alcohol-coated zinc-substituted cobalt ferrite nanoparticles: correlated effects of zinc content and applied magnetic field strength, Ceram. Int. 49 (21) (2023) 33934–33943.
[182] A. Manohar, K. Chintagumpala, K.H. Kim, Mixed Zn–Ni spinel ferrites: structure, magnetic hyperthermia and photocatalytic properties, Ceram. Int. 47 (5) (2021) 7052–7061.
[183] P.V. Ramana, K.S. Rao, K.R. Kumar, G. Kapusetti, M. Choppadandi, J.N. Kiran, K. H. Rao, A study of uncoated and coated nickel-zinc ferrite nanoparticles for magnetic hyperthermia, Mater. Chem. Phys. 266 (2021) 124546.
[184] M. Kaksonen, A. Roux, Mechanisms of clathrin-mediated endocytosis, Nat. Rev. Mol. Cell Biol. 19 (5) (2018) 313–326.
[185] O. Lunov, T. Syrovets, C. Loos, J. Beil, M. Delacher, K. Tron, G.U. Nienhaus, A. Musyanovych, V. Mailänder, K. Landfester, T. Simmet, Differential uptake of functionalized polystyrene nanoparticles by human macrophages and a monocytic cell line, ACS Nano 5 (3) (2011) 1657–1669.
[186] C. Gundu, V.K. Arruri, P. Yadav, U. Navik, A. Kumar, V.S. Amalkar, A. Vikram, R. R. Gaddam, Dynamin-independent mechanisms of endocytosis and receptor trafficking, Cells 11 (16) (2022) 2557.
[187] M. Sousa de Almeida, E. Susnik, B. Drasler, P. Taladriz-Blanco, A. Petri-Fink, B. Rothen-Rutishauser, Understanding nanoparticle endocytosis to improve targeting strategies in nanomedicine, Chem. Soc. Rev. 50 (9) (2021) 5397–5434.
[188] N. Shobhana, N.R. Naveen, P. Goudanavar, Magnetic precision: unleashing the therapeutic potential of paclitaxel-loaded nanoparticles in breast cancer treatment, Oral Oncology Reports 10 (2024) 100283.
[189] E. Benayas, A. Espinosa, M.T. Portolés, V. Vila-del Sol, M.P. Morales, M. C. Serrano, Cellular and molecular processes are differently influenced in primary neural cells by slight changes in the physicochemical properties of multicore magnetic nanoparticles, ACS Appl. Mater. Interfaces 15 (14) (2023) 17726–17741.
[190] S.D. Shirsat, P.V. Londhe, A.P. Gaikwad, M. Rizwan, S.S. Laha, V.M. Khot, V. Achal, T.A. Tabish, N.D. Thorat, Endosomal escape in magnetic nanostructures: recent advances and future perspectives, Materials Today Advances 22 (2024) 100484.
[191] A.K. Varkouhi, M. Scholte, G. Storm, H.J. Haisma, Endosomal escape pathways for delivery of biologicals, J. Contr. Release 151 (3) (2011) 220–228.
[192] Y. Gu, R. Piñol, R. Moreno-Loshuertos, C.D.S. Brites, J. Zeler, A. Martínez, G. Maurin-Pasturel, P. Fernández-Silva, J. Marco-Brualla, P. Téllez, R. Cases, R. N. Belsué, D. Bonvin, L.D. Carlos, A. Millán, Local temperature increments and induced cell death in intracellular magnetic hyperthermia, ACS Nano 17 (7) (2023) 6822–6832.
[193] I. Belhadj Slimen, T. Najar, A. Ghram, H. Dabbebi, M. Ben Mrad, M. Abdrabbah, Reactive oxygen species, heat stress and oxidative-induced mitochondrial damage. A review, Int. J. Hyperther. 30 (7) (2014) 513–523.
[194] C. Garrido, L. Galluzzi, M. Brunet, P.E. Puig, C. Didelot, G. Kroemer, Mechanisms of cytochrome c release from mitochondria, Cell Death Differ. 13 (9) (2006) 1423–1433.
[195] X. Chen, H. Wang, J. Shi, Z. Chen, Y. Wang, S. Gu, Y. Fu, J. Huang, J. Ding, L. Yu, An injectable and active hydrogel induces mutually enhanced mild magnetic hyperthermia and ferroptosis, Biomaterials 298 (2023) 122139.
[196] J.P. Kehrer, The Haber–Weiss reaction and mechanisms of toxicity, Toxicology 149 (1) (2000) 43–50.
[197] M.L. Kremer, Initial Steps in the Reaction of H2O2 with Fe2+ and Fe3+ Ions: Inconsistency in the Free Radical Theory, Reactions, 2023, pp. 171–175.
[198] S.S. Nazeer, A. Saraswathy, N. Nimi, H. Santhakumar, P. Radhakrishnapillai Suma, S.J. Shenoy, R.S. Jayasree, Near infrared-emitting multimodal nanosystem for in vitro magnetic hyperthermia of hepatocellular carcinoma and dual imaging of in vivo liver fibrosis, Sci. Rep. 13 (1) (2023) 12947.
[199] T. Mai, J.Z. Hilt, Magnetic nanoparticles: reactive oxygen species generation and potential therapeutic applications, J. Nanoparticle Res. 19 (7) (2017) 253.
[200] R.J. Wydra, P.G. Rychahou, B.M. Evers, K.W. Anderson, T.D. Dziubla, J.Z. Hilt, The role of ROS generation from magnetic nanoparticles in an alternating magnetic field on cytotoxicity, Acta Biomater. 25 (2015) 284–290.
[201] A. Sola-Leyva, Y. Jabalera, M.A. Chico-Lozano, M.P. Carrasco-Jiménez, G. R. Iglesias, C. Jimenez-Lopez, Reactive oxygen species (ROS) production in HepG2 cancer cell line through the application of localized alternating magnetic field, J. Mater. Chem. B 8 (34) (2020) 7667–7676.
[202] A.K. Hauser, K.W. Anderson, J.Z. Hilt, Peptide conjugated magnetic nanoparticles for magnetically mediated energy delivery to lung cancer cells, Nanomedicine (Lond) 11 (14) (2016) 1769–1785.
[203] R.S. Chouhan, M. Horvat, J. Ahmed, N. Alhokbany, S.M. Alshehri, S. Gandhi, Magnetic nanoparticles—a multifunctional potential agent for diagnosis and therapy, Cancers 13 (9) (2021) 2213.
[204] M. Domenech, I. Marrero-Berrios, M. Torres-Lugo, C. Rinaldi, Lysosomal membrane permeabilization by targeted magnetic nanoparticles in alternating magnetic fields, ACS Nano 7 (6) (2013) 5091–5101.
[205] M.J. Ko, S. Min, H. Hong, W. Yoo, J. Joo, Y.S. Zhang, H. Kang, D.-H. Kim, Magnetic nanoparticles for ferroptosis cancer therapy with diagnostic imaging, Bioact. Mater. 32 (2024) 66–97.
[206] C. Pucci, D. De Pasquale, A. Marino, C. Martinelli, S. Lauciello, G. Ciofani, Hybrid magnetic nanovectors promote selective glioblastoma cell death through a combined effect of lysosomal membrane permeabilization and chemotherapy, ACS Appl. Mater. Interfaces 12 (26) (2020) 29037–29055.
[207] M. Salimi, S. Sarkar, M. Hashemi, R. Saber, Treatment of breast cancer-bearing BALB/c mice with magnetic hyperthermia using dendrimer functionalized iron-oxide nanoparticles, Nanomaterials 10 (11) (2020) 2310.
[208] L. Beola, V. Grazú, Y. Fernández-Afonso, R.M. Fratila, M. de las Heras, J.M. de la Fuente, L. Gutiérrez, L. Asín, Critical parameters to improve pancreatic cancer treatment using magnetic hyperthermia: field conditions, immune response, and particle biodistribution, ACS Appl. Mater. Interfaces 13 (11) (2021) 12982–12996.
[209] A. Chauhan, S. Midha, R. Kumar, R. Meena, P. Singh, S.K. Jha, B.K. Kuanr, Rapid tumor inhibition via magnetic hyperthermia regulated by caspase 3 with time-dependent clearance of iron oxide nanoparticles, Biomater. Sci. 9 (8) (2021) 2972–2990.
[210] R.M. Patil, N.D. Thorat, P.B. Shete, P.A. Bedge, S. Gavde, M.G. Joshi, S.A. M. Tofail, R.A. Bohara, Comprehensive cytotoxicity studies of superparamagnetic iron oxide nanoparticles, Biochemistry and Biophysics Reports 13 (2018) 63–72.
[211] L. Rubio, I. Barguilla, J. Domenech, R. Marcos, A. Hernández, Biological effects, including oxidative stress and genotoxic damage, of polystyrene nanoparticles in different human hematopoietic cell lines, J. Hazard Mater. 398 (2020) 122900.
[212] L. Xuan, Z. Ju, M. Skonieczna, P.-K. Zhou, R. Huang, Nanoparticles-induced potential toxicity on human health: applications, toxicity mechanisms, and evaluation models, MedComm 4 (4) (2023) e327.
[213] H. Al Faruque, E.-S. Choi, H.-R. Lee, J.-H. Kim, S. Park, E. Kim, Targeted removal of leukemia cells from the circulating system by whole-body magnetic hyperthermia in mice, Nanoscale 12 (4) (2020) 2773–2786.
[214] N. Daviu, Y. Portilla, M. Gómez de Cedrón, A. Ramírez de Molina, D.F. Barber, DMSA-coated IONPs trigger oxidative stress, mitochondrial metabolic reprograming and changes in mitochondrial disposition, hindering cell cycle progression of cancer cells, Biomaterials 304 (2024) 122409.
[215] M. Ruzycka-Ayoush, K. Sobczak, I.P. Grudzinski, Comparative studies on the cytotoxic effects induced by iron oxide nanoparticles in cancerous and noncancerous human lung cells subjected to an alternating magnetic field, Toxicol. Vitro 95 (2024) 105760.
[216] H. Gu, S. Fu, Z. Cai, H. Ai, Polymer/iron oxide nanocomposites as magnetic resonance imaging contrast agents: polymer modulation and probe property control, Journal of Polymer Science n/ a (n/a) (2024).
[217] S. Behzadi, V. Serpooshan, W. Tao, M.A. Hamaly, M.Y. Alkawareek, E.C. Dreaden, D. Brown, A.M. Alkilany, O.C. Farokhzad, M. Mahmoudi, Cellular uptake of nanoparticles: journey inside the cell, Chem. Soc. Rev. 46 (14) (2017) 4218–4244.
[218] E. Fröhlich, Cellular targets and mechanisms in the cytotoxic action of non-biodegradable engineered nanoparticles, Curr. Drug Metabol. 14 (9) (2013) 976–988.
[219] P. Pradhan, J. Giri, G. Samanta, H.D. Sarma, K.P. Mishra, J. Bellare, R. Banerjee, D. Bahadur, Comparative evaluation of heating ability and biocompatibility of different ferrite-based magnetic fluids for hyperthermia application, J. Biomed. Mater. Res. B Appl. Biomater. 81B (1) (2007) 12–22.
[220] M. Calero, L. Gutiérrez, G. Salas, Y. Luengo, A. Lázaro, P. Acedo, M.P. Morales, R. Miranda, A. Villanueva, Efficient and safe internalization of magnetic iron oxide nanoparticles: two fundamental requirements for biomedical applications, Nanomed. Nanotechnol. Biol. Med. 10 (4) (2014) 733–743.
[221] D. Chen, X. Tang Q Fau - Li, X. Li X Fau - Zhou, J. Zhou X Fau - Zang, W.-q. Zang J Fau - Xue, J.-y. Xue Wq Fau - Xiang, C.-q. Xiang Jy Fau - Guo, C.Q. Guo, Biocompatibility of Magnetic Fe_3O_4 Nanoparticles and Their Cytotoxic Effect on MCF-7 Cells, (1178-2013 (Electronic)).
[222] M. Johannsen, B. Thiesen, A. Jordan, K. Taymoorian, U. Gneveckow, N. Waldöfner, R. Scholz, M. Koch, M. Lein, K. Jung, S.A. Loening, Magnetic fluid hyperthermia (MFH)reduces prostate cancer growth in the orthotopic Dunning R3327 rat model, Prostate 64 (3) (2005) 283–292.
[223] T.K. Jain, M.K. Reddy, M.A. Morales, D.L. Leslie-Pelecky, V. Labhasetwar, Biodistribution, clearance, and biocompatibility of iron oxide magnetic nanoparticles in rats, Mol. Pharm. 5 (2) (2008) 316–327.

[224] Y. Li, Y. Liu J Fau - Zhong, J. Zhong Y Fau - Zhang, Z. Zhang J Fau - Wang, L. Wang Z Fau - Wang, Y. Wang L Fau - An, M. An Y Fau - Lin, Z. Lin M Fau - Gao, D. Gao Z Fau - Zhang, D. Zhang, Biocompatibility of Fe_3O_4@Au Composite Magnetic Nanoparticles in Vitro and in Vivo, (1178-2013 (Electronic)).

[225] S. Jeon, B.C. Park, S. Lim, H.Y. Yoon, Y.S. Jeon, B.-S. Kim, Y.K. Kim, K. Kim, Heat-generating iron oxide multigranule nanoclusters for enhancing hyperthermic efficacy in tumor treatment, ACS Appl. Mater. Interfaces 12 (30) (2020) 33483–33491.

[226] X.L. Liu, Y. Yang, C.T. Ng, L.Y. Zhao, Y. Zhang, B.H. Bay, H.M. Fan, J. Ding, Magnetic vortex nanorings: a new class of hyperthermia agent for highly efficient in vivo regression of tumors, Adv. Mater. 27 (11) (2015) 1939–1944.

[227] G.N.A. Rego, M.P. Nucci, J.B. Mamani, F.A. Oliveira, L.C. Marti, I.S. Filgueiras, J. M. Ferreira, C.C. Real, D.D. Faria, P.L. Espinha, D.M.C. Fantacini, L.E.B. Souza, D. T. Covas, C.A. Buchpiguel, L.F. Gamarra, Therapeutic efficiency of multiple applications of magnetic hyperthermia technique in glioblastoma using aminosilane coated iron oxide nanoparticles: in vitro and in vivo study, Int. J. Mol. Sci. 21 (3) (2020) 958.

[228] J. Hamzehalipour Almaki, R. Nasiri, A. Idris, M. Nasiri, F.A. Abdul Majid, D. Losic, Trastuzumab-decorated nanoparticles for in vitro and in vivo tumor-targeting hyperthermia of HER2+ breast cancer, J. Mater. Chem. B 5 (35) (2017) 7369–7383.

[229] X. Yan, T. Sun, Y. Song, W. Peng, Y. Xu, G. Luo, M. Li, S. Chen, W.-W. Fang, L. Dong, S. Xuan, T. He, B. Cao, Y. Lu, In situ thermal-responsive magnetic hydrogel for multidisciplinary therapy of hepatocellular carcinoma, Nano Lett. 22 (6) (2022) 2251–2260.

[230] M. Fontes de Paula Aguiar, J. Bustamante Mamani, T. Klei Felix, R. Ferreira dos Reis, H. Rodrigues da Silva, L.P. Nucci, M.P. Nucci-da-Silva, L.F. Gamarra, Magnetic targeting with superparamagnetic iron oxide nanoparticles for in vivo glioma 6 (5) (2017) 449–472.

[231] H.F. Rodrigues, F.M. Mello, L.C. Branquinho, N. Zufelato, E.P. Silveira-Lacerda, A. F. Bakuzis, Real-time infrared thermography detection of magnetic nanoparticle hyperthermia in a murine model under a non-uniform field configuration, Int. J. Hyperther. 29 (8) (2013) 752–767.

[232] A. Ahmed, E. Kim, S. Jeon, J.-Y. Kim, H. Choi, Closed-loop temperature-controlled magnetic hyperthermia therapy with magnetic guidance of superparamagnetic iron-oxide nanoparticles, Advanced Therapeutics 5 (2) (2022) 2100237.

[233] E.K. Mohamed, M.M. Fathy, N.A. Sadek, D.E. Eldosoki, The effects of rutin coat on the biodistribution and toxicities of iron oxide nanoparticles in rats, J. Nanoparticle Res. 26 (3) (2024) 49.

[234] S. Piehler, H. Dähring, J. Grandke, J. Göring, P. Couleaud, A. Aires, A. L. Cortajarena, J. Courty, A. Latorre, Á. Somoza, U. Teichgräber, I. Hilger, Iron oxide nanoparticles as carriers for DOX and magnetic hyperthermia after intratumoral application into breast cancer in mice: impact and future perspectives, Nanomaterials 10 (16) (2020) 1016.

[235] P.T. Ha, T.T.H. Le, T.Q. Bui, H.N. Pham, A.S. Ho, L.T. Nguyen, Doxorubicin release by magnetic inductive heating and in vivo hyperthermia-chemotherapy combined cancer treatment of multifunctional magnetic nanoparticles, New J. Chem. 43 (14) (2019) 5404–5413.

[236] M. Norouzi, V. Yathindranath, J.A. Thliveris, B.M. Kopec, T.J. Siahaan, D. W. Miller, Doxorubicin-loaded iron oxide nanoparticles for glioblastoma therapy: a combinational approach for enhanced delivery of nanoparticles, Sci. Rep. 10 (1) (2020) 11292.

[237] K. El-Boubbou, O.M. Lemine, R. Ali, S.M. Huwaizi, S. Al-Humaid, A. AlKushi, Evaluating magnetic and thermal effects of various Polymerylated magnetic iron oxide nanoparticles for combined chemo-hyperthermia, New J. Chem. 46 (12) (2022) 5489–5504.

[238] B.T. Mai, P.B. Balakrishnan, M.J. Barthel, F. Piccardi, D. Niculaes, F. Marinaro, S. Fernandes, A. Curcio, H. Kakwere, G. Autret, R. Cingolani, F. Gazeau, T. Pellegrino, Thermoresponsive iron oxide nanocubes for an effective clinical translation of magnetic hyperthermia and heat-mediated chemotherapy, ACS Appl. Mater. Interfaces 11 (6) (2019) 5727–5739.

[239] W. Lin, X. Xie, Y. Yang, X. Fu, H. Liu, Y. Yang, J. Deng, Thermosensitive magnetic liposomes with doxorubicin cell-penetrating peptides conjugate for enhanced and targeted cancer therapy, Drug Deliv. 23 (9) (2016) 3436–3443.

[240] F.L. Tansi, F. Fröbel, W.O. Maduabuchi, F. Steiniger, M. Westermann, R. Quaas, U.K. Teichgräber, I. Hilger, Effect of matrix-modulating enzymes on the cellular uptake of magnetic nanoparticles and on magnetic hyperthermia treatment of pancreatic cancer models in vivo, Nanomaterials 11 (2) (2021) 438.

[241] Z.-Q. Zhang, S.-C. Song, Multiple hyperthermia-mediated release of TRAIL/SPION nanocomplex from thermosensitive polymeric hydrogels for combination cancer therapy, Biomaterials 132 (2017) 16–27.

[242] M. Gogoi, M.K. Jaiswal, H.D. Sarma, D. Bahadur, R. Banerjee, Biocompatibility and therapeutic evaluation of magnetic liposomes designed for self-controlled cancer hyperthermia and chemotherapy, Integr. Biol. 9 (6) (2017) 555–565.

[243] J. Tang, H. Zhou, J. Liu, J. Liu, W. Li, Y. Wang, F. Hu, Q. Huo, J. Li, Y. Liu, C. Chen, Dual-Mode imaging-guided synergistic chemo- and magnetohyperthermia therapy in a versatile nanoplatform to eliminate cancer stem cells, ACS Appl. Mater. Interfaces 9 (28) (2017) 23497–23507.

[244] A. Manigandan, V. Handi, N.S. Sundaramoorthy, R. Dhandapani, J. Radhakrishnan, S. Sethuraman, A. Subramanian, Responsive nanomicellar theranostic cages for metastatic breast cancer, Bioconjugate Chem. 29 (2) (2018) 275–286.

[245] K.-Y. Qian, Y. Song, X. Yan, L. Dong, J. Xue, Y. Xu, B. Wang, B. Cao, Q. Hou, W. Peng, J. Hu, K. Jiang, S. Chen, H. Wang, Y. Lu, Injectable ferrimagnetic silk fibroin hydrogel for magnetic hyperthermia ablation of deep tumor, Biomaterials 259 (2020) 120299.

[246] E. Guisasola, L. Asín, L. Beola, J.M. de la Fuente, A. Baeza, M. Vallet-Regí, Beyond traditional hyperthermia: in vivo cancer treatment with magnetic-responsive mesoporous silica nanocarriers, ACS Appl. Mater. Interfaces 10 (15) (2018) 12518–12525.

[247] Y. Zhang, Y. Zhang, J. Li, C. Liang, K. Shi, S. Wang, X. Gao, B. Yan, Y. Lyu, X. Liu, H. Fan, Impact of nanoheater subcellular localization on the antitumor immune efficacy of magnetic hyperthermia, Nano Today 56 (2024) 102226.

[248] K.A. Court, H. Hatakeyama, S.Y. Wu, M.S. Lingegowda, C. Rodríguez-Aguayo, G. López-Berestein, L. Ju-Seog, C. Rinaldi, E.J. Juan, A.K. Sood, M. Torres-Lugo, HSP70 inhibition synergistically enhances the effects of magnetic fluid hyperthermia in ovarian cancer, Mol. Cancer Therapeut. 16 (5) (2017) 966–976.

[249] J.M. Paez-Muñoz, F. Gámez, Y. Fernández-Afonso, R. Gallardo, M. Pernia Leal, L. Gutiérrez, J.M. de la Fuente, C. Caro, M.L. García-Martín, Optimization of iron oxide nanoparticles for MRI-guided magnetic hyperthermia tumor therapy: reassessing the role of shape in their magnetocaloric effect, J. Mater. Chem. B 11 (46) (2023) 11110–11120.

[250] T. Kobayashi, Y. Kida, T. Tanaka, K. Hattori, M. Matsui, Y. Amemiya, Interstitial hyperthermia of malignant brain tumors by implant heating system: clinical experience, J. Neuro Oncol. 10 (2) (1991) 153–163.

[251] M. Johannsen, U. Gneveckow, K. Taymoorian, B. Thiesen, N. Waldöfner, R. Scholz, K. Jung, A. Jordan, P. Wust, S.A. Loening, Morbidity and quality of life during thermotherapy using magnetic nanoparticles in locally recurrent prostate cancer: results of a prospective phase I trial, Int. J. Hyperther. 23 (3) (2007) 315–323.

[252] MagForce Nanotechnologies AG Applies for European Regulatory Approval of its Nano-Cancer® Therapy, Business Wire, 2009, p. NA.

[253] O. Grauer, M. Jaber, K. Hess, M. Weckesser, W. Schwindt, S. Maring, J. Wölfer, W. Stummer, Combined intracavitary thermotherapy with iron oxide nanoparticles and radiotherapy as local treatment modality in recurrent glioblastoma patients, J. Neuro Oncol. 141 (1) (2019) 83–94.

[254] W.J. Atkinson, I.A. Brezovich, D.P. Chakraborty, Useable frequencies in hyperthermia with thermal seeds, IEEE (Inst. Electr. Electron. Eng.) Trans. Biomed. Eng. BME-31 (1) (1984) 70–75.

[255] B. Herrero de la Parte, I. Rodrigo, J. Gutiérrez-Basoa, S. Iturrizaga Correcher, C. Mar Medina, J.J. Echevarría-Uraga, J.A. Garcia, F. Plazaola, I. García-Alonso, Proposal of new safety limits for in vivo experiments of magnetic hyperthermia antitumor therapy, Cancers 14 (13) (2022) 3084.

[256] H. Yan, W. Shang, X. Sun, L. Zhao, J. Wang, Z. Xiong, J. Yuan, R. Zhang, Q. Huang, K. Wang, B. Li, J. Tian, F. Kang, S.-S. Feng, "All-in-One" nanoparticles for trimodality imaging-guided intracellular photo-magnetic hyperthermia therapy under intravenous administration, Adv. Funct. Mater. 28 (9) (2018) 1705710.

[257] M. Chen, Y. Fu, Y. Liu, B. Zhang, X. Song, X. Chen, Z. Zhu, H. Gao, J. Yang, X. Shi, NIR-Light-Triggered mild-temperature hyperthermia to overcome the cascade cisplatin resistance for improved resistant tumor therapy, Adv. Healthcare Mater. 13 (11) (2024) 2303667.

[258] A. Espinosa, J. Reguera, A. Curcio, Á. Muñoz-Noval, C. Kuttner, A. Van de Walle, L.M. Liz-Marzán, C. Wilhelm, Janus magnetic-plasmonic nanoparticles for magnetically guided and thermally activated cancer therapy, Small 16 (11) (2020) 1904960.

[259] X. Ma, Y. Wang, X.-L. Liu, H. Ma, G. Li, Y. Li, F. Gao, M. Peng, H.M. Fan, X.-J. Liang, Fe3O4–Pd Janus nanoparticles with amplified dual-mode hyperthermia and enhanced ROS generation for breast cancer treatment, Nanoscale Horizons 4 (6) (2019) 1450–1459.

[260] A. Espinosa, R. Di Corato, J. Kolosnjaj-Tabi, P. Flaud, T. Pellegrino, C. Wilhelm, Duality of iron oxide nanoparticles in cancer therapy: amplification of heating efficiency by magnetic hyperthermia and photothermal bimodal treatment, ACS Nano 10 (2) (2016) 2436–2446.

[261] J.B. Vines, J.-H. Yoon, N.-E. Ryu, D.-J. Lim, H. Park, Gold nanoparticles for photothermal cancer therapy, Front. Chem. 7 (2019).

[262] M. Lázaro, Á.V. Delgado, G.R. Iglesias, Magneto-photothermal synergy applied to gold-coated magnetic nanoparticles, J. Magn. Magn Mater. 591 (2024) 171718.

[263] A. Espinosa, M. Bugnet, G. Radtke, S. Neveu, G.A. Botton, C. Wilhelm, A. Abou-Hassan, Can magneto-plasmonic nanohybrids efficiently combine photothermia with magnetic hyperthermia? Nanoscale 7 (45) (2015) 18872–18877.

[264] L. Wang, W. Zou, J. Shen, S. Yang, J. Wu, T. Ying, X. Cai, L. Zhang, J. Wu, Y. Zheng, Dual-functional laser-guided magnetic nanorobot collectives against gravity for on-demand thermo-chemotherapy of peritoneal metastasis, Adv. Healthcare Mater. 13 (9) (2024) 2303361.

[265] E.S. Abu Serea, I. Orue, J.Á. García, S. Lanceros-Méndez, J. Reguera, Enhancement and tunability of plasmonic-magnetic hyperthermia through shape and size control of Au:Fe3O4 Janus nanoparticles, ACS Appl. Nano Mater. 6 (19) (2023) 18466–18479.

[266] B. Muzzi, M. Albino, A. Gabbani, A. Omelyanchik, E. Kozenkova, M. Petrecca, C. Innocenti, E. Balica, A. Lavacchi, F. Scavone, C. Anceschi, G. Petrucci, A. Ibarra, A. Laurenzana, F. Pineider, V. Rodionova, C. Sangregorio, Star-shaped magnetic-plasmonic Au@Fe3O4 nano-heterostructures for photothermal therapy, ACS Appl. Mater. Interfaces 14 (25) (2022) 29087–29098.

[267] S. Fiorito, N. Soni, N. Silvestri, R. Brescia, H. Gavilán, J.S. Conteh, B.T. Mai, T. Pellegrino, Fe3O4@Au@Cu2−xS heterostructures designed for tri-modal therapy: photo- magnetic hyperthermia and 64Cu radio-insertion, Small 18 (18) (2022) 2200174.

[268] R. Hu, M. Zheng, J. Wu, C. Li, D. Shen, D. Yang, L. Li, M. Ge, Z. Chang, W. Dong, Core-shell magnetic gold nanoparticles for magnetic field-enhanced radio-photothermal therapy in cervical cancer, Nanomaterials 7 (5) (2017) 111.

[269] A. Yilmazer, Z. Eroglu, C. Gurcan, A. Gazzi, O. Ekim, B. Sundu, C. Gokce, A. Ceylan, L. Giro, M.A. Unal, F. Arı, A. Ekicibil, O. Ozgenç Çinar, B.I. Ozturk, O. Besbinar, M. Ensoy, D. Cansaran-Duman, L.G. Delogu, O. Metin, Synergized photothermal therapy and magnetic field induced hyperthermia via bismuthene for lung cancer combinatorial treatment, Materials Today Bio 23 (2023) 100825.
[270] S. Zuo, J. Wang, X. An, Y. Zhang, Janus magnetic nanoplatform for magnetically targeted and protein/hyperthermia combination therapies of breast cancer, Front. Bioeng. Biotechnol. 9 (2022).
[271] M.D. Hirschey, R.J. DeBerardinis, A.M.E. Diehl, J.E. Drew, C. Frezza, M.F. Green, L.W. Jones, Y.H. Ko, A. Le, M.A. Lea, J.W. Locasale, V.D. Longo, C.A. Lyssiotis, E. McDonnell, M. Mehrmohamadi, G. Michelotti, V. Muralidhar, M.P. Murphy, P. L. Pedersen, B. Poore, L. Raffaghello, J.C. Rathmell, S. Sivanand, M.G. Vander Heiden, K.E. Wellen, Dysregulated metabolism contributes to oncogenesis, Semin. Cancer Biol. 35 (2015) S129–S150.
[272] W. Ying, Y. Zhang, W. Gao, X. Cai, G. Wang, X. Wu, L. Chen, Z. Meng, Y. Zheng, B. Hu, X. Lin, Hollow magnetic nanocatalysts drive starvation–chemodynamic–hyperthermia synergistic therapy for tumor, ACS Nano 14 (8) (2020) 9662–9674.
[273] K. Yu, H. Zhou, Y. Xu, Y. Cao, Y. Zheng, B. Liang, Engineering a triple-functional magnetic gel driving mutually-synergistic mild hyperthermia-starvation therapy for osteosarcoma treatment and augmented bone regeneration, J. Nanobiotechnol. 21 (1) (2023) 201.
[274] X. Xing, S. Zhao, T. Xu, L. Huang, Y. Zhang, M. Lan, C. Lin, X. Zheng, P. Wang, Advances and perspectives in organic sonosensitizers for sonodynamic therapy, Coord. Chem. Rev. 445 (2021) 214087.
[275] Y.-J. Ho, C.-H. Wu, Q.-f. Jin, C.-Y. Lin, P.-H. Chiang, N. Wu, C.-H. Fan, C.-M. Yang, C.-K. Yeh, Superhydrophobic drug-loaded mesoporous silica nanoparticles capped with β-cyclodextrin for ultrasound image-guided combined antivascular and chemo-sonodynamic therapy, Biomaterials 232 (2020) 119723.
[276] M. Chen, X. Liang, C. Gao, R. Zhao, N. Zhang, S. Wang, W. Chen, B. Zhao, J. Wang, Z. Dai, Ultrasound triggered conversion of porphyrin/camptothecin-fluoroxyuridine triad microbubbles into nanoparticles overcomes multidrug resistance in colorectal cancer, ACS Nano 12 (7) (2018) 7312–7326.
[277] Q. Feng, W. Zhang, X. Yang, Y. Li, Y. Hao, H. Zhang, L. Hou, Z. Zhang, pH/ultrasound dual-responsive gas generator for ultrasound imaging-guided therapeutic inertial cavitation and sonodynamic therapy, Adv. Healthcare Mater. 7 (5) (2018) 1700957.
[278] Y. He, J. Wan, Y. Yang, P. Yuan, C. Yang, Z. Wang, L. Zhang, Multifunctional polypyrrole-coated mesoporous TiO2 nanocomposites for photothermal, sonodynamic, and chemotherapeutic treatments and dual-modal ultrasound/photoacoustic imaging of tumors, Adv. Healthcare Mater. 8 (9) (2019) 1801254.
[279] Y. Liang, M. Zhang, Y. Zhang, M. Zhang, Ultrasound sonosensitizers for tumor sonodynamic therapy and imaging: a new direction with clinical translation, Molecules 28 (18) (2023) 6484.
[280] Y. Zhang, Y. Xu, D. Sun, Z. Meng, W. Ying, W. Gao, R. Hou, Y. Zheng, X. Cai, B. Hu, X. Lin, Hollow magnetic nanosystem-boosting synergistic effect between magnetic hyperthermia and sonodynamic therapy via modulating reactive oxygen species and heat shock proteins, Chem. Eng. J. 390 (2020) 124521.
[281] F. Gao, G. He, H. Yin, J. Chen, Y. Liu, C. Lan, S. Zhang, B. Yang, Titania-coated 2D gold nanoplates as nanoagents for synergistic photothermal/sonodynamic therapy in the second near-infrared window, Nanoscale 11 (5) (2019) 2374–2384.
[282] Y. Zhang, H. Wang, X. Jia, S. Du, Y. Yin, X. Zhang, Cascade catalytic nanoplatform for enhanced starvation and sonodynamic therapy, J. Drug Target. 28 (2) (2020) 195–203.
[283] E. Aram, M. Moeni, R. Abedizadeh, D. Sabour, H. Sadeghi-Abandansari, J. Gardy, A. Hassanpour, Smart and multi-functional magnetic nanoparticles for cancer treatment applications: clinical challenges and future prospects, Nanomaterials 12 (20) (2022) 3567.
[284] A.L. Onugwu, O.L. Ugorji, C.A. Ufondu, S.A. Ihim, A.C. Echezona, C.S. Nwagwu, S.O. Onugwu, S.W. Uzondu, C.P. Agbo, J.D. Ogbonna, A.A. Attama, Nanoparticle-based delivery systems as emerging therapy in retinoblastoma: recent advances, challenges and prospects, Nanoscale Adv. 5 (18) (2023) 4628–4648.
[285] C. Qiu, F. Xia, J. Zhang, Q. Shi, Y. Meng, C. Wang, H. Pang, L. Gu, C. Xu, Q. Guo, J. Wang, Advanced Strategies for Overcoming Endosomal/Lysosomal Barrier in Nanodrug Delivery, Research 6 0148.
[286] T. Kobayashi, K. Kakimi, E. Nakayama, K. Jimbow, Antitumor immunity by magnetic nanoparticle-mediated hyperthermia, Nanomedicine 9 (11) (2014) 1715–1726.
[287] Y. Chao, G. Chen, C. Liang, J. Xu, Z. Dong, X. Han, C. Wang, Z. Liu, Iron nanoparticles for low-power local magnetic hyperthermia in combination with immune checkpoint blockade for systemic antitumor therapy, Nano Lett. 19 (7) (2019) 4287–4296.
[288] P.T. Yin, S. Shah, N.J. Pasquale, O.B. Garbuzenko, T. Minko, K.-B. Lee, Stem cell-based gene therapy activated using magnetic hyperthermia to enhance the treatment of cancer, Biomaterials 81 (2016) 46–57.